5

LUNAR MINERALS

James Papike, Lawrence Taylor, and Steven Simon

The lunar rocks described in the next chapter are unique to the Moon. Their special characteristics—especially the complete lack of water, the common presence of metallic iron, and the ratios of certain trace chemical elements—make it easy to distinguish them from terrestrial rocks. However, the minerals that make up lunar rocks are (with a few notable exceptions) minerals that are also found on Earth.

Both lunar and terrestrial rocks are made up of minerals. A *mineral is* defined as a solid chemical compound that (1) occurs naturally; (2) has a definite chemical composition that varies either not at all or within a specific range; (3) has a definite ordered arrangement of atoms; and (4) can be mechanically separated from the other minerals in the rock. *Glasses* are solids that may have compositions similar to minerals, but they lack the ordered internal arrangement of atoms.

Minerals have provided the keys to understanding lunar rocks because their compositions and atomic structures reflect the physical and chemical conditions under which the rocks formed. Analyses of lunar minerals, combined with the results of laboratory experiments and studies of terrestrial rocks, have enabled scientists to determine key parameters—temperature, pressure, cooling rate, and the partial pressures of such gases as oxygen, sulfur, and carbon monoxide—that existed during formation of the lunar rocks.

The fact that minerals are mechanically separable from the rest of the rock is also a critical characteristic in considering the economic extraction of resources from lunar materials. For terrestrial resources, mechanical separation without further processing is rarely adequate to concentrate a potential resource to high value (placer gold deposits are a well-known exception). However, such separation is an essential initial step in concentrating many economic materials and, as described later (Chapter 11), mechanical separation could be important in obtaining lunar resources as well.

A mineral may have a specific, virtually unvarying composition (e.g., quartz, SiO_2), or the composition may vary in a regular manner between two or more *endmember* components. Most lunar and terrestrial minerals are of the latter type. An example is *olivine,* a mineral whose composition varies between the compounds Mg_2SiO_4 and Fe_2SiO_4. The intermediate members, produced by the variable substitution of Mg and Fe, are called *solid solutions* and can be represented by the formula $(Mg,Fe)_2SiO_4$, a notation indicating that the elements inside the parentheses may substitute for each other. The *crystal structure* of a mineral reflects the regular and ordered arrangement of atoms within it. Within this structure, positively charged *cations* (generally metals such as Si, Al, Mg, Ti, and Fe) are linked into complicated geometric networks with negatively charged *anions* (chiefly O). Within the crystal structure, each cation is shared (*coordinated*) with several anions. Coordination with four anions produces an arrangement of anions surrounding a cation in *tetrahedral* or *fourfold coordination,* while coordination with six anions is called *octahedral* or *sixfold coordination.* These tetrahedral and octahedral units combine to form

larger structures—chains, sheets, or three-dimensional networks—to build up the mineral. Within these networks, certain ions normally occupy specific sites that are given special designations such as M1 and M2 (for metals) and O1 and O2 (for oxygen atoms). The appendix to this chapter lists compositions of important lunar minerals as oxide weight percents and also, in most cases, as cation proportions. Table A5.1 explains the rock descriptions used to indicate which rock types the mineral analyses are from.

The crystal structures of minerals, and the relations between different ions in the structure, provide important clues not only about the nature of the mineral, but also about its origin. The structures can be established using X-ray diffraction methods, and X-ray crystallography was an important and well-established discipline long before the return of lunar samples.

In defining the structure of a mineral, the key element is the *unit cell.* This is a stackable volume of atoms that defines the structure; the crystal is then built up by the infinite stacking of the unit cell in all directions. The unit cell is a three-dimensional prism normally several Angstrom units (Å) on a side (1 Å = 10^{-10} m). Unit cells are defined by specifying the lengths of their *crystallographic axes* (e.g., *a, b, c*) and the angles between them (α, β, γ). Careful measurement of unit cells is especially important, because unit cell parameters can be indicators of the composition, conditions of formation, and cooling histories of the minerals involved, and therefore of the rocks that contain them.

Lunar rocks are made up of minerals and glasses. Some lunar rocks, called *breccias,* also contain fragments of older rocks. Silicate minerals, composed dominantly of silicon and oxygen, are the most abundant constitutents, making up over 90% by volume of most lunar rocks. The most common silicate minerals are *pyroxene,* $(Ca,Fe,Mg)_2Si_2O_6$; *plagioclase feldspar,* $(Ca,Na)(Al,Si)_4O_8$; and *olivine,* $(Mg,Fe)_2SiO_4$. *Potassium feldspar* ($KAlSi_3O_8$) and the silica (SiO_2) minerals (e.g., *quartz*), although abundant on Earth, are notably rare on the Moon. Minerals containing oxidized iron (Fe^{3+} rather than Fe^{2+}) are absent on the Moon. The most striking aspect of lunar mineralogy, however, is the total lack of minerals that contain water, such as clays, micas, and amphiboles.

Oxide minerals, composed chiefly of metals and oxygen, are next in abundance after silicate minerals. They are particularly concentrated in the mare basalts, and they may make up as much as 20% by volume of these rocks. The most abundant oxide mineral is *ilmenite,* $(Fe,Mg)TiO_3$, a black, opaque mineral that reflects the high TiO_2 contents of many mare basalts. The second most abundant oxide mineral, *spinel,* has a widely varying composition and actually consists of a complex series of solid solutions. Members of this series include: *chromite,* $FeCr_2O_4$; *ulvöspinel,* Fe_2TiO_4; *hercynite,* $FeAl_2O_4$; and *spinel* (*sensu stricto*), $MgAl_2O_4$. Another oxide phase, which is only abundant in titanium-rich lunar basalts, is *armalcolite,* $(Fe,Mg)Ti_2O_5$. As with the silicate minerals, no oxide minerals containing water (e.g., limonite) are native to the Moon. There was some debate about the origin of rare FeOOH found in some samples, but it is now generally believed that this material formed after contamination by terrestrial water (section 5.2.4).

Two additional minerals are noteworthy because, although they occur only in small amounts, they reflect the highly-reducing, low-oxygen environment under which the lunar rocks formed. *Native iron* (*Fe*) is ubiquitous in lunar rocks; this metal commonly contains small amounts of Ni and Co as well. *Troilite,* relatively pure FeS, is a common minor component; it holds most of the sulfur in lunar rocks. The sulfur that is not held in troilite can be mobilized during impact events, producing further sulfurization of native Fe (see below, section 5.3.1).

Rare lunar minerals include *apatite* $[Ca_5(PO_4)_3(OH,F,Cl)]$, which contains only F or Cl and no OH on the Moon, and the associated mineral *whitlockite* $[Ca_3(PO_4)_2]$. Rare sulfides, phosphides, and carbides occur in a variety of lunar rocks. Among these are a few that are largely of meteoritic origin and are very rare indeed: *schreibersite* $[(Fe,Ni)_3P]$, *cohenite* $[(Fe,Ni)_3C]$, and *niningerite* [(Mg,Fe,Mn)S]. In detail, lunar mineralogy becomes quite complex when rare minerals are considered. An excellent summary of known and suspect lunar minerals, compiled soon after the Apollo era, can be found in *Frondel* (1975).

Not all lunar minerals are described in detail in this chapter. It will be seen that the chapter devotes almost as much text to the description of some minor minerals as to the abundant ones. Although this may seem odd from a pragmatic viewpoint, many minor minerals provide unique and important scientific information that the more abundant ones do not. Furthermore, from the point of view of possible resource utilization, abundance is only one factor to be considered. Composition and ease of separation are also important, and even rare minerals can be valuable economic resources. At one extreme of potential economic use, the abundance of plagioclase is so great in some lunar highland rocks and soils that no concentration would be necessary for some proposed uses (e.g., glass manufacture). At the other extreme, native Fe metal is rare but might still be valuable because concen-

TABLE 5.1. Modal proportions (vol.%) of minerals and glasses in soils from the Apollo (A) and Luna (L) sampling sites (90–20 μm fraction, not including fused-soil and rock fragments).

	A-	A-	A-14	A-(H)	A-(M)	A-16	A-(H)	A-(M)	L-16	L-20	L-
Plagioclase	21.4	23.2	31.8	34.1	12.9	69.1	39.3	34.1	14.2	52.1	20.9
Pyroxene	44.9	38.2	31.9	38.0	61.1	8.5	27.7	30.1	57.3	27.0	51.6
Olivine	2.1	5.4	6.7	5.9	5.3	3.9	11.6	0.2	10.0	6.6	17.5
Silica	0.7	1.1	0.7	0.9	-	0.0	0.1	-	0.0	0.5	1.7
Ilmenite	6.5	2.7	1.3	0.4	0.8	0.4	3.7	12.8	1.8	0.0	1.0
Mare Glass	16.0	15.1	2.6	15.9	6.7	0.9	9.0	17.2	5.5	0.9	3.4
Highland Glass	8.3	14.2	25.0	4.8	10.9	17.1	8.5	4.7	11.2	12.8	3.8
Others	-	-	-	-	2.3	-	-	0.7	-	-	
Total	99.9	99.9	100.0	100.0	100.0	99.9	99.9	99.8	100.0	99.9	99.9

Data from *Papike et al.* (1982), *Simon et al.* (1982), *Laul et al.* (1978a), and Papike and Simon (unpublished). (H) Denotes highland. (M) Denotes mare.

tration and collection may be possible. Finally, it is important to emphasize that, although our catalog of lunar mineral types is large, there are almost certainly some minerals on the Moon that are not represented in our currently small and geographically limited sample collection. At the time this book was being prepared, another new mineral was discovered in the Apollo lunar sample collection (*yoshiokaite;* see *Vaniman and Bish,* 1990). More surprises are to be expected as we explore the geochemically distinct and unsampled parts of the Moon (Chapter 10).

5.1. SILICATE MINERALS

The silicate minerals, especially pyroxene, plagioclase feldspar, and olivine, are the most abundant minerals in rocks of the lunar crust and mantle. These silicate minerals, along with other minerals and glasses, make up the various mare basaltic lavas and the more complex suite of highland rocks (melt rocks, breccias, and plutonic rocks) discussed in Chapter 6. Meteoroid impacts over time have broken up and pulverized the lunar bedrock to produce a blanket of powdery *regolith* (a term for fragmental and unconsolidated rock debris) several meters thick, which forms the interface between the Moon and its space environment (see Chapter 7). The regolith therefore provides a useful sample of lunar minerals from a wide range of rocks, and Table 5.1 shows the average volume percentages of minerals in regolith collected at the Apollo and Luna sites (see section 2.1 for locations). The data are for the 90–20 μm size fraction, normalized so that the rock fragments are subtracted from the total. The resulting soil *modes* (composition by volume percent) show the predominance of silicate minerals, especially pyroxene (8.5 to 61.1 vol.%), plagioclase feldspar (12.9 to 69.1 vol.%), and olivine (0.2 to 17.5 vol.%).

Figure 5.1 shows the modal proportions of the same three silicate phases. Several features are apparent. First, olivine is usually subordinate to pyroxene and plagioclase, and its maximum abundance occurs in the Luna 24 regolith. Second, there is a wide range of pyroxene/plagioclase ratios; the Apollo 15 mare soils are richest in pyroxene, and the Apollo 16 soils are richest in plagioclase. Because of these variations, any processing scheme designed to extract specific elements from minerals in the regolith will have to consider the variations in mineral abundances across the Moon.

5.1.1. Pyroxene

Pyroxenes are the most chemically complex of the major silicate phases in lunar rocks. They are also informative recorders of the conditions of formation and the evolutionary history of these rocks. Pyroxenes are compositionally variable solid solutions, and they contain most of the major chemical elements present in the host rocks. Figure 5.2 shows the pyroxene crystal structure, which basically consists of chains built up from linked silicon-oxygen tetrahedra, combined with metal-oxygen octahedra. Oxygen atoms define the corners of all of the polyhedral sites shown, and the cations (Si and other metals) are located inside the polyhedra. The structure is composed of *octahedral layers* containing infinite chains of edge-sharing bands of six-cornered (octahedral) polyhedra (called the M1 sites); the chains run parallel to the crystallographic c-axis. These chains are cross-linked by distorted six-cornered octahedra or larger eight-cornered

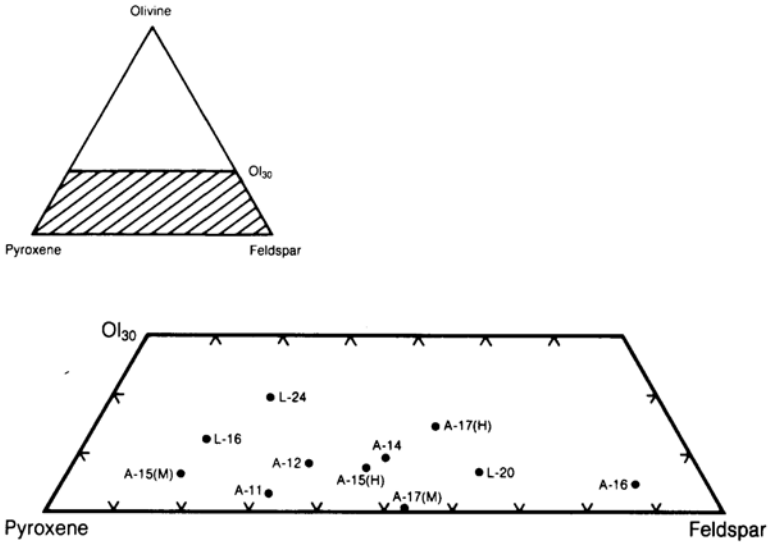

Fig. 5.1. Triangular plot showing modal (vol.%) proportions of pyroxene, olivine, and plagioclase feldspar in the 90-20 μm fractions of typical lunar soils. Soil compositions lie in the trapezoidal area bounded by pyroxene-feldspar-olivine (30%). Sampling sites are indicated, e.g., A-12 is Apollo 12 and L-20 is Luna 20. (H) indicates highland soil while (M) indicates mare soil.

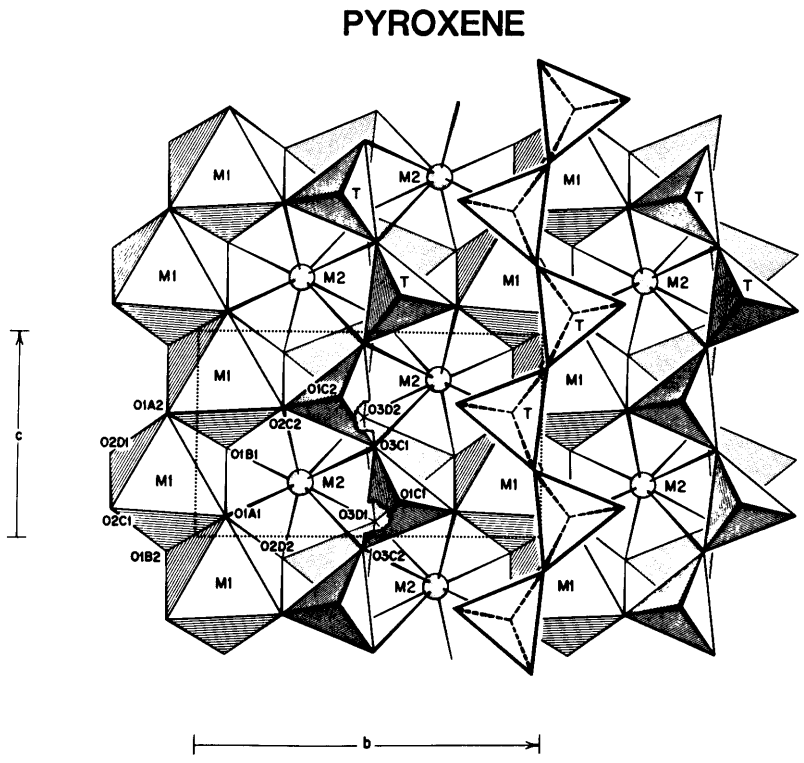

Fig. 5.2. Crystal structure of pyroxene, composed of polyhedra defined by oxygen atoms (O positions). These polyhedra vary in size, from the smaller T (tetrahedral sites) to larger Ml (octahedral sites) and M2 (distorted six to eight coordinated sites). Symbols 01A2, O1B1, etc. represent symmetrically distinct oxygen positions; *b* and *c* show the orientation and dimension of the *unit cell* (dotted outline) along the *b* and c axes of the crystal.

polyhedra (collectively called the M2 sites). These M1-M2 layers are in turn separated from each other by layers composed of infinite chains of silicon-oxygen tetrahedra that also run parallel to the crystallographic c-axis.

In such a structure, the M1 and M2 sites provide a variety of volumes; as a result, pyroxenes can accommodate a wide variety of cations, and these cations reflect much of the chemistry and crystallization history of the rocks in which they occur. Ca, Na, Mn, Mg, and Fe^{2+} are accommodated in the large distorted six- to eight-cornered M2 site; Mn, Fe^{2+}, Mg, Cr^{3+}, Cr^{2+}, Ti^{4+}, Ti^{3+}, and Al occur in the six-cornered M1 site; and Al and Si occupy the small four-cornered tetrahedral site. Potassium is too large to be accommodated in any of the pyroxene crystallographic sites.

Pyroxene chemical analyses are listed in Table A5.2 for mare basalts, in Table A5.3 for highland clast-poor melt rocks and crystalline melt breccias (section 6.4) as well as KREEP rocks (section 6.3.2), and in Table A5.4 for coarse-crystalline highland igneous rocks (anorthosites and Mg-rich rocks; sections 6.3.3 and 6.3.4). These tables show that Fe^{3+} (which would be listed as Fe_2O_3) does not occur in lunar pyroxenes and that sodium is in low abundance.

Figures 5.3, 5.4, and 5.5 illustrate the range of lunar pyroxene compositions, in terms of the end-member components $MgSiO_3$ (*enstatite*), $CaSiO_3$ (*wollastonite*), and $FeSiO_3$ (*ferrosilite*). The diagram shown is a quadrilateral that represents the lower half of the complete triangular plot. This convention is used because compositions more calcium-rich than Ca:Mg = 1:1 or Ca:Fe = 1:1 do not crystallize with the pyroxene structure. The solid dots indicate specific analyses from Tables A5.2, A5.3, and A5.4, while the short dashed lines define the total range of known compositions for those lunar rock types. The long dashed lines in Fig. 5.5, which connect pairs of high-Ca and low-Ca pyroxenes, are called *tie-lines*. These tie-lines connect pairs of pyroxenes that formed in slowly-cooled lunar rocks, in which the component minerals were close to thermal and chemical equilibrium. Much of the chemical variability of pyroxenes is illustrated on pyroxene quadrilateral plots discussed above. More detailed discussion of the correlation between pyroxene

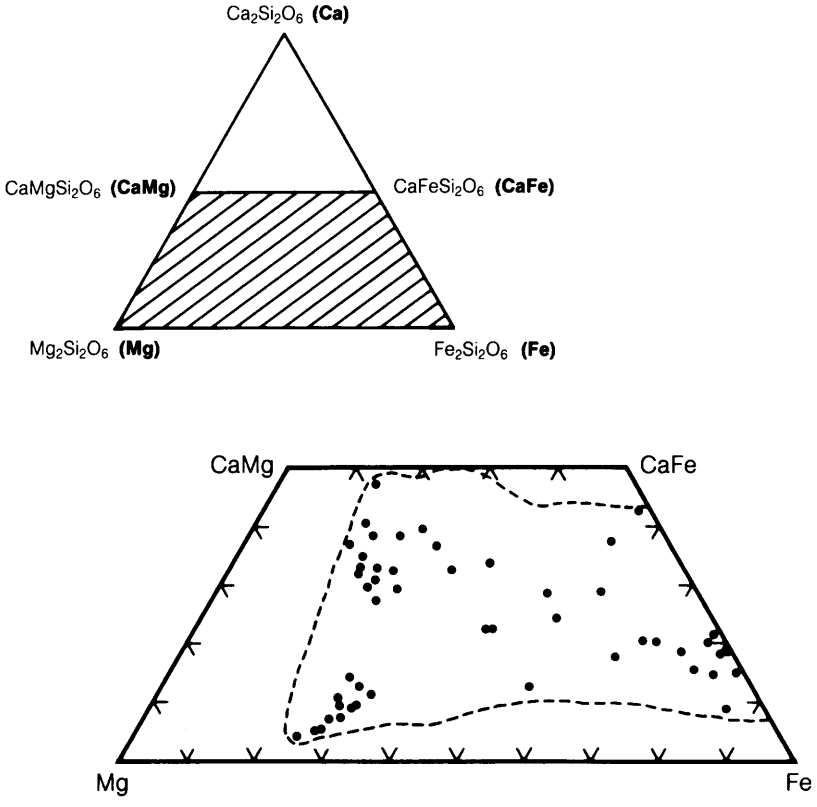

Fig. 5.3. Compositions of pyroxenes from mare basalts, shown in the "pyroxene quadrilateral" part of the triangle $Ca_2Si_2O_6$ (Ca) — $Mg_2Si_2O_6$ (Mg) — $Fe_2Si_2O_6$ (Fe). Inset diagram shows the pyroxene mineral compositions corresponding to the corners of the "quadrilateral" (shaded area) that includes all possible pyroxene Ca:Mg:Fe compositions. Dots represent analyses in Table A5.2. Dashed line encloses the total range of mare basalt pyroxene

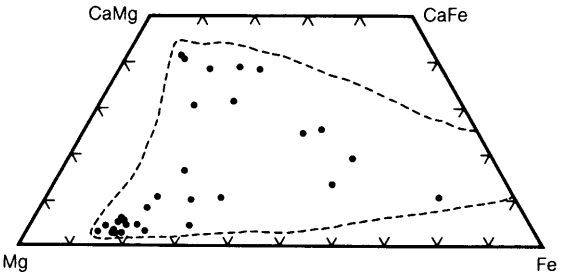

Fig. 5.4. Compositions of pyroxenes from highland breccias, clast-poor melt rocks, and KREEP rocks, shown in the "pyroxene quadrilateral." Dots represent analyses in Table A5.3. Dashed line encloses the total range of pyroxene compositions reported in the literature for these highland rock types.

compositions, rock types, and cooling rates can be found in *Papike et al.* (1976) and *BVSP* (1981) for mare basalts, and in *Vaniman and Papike* (1980) for lunar highland melt rocks.

Although the major elements that define the quadrilateral plot (Ca, Mg, and Fe) show the important variations discussed above, the other, less abundant elements also show important trends. These other elements include Al, Ti, Cr, and Na. Sodium usually occurs in low concentrations in lunar pyroxenes because of its generally low abundance in lunar rocks. However, the contents of Al, Ti, and Cr in lunar pyroxenes can be significant (see Tables A5.2, A5.3, and A5.4). The very low abundance (partial pressure) of oxygen gas during the crystallization of lunar rocks has resulted in reduced valence states for some Ti atoms (Ti^{3+} rather than Ti^{4+}) and Cr atoms (Cr^{2+} rather than Cr^{3+}). These

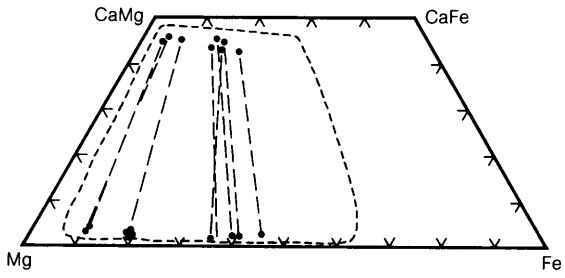

Fig. 5.5. Compositions of pyroxenes from highland coarse-crystalline igneous rocks (ferroan anorthosites and Mg-rich rocks), shown in the "pyroxene quadrilateral." Dots represent analyses in Table A5.4. Dashed line encloses the total range of pyroxene compositions reported in the literature for these highland rock types. Straight dashed lines connect compositions of high-Ca and low-Ca pyroxenes that coexist in the same rock.

lower valence states are very rare in Ti and Cr of terrestrial pyroxenes. For example, *Sung et al.* (1974) suggest that as much as 30–40% of the Ti in Apollo 17 mare basalts occurs in the trivalent state and that most of this reduced Ti is in pyroxenes.

Lunar pyroxenes also show substantial *subsolidus* reactions (i.e., recrystallization and other changes that take place below melting temperatures). Considerable work has been done to interpret the resulting features. It was discovered soon after the return of the Apollo 11 samples that submicroscopic, subsolidus separation (*exsolution*) of two distinct pyroxenes [*augite* (high-Ca clinopyroxene) and *pigeonite* (low-Ca clinopyroxene)] had taken place within originally uniform pyroxene crystals (e.g., *Ross et al.,* 1970). This process produced distinctive microscopic and submicroscopic *exsolution lamellae,* i.e., thin layers of pigeonite in augite, or vice versa. *Papike et al.* (1971) attempted to relate these exsolution features to the relative cooling histories of mare basalts. They pointed out that certain parameters of the pyroxene crystal unit cell (the length b and the angle β) could be used to estimate the compositions of the intergrown augite and pigeonite. They also suggested that Δ/β (β pigeonite—β augite) could be used to indicate the degree of subsolidus exsolution and thus the relative annealing temperatures of the exsolved pyroxenes. *Takeda et al.* (1975) summarized similar exsolution data for pyroxene grains from Apollo 12 and 15 basalts. They compared the relative cooling rates (determined from exsolution studies) with absolute cooling rates determined from experimental studies. *Ross et al.* (1973) experimentally determined the 1-atmosphere augite-pigeonite stability relations for pyroxene grains from mare basalt 12021. *Grove* (1982) used exsolution lamellae in lunar clinopyroxenes as cooling rate indicators, and his results were calibrated experimentally. These studies all indicate that the cooling and subsolidus equilibration of igneous and metamorphic pyroxenes is a slow process; estimated cooling rates range from 1.5° to 0.2°C/hr for lava flows 6 m thick (e.g., model cooling rates for Apollo 15 mare lavas; *Takeda et al.,* 1975).

Shock lamellae can be produced in pyroxenes by the shock waves due to meteoroid impact. However, these features are relatively rare, and they are much less well characterized than the analogous shock lamellae in plagioclase (*Schall and Hörz,* 1977).

5.1.2. Plagioclase Feldspar

The silicate mineral *feldspar* has a framework structure of three-dimensionally linked SiO_4 and AlO_4 tetrahedra (Fig. 5.6). The ratio Si:Al varies between 3:1 and 1:1. Ordering (i.e., nonrandom

placement) of Si and Al in specific tetrahedral sites can lead to complexities such as discontinuities in the crystal structure. Within this three-dimensional framework of tetrahedra containing Si and Al, much larger volumes with 8 to 12 corners occur that accommodate large cations (Ca, Na, K, Fe, Mg, Ba).

Aside from rare potassium- and barium-enriched feldspars (discussed below in section 5.1.5), most lunar feldspars belong to the plagioclase series, which consists of solid crystalline solutions between albite ($NaAlSi_3O_8$) and anorthite ($CaAl_2Si_2O_8$). Because of the alkali-depleted nature of the Moon (Chapter 8), lunar plagioclases are also depleted in Na (the albite component) relative to terrestrial plagioclases. Tables A5.5, A5.6, and A5.7 list lunar plagioclase compositions for mare basalts, for clast-poor melt rocks and crystalline melt breccias (section 6.4), as well as KREEP rocks (section 6.3.2),

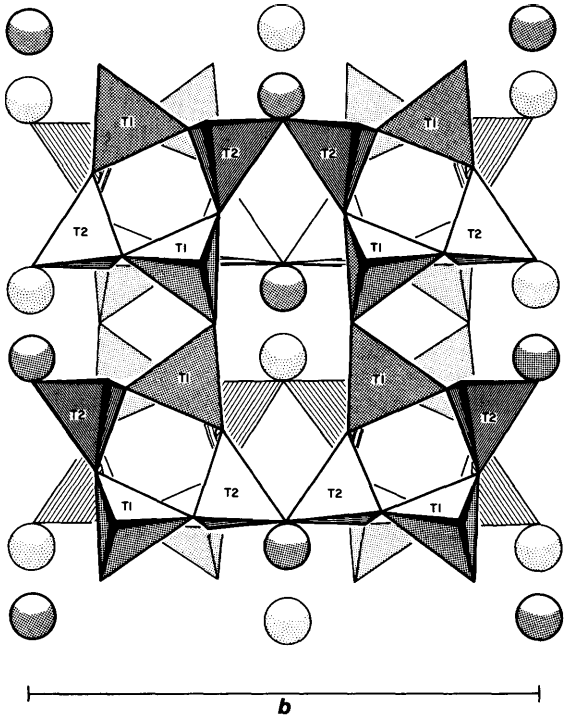

Fig. 5.6. Crystal structure of feldspar, which is composed of tetrahedra (T 1, T2) with oxygen atoms at the apices, combined with larger polyhedra. This structure forms several varieties of feldspar, depending on the chemical composition of the larger cations (shown as spheres). Spheres represent Ca atoms in anorthite, Na in albite, K in potassium feldspar, and Ba in celsian. The ratio of Al:Si within the tetrahedral sites varies from 1:1 when the large cations (spheres) have divalent charge (e.g., Ca) to 1:3 when the large spheres are monovalent (e.g., Na). T1 and T2 are two symmetrically distinct tetrahedral sites in high-temperature feldspar, in which the placement of Si and Al within the tetrahedral sites is random (*disordered*); *b is* the unit cell dimension along the *b* axis of the crystal.

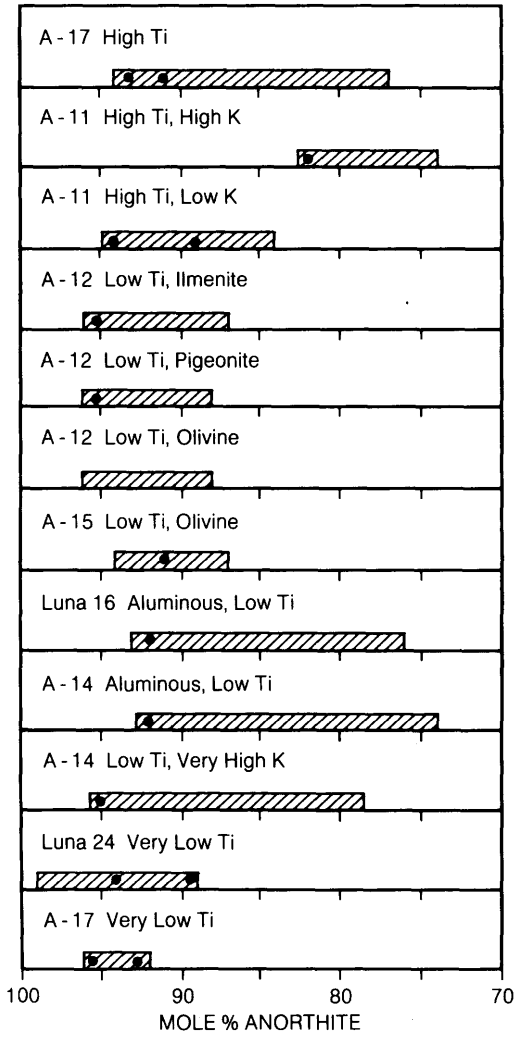

Fig. 5.7. Range of compositional variation in plagioclase feldspars from lunar mare basalts, shown as mol.% anorthite ($CaAl_2Si_2O_8$) in the albite ($NaAlSi_3O_8$)-anorthite ($CaAl_2Si_2O_8$) solid solution. Dots represent analyses in Table A5.5. Patterned areas represent the ranges for all mare basalt plagioclases reported in the literature. Mare rock types are described in Table A5.1 and in section 6.1.

and for coarse-crystalline highland igneous rocks (anorthosites and Mg-rich rocks; sections 6.3.3 and 6.3.4). The maximum chemical variation involves solid solution between albite and anorthite, a variability that can also be described as the coupled substitution between NaSi and CaAl, in which the CaAl component represents anorthite. Figure 5.7 illustrates the compositional range of this substitution in plagioclase feldspars from mare basalts. The Ca abundance in the plagioclase (mole% anorthite) correlates positively with the Ca/Na ratio in the host basalts (e.g., *Papike et al.,* 1976; *BVSP,* 1981).

Plagioclases from highland impact melts, from breccias, and from KREEP rocks such as "IKFM" (Fig. 5.8) have more Na-rich compositions (i.e., less anorthite) along with their enrichment in the geochemically similar elements potassium (K), rare earth elements (REE), and phosphorus (P), the association of minor elements referred to as KREEP (see sections 2.4 and 6.3.2). Plagioclases from coarse-crystalline igneous rocks have more restricted compositions (Fig. 5.9); however, there is a positive correlation between the alkali content of the host rock and the plagioclase (note the Na-rich plagioclase from a particular rock type, alkali anorthosite, which is itself also Na-rich).

An interesting aspect of mare basalt plagioclases concerns the problem of where the observed Fe and Mg fit into the crystal structure. *Smith* (1974), in reviewing this problem, pointed out that (1) the Fe content in mare basalt plagioclase is higher than that in plagioclase from lunar highland rocks and (2) the Fe content is positively correlated with albite (NaSi) content. *Weill et al.* (1971) noted peculiarities in lunar plagioclase cation ratios, and suggested that they might result from substitution of the theoretical "Schwantke molecule," $Ca_{0.5}\square_{0.5}AlSi_3O_8$ where $\square$ = a vacant site normally occupied by a large cation (Na or Ca). *Wenk and Wilde* (1973) reviewed all available chemical data to accurately define the chemical components in lunar plagioclase. They concluded that (1) the deficiency of Al+Si in the tetrahedral sites (up to 0.06 atoms per eight-oxygen formula unit) is largely compensated by Fe and Mg substitution in the same tetrahedral sites; (2) the Ca/Na ratio in the octahedral large-cation sites increases correspondingly to maintain charge balance; and (3) the vacancy-coupled substitution of $Ca+\square$ (the "Schwantke molecule") for 2Na probably also occurs but is much less significant. *Wenk and Wilde* (1973) also made the interesting observation that the apparent number of vacancies increases with increasing Fe+Mg content. They suggested that the progressive substitution of the larger Fe and Mg ions for the smaller Si in the tetrahedral sites decreases the volume of interstitial space available for the Iarge Ca and Na atoms. *Longhi et al.* (1976) identified the same Fe and Mg components by using a slightly

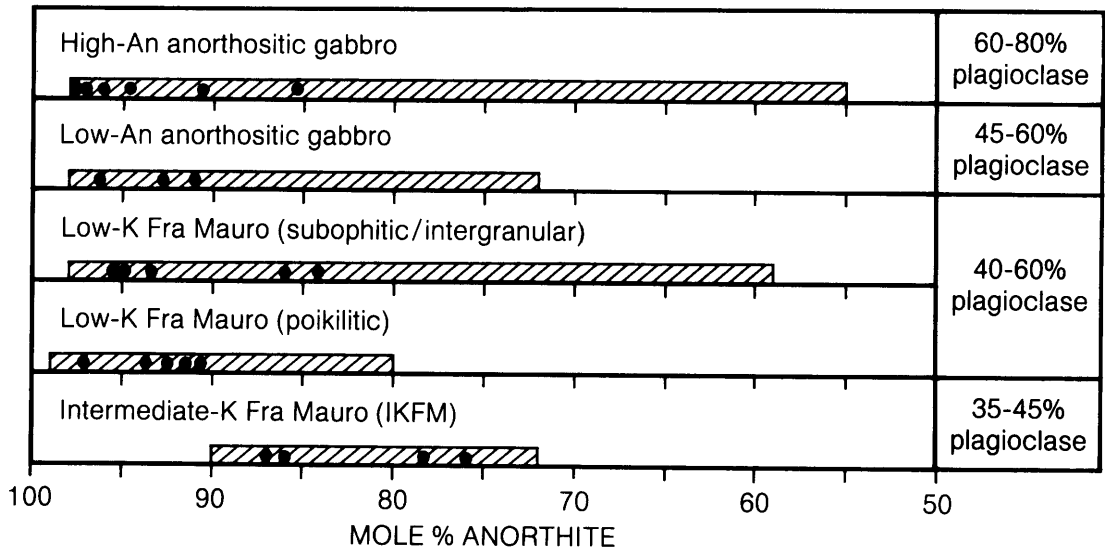

Fig. 5.8. Range of compositional variation in plagioclase feldspars from lunar highland breccias, clast-poor melt rocks, and KREEP rocks, shown as mol.% anorthite ($CaAl_2Si_2O_8$) in the albite ($NaAlSi_3O_8$)-anorthite ($CaAl_2Si_2O_8$) solid solution. Dots represent analyses in Table A5.6. Patterned areas represent the ranges for plagioclases reported in the literature for these highland rock types. The rock types listed use the nomenclature of *Vaniman and Papike* (1980); those at the top generally have more plagioclase than those at the bottom.

different approach. *Schurmann and Hafner* (1972) and *Hafner et al.* (1973), using Mössbauer and electron spin resonance techniques, showed that most of the iron in lunar plagioclase is present as Fe^{2+}. These studies all indicate that divalent Mg and Fe are important components in the tetrahedral structural sites in lunar plagioclase.

Plagioclase, like pyroxene, may undergo subsolidus reactions. *Smith and Steele* (1974) suggested that the grains of pyroxene and silica minerals observed as inclusions inside the plagioclase crystals of slowly-cooled highland plutonic rocks (e.g., anorthosites) may have formed by solid-state exsolution of the necessary elements (Ca, Fe, Mg, Si, etc.) from the original plagioclase grain. The original plagioclase, when first crystallized, would have had high contents of Fe and Mg in its tetrahedral sites, perhaps comparable to the Fe and Mg contents of plagioclases in mare basalts. *Smith and Steele* (1974) proposed that, with falling temperature, the plagioclase component $CaSi_3(Mg,Fe^{2+})O_8$ broke down into pyroxene, $Ca(Mg,Fe^{2+})Si_2O_6$, and a silica mineral (SiO_2). However, this interesting suggestion was not supported by the subsequent results of *Dixon and Papike* (1975), who found that the volume of SiO_2 inclusions in plagioclases from anorthosites is much too low relative to the pyroxene inclusions for the two minerals to have formed by such a reaction. These authors preferred the explanation that the pyroxene inclusions and the plagioclase precipitated together from the original melt and later reacted during thermal annealing according to the exchange reaction: Ca(pyroxene) + Fe(plagioclase) = Fe(pyroxene) + Ca(plagioclase). As a result, the plagioclase became more Ca-rich and the pyroxene more Fe-rich with time.

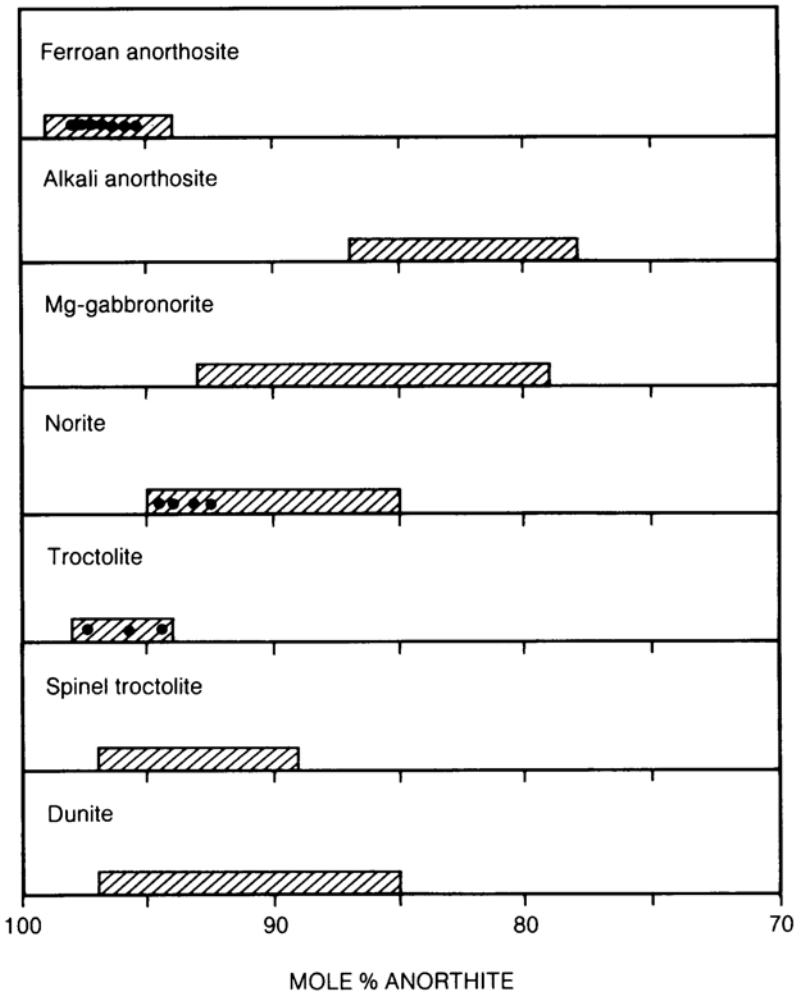

Fig. 5.9. Range of compositional variation in plagioclase feldspars from highland coarse-crystalline igneous rocks (ferroan anothosites, alkali anorthosites, and five types of Mg-rich rocks), shown as mol.% anorthite ($CaAl_2Si_2O_8$) in the albite ($NaAlSi_3O_8$)-anorthite ($CaAl_2Si_2O_8$) solid solution. Dots represent analyses in Table A5.7. Patterned areas represent the ranges for plagioclases from all such rocks reported in the literature. See section 6.3 for description of rock types.

5.1.3. Olivine

The crystal structure of olivine, $(Mg,Fe)_2SiO_4$, consists of serrated chains formed of edge-sharing octahedra. These chains run parallel to the crystallographic c-axis (Fig. 5.10). The octahedral chains are cross-linked by isolated SiO_4 tetrahedra. The major cations in the octahedral sites, Fe^{2+} and Mg, are distributed with a high degree of disorder (randomness) over both the M1 and M2 octahedral sites. However, the small amounts of Ca that may occur in olivine occupy only the M2 site (see *Papike and Cameron,* 1976, for a review).

Representative olivine analyses are listed in Tables A5.8 for mare basalts, A5.9 for highland clast-poor melt rocks and crystalline melt breccias (section 6.4), and A5.10 for coarse-crystalline high-land igneous rocks (anorthosites and Mg-rich rocks; sections 6.3.3 and 6.3.4). The major compositional variation within olivines is caused by exchange of Fe for Mg; this exchange, and the resulting variations in composition, are represented by the ratio Fe/(Fe + Mg). The Fe end member, Fe_2SiO_4, is *fayalite,* and the Mg end member, Mg_2SiO_4, is *forsterite.* Figures 5.11, 5.12, and 5.13 illustrate the variations between forsterite and fayalite within olivines from mare rocks, highland impact melts or breccias, and highland coarse-crystalline igneous rocks.

The most magnesian mare basalt olivine grains contain only 20% fayalite (Fa), represented by the notation Fa_{20} (i.e., 80 mol.% forsterite and 20% fayalite in the solid solution series forsterite—fayalite, Mg_2SiO_4—Fe_2SiO_4). Most mare basalt olivines have compositions in the range Fa_{20}-Fa_{70} (Fig. 5.11).

Very few olivines in mare basalts have compositions in the range Fa_{70}-Fa_{100}; however, a number of mare basalts do contain very Fe-rich olivine (Fa_{90}-Fa_{100}). These olivines are part of an equilibrium three-phase assemblage (Ca,Fe pyroxene — Fe olivine — silica) that crystallized stably from the late-stage iron-enriched portions of mare basalt melts. Some mare basalts, which cooled quickly during the late stages of crystallization, contain instead either an Fe-rich pyroxene that crystallized metastably relative to the normal three-phase assemblage or a related silicate mineral, pyroxferroite (see section 5.1.5). The formation of extremely Fe-rich pyroxene violates a so-called "forbidden region" at the Fe-apex of the "pyroxene quadrilateral" (the *Fe* corner of Figs. 5.3–5.5; see *Lindsley and Munoz,* 1969, for details).

Other significant elements in lunar olivines are Ca, Mn, Cr, and Al. Calcium varies directly with the Fe content, and it may be an indicator of the cooling rate (*Smith,* 1974). The experimental data of *Donaldson et al.* (1975) support this contention. Olivines in mare basalts are significantly enriched in Cr relative to olivines in terrestrial basalts. Cr_2O_3 values, which are commonly below detection limits (~0.1 wt.%) in terrestrial olivines (*Smith,* 1974), range up to 0.6 wt.% in lunar olivines. Much or all of this Cr may be in the reduced Cr^{2+} valence state, and *Haggerty et al.* (1970) identified significant Cr^{2+} in lunar olivine using optical absorption techniques. Cr^{2+} is more readily accommodated into the olivine structure than is Cr^{3+}, which is the normal valence state for Cr in terrestrial olivines. The presence of Cr^{2+} is another result of the low oxygen partial pressures that

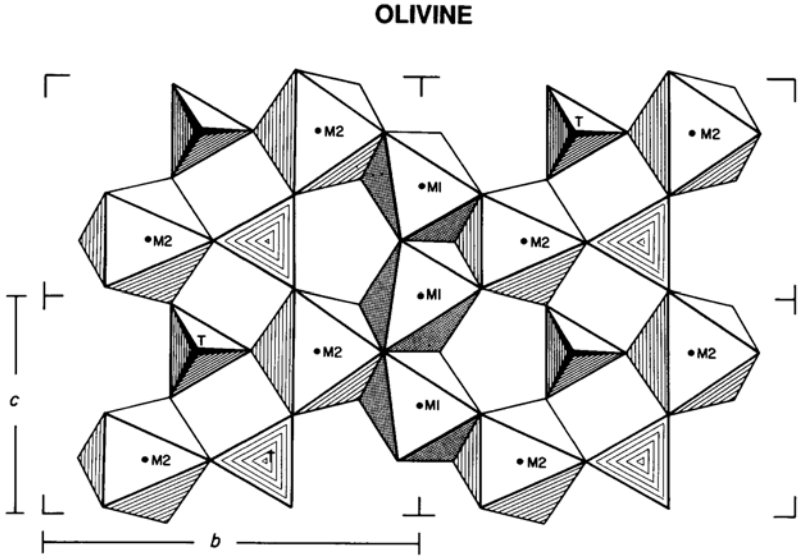

Fig. 5.10. Crystal structure of olivine, which is composed of tetrahedra (T) and octahedra (Ml, M2) defined by oxygen atoms. Small cations (almost entirely Si^{4+}) are located within the tetrahedra; larger cations (mostly Fe^{2+} and Mg^{2+}) are located within the two symmetrically distinct octahedral sites (M1 and M2). The bars *b* and *c* indicate the orientation and dimension of the unit cell along the *b* and *c* axes of the crystal.

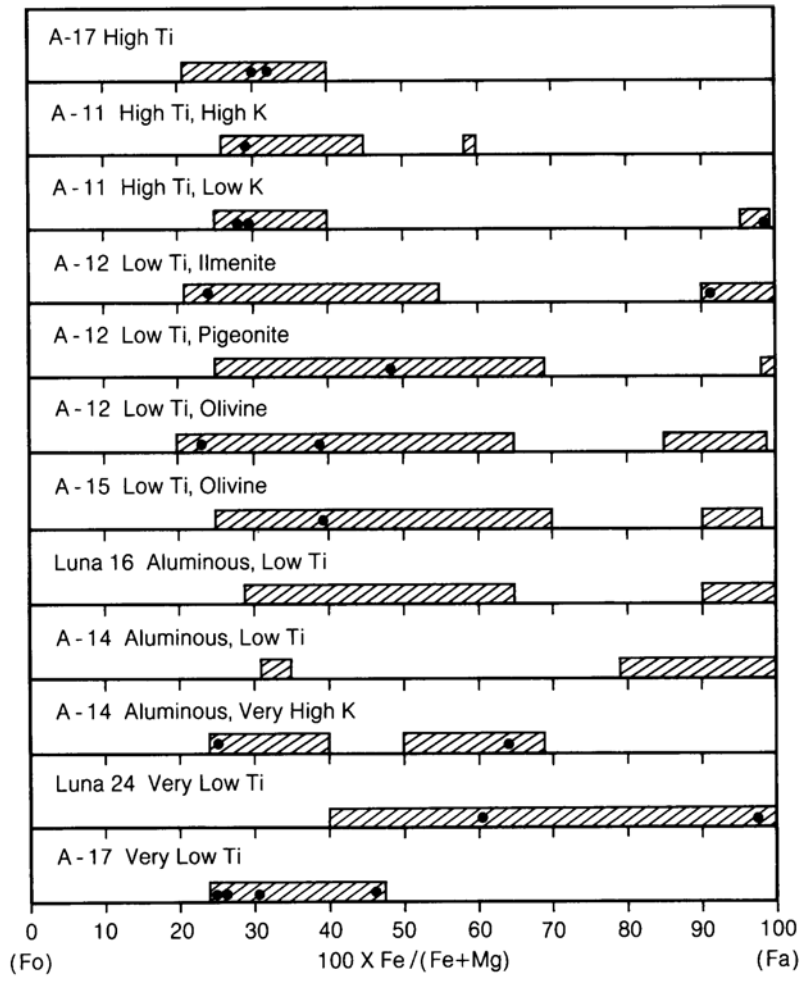

Fig. 5.11. Variation of the atomic ratio Fe/(Fe + Mg) in olivines from lunar mare basalts. Compositions lie between the end members forsterite (Fo), Mg_2SiO_4, at 0, and fayalite (Fa), $Fe^{2+}{}_2SiO_4$, at 100. Dots represent analyses in Table A5.8. Patterned areas represent the entire compositional range for mare basalt olivines reported in the literature.

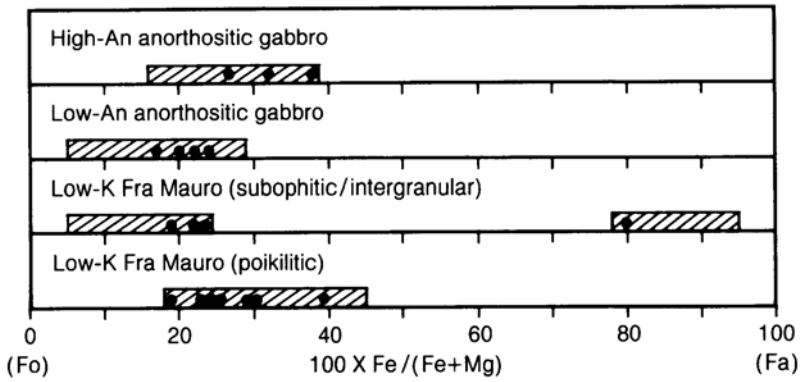

Fig. 5.12. Variation of the atomic ratio Fe/(Fe + Mg) in olivines from lunar highland clast-poor melt rocks. Compositions lie between the end members forsterite (Fo), Mg_2SiO_4, and fayalite (Fa), $Fe^{2+}{}_2SiO_4$. Dots represent analyses in Table A5.9. Patterned areas represent the entire compositional range for highland melt rock olivines reported in the literature.

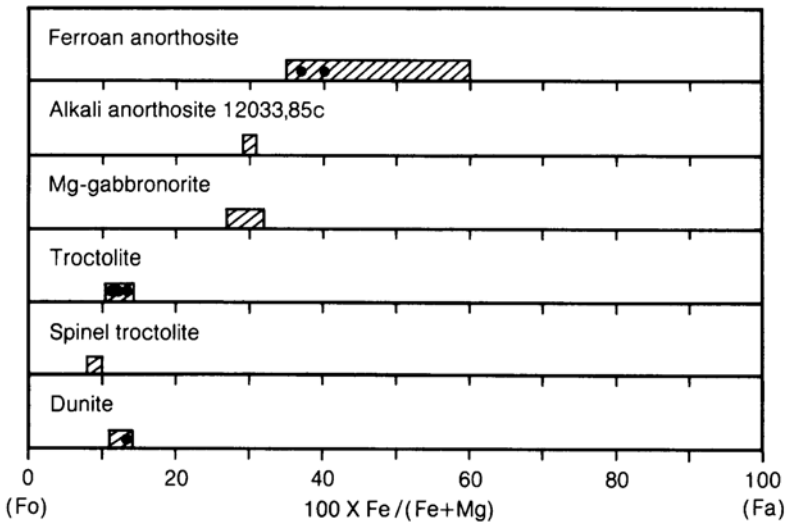

Fig. 5.13. Variation of the atomic ratio Fe/(Fe + Mg) in olivines from lunar highland coarse-crystalline igneous rocks (anorthosites and Mg-rich rocks). Compositions lie between forsterite (Fo), Mg_2SiO_4, and fayalite (Fa), $Fe^{2+}{}_2SiO_4$. Dots represent analyses in Table A5.10. Patterned areas represent the entire compositional range for lunar plutonic rock olivines

existed during mare basalt crystallization. Similarly, Cr^{2+} is much more abundant in lunar pyroxenes than in terrestrial pyroxenes (*BVSP*, 1981).

5.1.4. Silica Minerals: Quartz, Cristobalite, and Tridymite

Silica minerals include several structurally different minerals, all of which have the simple formula SiO_2. These minerals are generally rare on the Moon. This rarity is one of the major mineralogic differences between the Moon and the Earth, where silica minerals are abundant in such common rocks as granite, sandstone, and chert. The relative absence of silica minerals on the Moon is a result of several factors. For one thing, the Moon has apparently not evolved chemically beyond the formation of a low-silica, high-alumina anorthositic crust (see section 2.4), so that high-silica granitic rocks are rare. For another, the Moon lacks hydrous and hydrothermal systems like those that can crystallize silica on Earth.

Despite their rarity on the Moon, the silica minerals are nevertheless important in classifying and unraveling the origin of some lunar rocks (section 6.3). Furthermore, lunar crustal rocks that contain silica minerals may be more abundant than their meager representation among the returned Apollo and Luna samples suggests. The silica minerals tend to concentrate along with chemical elements that are also rare on the Moon, such as the KREEP elements (sections 6.3.2 and 6.3.5). For these reasons, the lunar silica minerals deserve greater consideration than their rarity would otherwise warrant.

The silica minerals found on the Moon are *cristobalite, quartz,* and *tridymite.* In spite of the intense impact cratering of the Moon, it is interesting that the high-pressure polymorphs of SiO_2, *coesite* and *stishovite,* which are known from young terrestrial impact craters, have not been found on the Moon. Explanations for their absence include the rarity of silica grains in the original target rocks and probable volatilization of silica during impact events in the high vacuum at the lunar surface.

The crystal structures of the silica minerals are distinctly different, but they all consist of frameworks of SiO_4 tetrahedra in which each tetrahedral corner is shared with another tetrahedron. A comparison of silica mineral structures, along with structure diagrams, can be found in *Papike and Cameron* (1976). All of the silica mineral structures contain little or no room for cations larger than Si^{4+}, hence the relatively pure SiO_2 composition of these minerals. The structures become more open in going from quartz to cristobalite to tridymite, and the general abundance of impurities increases accordingly.

Quartz occurs in a few granite-like (*felsite*) clasts (e.g., sample 12013, section 6.3.5) as needle-shaped crystals that probably represent structural transformation (*inversion*) of original tridymite (*Quick et al.,* 1981a). Some tridymite is preserved in these felsite clasts. The other rock type in which quartz is abundant is the rare fragments of coarse-grained lunar granites. The largest lunar granite clast yet found, from Apollo 14 breccia 14321, weighs 1.8 g and contains 40 vol.% quartz (*Warren et al.,* 1983). A smaller granite clast from sample 14303 was

estimated to have 23 vol.% quartz (*Warren et al.,* 1983). Based on their isotopic work on the large clast, *Shih et al.* (1985) suggested that the sample crystallized in a deep-seated plutonic environment about 4.1 b.y. ago, and it therefore did not form during the earlier crystallization of the magma ocean about 4.5 to 4.3 b.y. ago (section 2.4). Consistent with the general absence of hydrous minerals on the Moon, the lunar granites do not contain mica or amphibole, as would granites on Earth.

The most common silica mineral in mare basalt lavas is not quartz but cristobalite, which can constitute up to 5 vol.% of some basalts. This situation contrasts with the general absence of all silica minerals in terrestrial basalts. Lunar cristobalite commonly has twinning and curved fractures, indicating that it has inverted from a high-temperature crystal structure to a low-temperature one during cooling of the lavas (*Dence et al.,* 1970; *Champness et al.,* 1971). Other mare basalts contain crystals of the silica mineral tridymite that have incompletely inverted to cristobalite, producing rocks that contain both tridymite and cristobalite. In a study of Apollo 12 basalts, *Sippel* (1971) found that the coarser-grained samples contained tridymite and cristobalite, while the finer-grained basalts contained cristobalite and quartz. Unfortunately, these mineral pairs are stable over fairly large temperature ranges and can also form metastably, outside of their equilibrium stability fields, so they are not useful for inferring the temperatures of lava crystallization.

Cristobalite tends to occur as irregular grains wedged between other crystals, while tridymite forms lathlike crystals. *Klein et al.* (1971) observed tridymite laths enclosed by pyroxene and plagioclase and suggested that tridymite was an early crystallizing phase.

Table A5.11 a lists some representative analyses of cristobalite (analyses 13-15) and tridymite (analysis 16). Although the lunar silica minerals are nearly pure SiO_2, they contain such typical contaminants as Al_2O_3, TiO_2, CaO, FeO, and Na_2O.

In contrast to lunar basalts, terrestrial basalts typically lack any evidence for crystallization of silica minerals from the melt. In those cases where silica minerals are observed in terrestrial basalts, they generally occur as rounded or embayed crystals of quartz that have been partly absorbed by the surrounding basaltic magma. These textures are ambiguous, and it is difficult to decide whether this quartz formed directly from the basaltic magma or whether it represents accidental inclusions picked up from other rocks through which the magma flowed. This is not the case in lunar mare basalts, where silica minerals have clearly crystallized from the magma.

5.1.5. Other Silicate Minerals

Several other silicate minerals occur only rarely in lunar rocks. Some of these (e.g., *tranquillityite* and *pyroxferroite*) are unique to the Moon. Others, like *zircon* and *potassium feldspar* (*K feldspar*), are rare on the Moon but common on Earth. These minerals occur in lunar basalts in small patches of high-silica residual melt formed during the last stages of crystallization of the mare lavas, and they are often accompanied by a silica mineral such as cristobalite. The same minerals also occur in unusual high-silica ("KREEPy") highland rocks, which may have formed from a similar residual melt produced during large-scale crystallization of ancient highland igneous rocks (see sections 2.4.3 and 2.4.4).

Despite the rarity of these minerals on the Moon, they are important because (1) they act as recorders of the last stages of basalt crystallization and (2) they are commonly enriched in rare earth elements (REE) and in radioactive elements, some of which are useful in dating the samples.

As the basalt bedrock is gradually pulverized by meteoroid impacts, these rare silicate minerals are released into the lunar soil. These minerals are fine-grained to begin with and, in the case of K-feldspar and cristobalite, are easily broken. As a result, the rare silicate minerals tend to become concentrated in the finer soil fractions. In mare terranes, the finest soil fractions have different compositions from the bulk soils; they are enriched in REE, in radioactive elements, and in Al, K, and Na contained in feldspars. This variation of regolith composition with grain size is discussed in more detail in section 7.5.3.

Tranquillityite. *Tranquillityite* [$Fe_8(Y+Zr)_2Ti_3Si_3O_{24}$] is named for the Apollo 11 landing site in Mare Tranquillitatis. This mineral was first described in Apollo 11 samples as "new mineral A" (*Ramdohr and El Goresy,* 1970). Chemical analyses of tranquillityite, together with the structural formula, X-ray data, and density (4.7 g/cm^3) were first published by *Lovering et al.* (1971). Some of their analyses of tranquillityite from Apollo 11 and Apollo 12 basalts are listed in Table A5.11b.

Tranquillityite characteristically occurs in lunar mare basalts, where it forms small (<100-μm) lath-shaped crystals associated with other rare minerals such as pyroxferroite and apatite in small pockets where the last minerals to crystallize are clustered. Tranquillityite is semiopaque; it has a nonpleochroic (constant in all crystal directions) deep red color in transmitted light (due to its high TiO_2 content) and a gray to dark gray color in reflected light. *Lovering et al.* (1971) determined crystallographic dimensions for what appeared to be well-crystallized tranquillityite. However, further X-ray diffraction studies

showed that some tranquillityites tend to be *metamict,* a state in which the original crystallographic order is partly or completely destroyed by radiation produced by decay of the relatively large amounts of U (~40–1000 µg/g) that they contain (*Gatehouse et al.,* 1977; *Lovering and Wark,* 1971). *Gatehouse et al.* (1977) were able to anneal this damage and recrystallize lunar tranquillityite grains by heating them to 800°C. Those heated in air formed a face-centered cubic crystal structure similar to fluorite (CaF_2), with an edge dimension of 4.85 Å. Grains reconstituted in vacuum formed with a slight rhombohedral distortion from cubic symmetry (edge dimension = 4.743 Å). Heating above 900°C caused the tranquillityite structure to break down (*Gatehouse et al.,* 1977). This result is consistent with the observation that tranquillityite is not found in metamorphosed (highly heated) basalt clasts (*Lovering and Wark,* 1975), in which it appears to have broken down, in part, to zircon.

Zircon. *Zircon,* ideally $ZrSiO_4$, is important not only because it tends to concentrate REE, but also because it is useful for age-dating the rocks in which it formed. Zircon is a refractory mineral that resists remelting and often incorporates Hf, Th, and U into its crystal structure, making it well-suited for U-Pb dating (e.g., *Compston et al.,* 1984). Zircons also have a high retentivity for *fission tracks,* microscopic linear zones of damage produced by the recoil of U atoms that decay in the crystal by spontaneous fission. Zircon is especially suitable for age determinations based on the density of such tracks within the crystal (*Braddy et al.,* 1975).

The main source of lunar zircons appears to be the rare, high-silica granitic rocks (*Lovering and Wark,* 1975). For example, rock 12013, a KREEPy granitic rock, contains 2200 µg/g Zr (*LSPET,* 1970), which corresponds to approximately 0.1% zircon (*Drake et al.,* 1970). In this sample, zircons range from 4 to 80 µm in size. *Taylor et al.* (1980) found 0.6 vol.% zircon in a fragment of a similar rock type (quartz monzodiorite) from melt breccia 15405, and *Keil et al.* (1971) reported zircon in a "12013-like lithic fragment." *Gay et al.* (1972) found zircon in an anorthosite clast in breccia 14321. Representative analyses of these zircons are listed in Table A5.11a. Optical and physical properties of lunar zircons are described in *Braddy et al.* (1975).

Because of the rarity of lunar granitic rocks and the durability of zircons, most zircons are found as isolated grains in soils and breccias. Zircons can also be found in metamorphosed basalt clasts, where they possibly form by the breakdown of original tranquillityite (*Lovering and Wark,* 1975). For their fission track study, *Braddy et al.* (1975) separated zircons from the "sawdust" left after breccia 14321 was cut for other studies. From 20 g of this sawdust they recovered 93 zircons, 70 of which were >100 µm in diameter. The zircons varied in U content from 15 to 400 µg/g, with a median content of 50 µg/g. *Braddy et al.* (1975), using methods of thermal annealing followed by etching, showed that zircons are excellent recorders of fission tracks.

Although they are rare, small, and difficult to work with, zircons are very important in dating lunar samples, especially very old (>4 b.y.) highland rocks. Uranium-lead dating of lunar zircons, using ion microprobe analysis techniques (*Compston et al.,* 1984), has shown that zircons can survive the intense shock and heating of meteorite bombardment without serious disruption of their U-Pb systematics; they can therefore preserve the original rock ages. *Compston et al.* (1984) analyzed four zircons from a *clast* (a fragment of an older rock) within breccia 73217 and successfully determined a formation age for the clast of about 4356 m.y., a measurement that would otherwise not have been obtained.

Pyroxferroite. Although *pyroxferroite* had been synthesized in the laboratory (*Lindsley,* 1967), the mineral was not observed in natural rocks until the return of the Apollo 11 samples. Pyroxferroite is an iron-rich *pyroxenoid* (*a* mineral structurally similar to pyroxene), whose formula is approximately $Ca_{1/7}Fe_{6/7}SiO_3$, with limited substitution of Mg for Fe. Some representative analyses are listed in Table A5.11a. *Burnham* (1971) determined that the pyroxferroite structure is based on a repeating pattern of seven SiO_4 tetrahedra; this structure is the same as that of a rare terrestrial mineral, *pyroxmangite*. *Chao et al.* (1970) published some of the first X-ray, physical, and chemical data for pyroxferroite.

Pyroxferroite is found in mare basalts and Fe-rich basalts (*ferrobasalts* such as those at the Luna 24 site). As these rocks cooled, the compositions of the crystallizing pyroxenes changed, moving toward the CaFe-Fe side of the pyroxene quadrilateral (Fig. 5.3), and approaching the pyroxferroite composition. However, experimental studies by *Lindsley and Burnham* (1970) showed that pyroxferroite is only stable at approximately 10 kbar pressure, which on the Moon corresponds to a depth in the crust of several hundred kilometers (*Chao et al.,* 1970). Although the lunar mare basalt magmas may have been derived from such depths, it is highly unlikely that they crystallized under such high pressures. Therefore it is probable that pyroxferroite crystallized *metastably* (out of equilibrium) during rapid near-surface cooling of the basalts. To test this hypothesis, *Lindsley et al.* (1972) heated pyroxferroite crystals and found that those kept at 900°C for three days decomposed, forming the stable mineral assemblage

Ca-rich pyroxene + fayalite (Fe_2SiO_4) + tridymite (SiO_2). This result indicates that the lunar basalts cooled to below 900°C within three days after crystallization of pyroxferroite. If they had remained above this temperature for a longer time, the pyroxferroite would have broken down to the three stable minerals.

Potassium feldspar. Another late-stage mineral found in lunar basalts is potassium feldspar, $KAlSi_3O_8$. Because the other basalt minerals (e.g., pyroxene, olivine, and plagioclase feldspar) accept very little of the relatively large K^+ ion into their structures, it becomes concentrated in the residual melt that remains after most minerals have crystallized. Early investigators were therefore not surprised to find minor amounts of late-formed potassium feldspar in Apollo 11 basalts (e.g., *Agrell et al.,* 1970; *Keil et al.,* 1970). *Albee and Chodos* (1970) observed a "K-rich phase" that approached potassium feldspar in composition but was nonstoichiometric.

In high-silica highland rocks, which have granitic or so-called "KREEPy" compositions, potassium feldspar is commonly neither minor nor fine-grained. In sample 12013, a KREEPy breccia that itself contains two different breccias (gray and black), there are abundant patches of fine-grained granitic material (*felsite*) that contain 50% potassium feldspar, 40% silica minerals, 5% Fe-rich augite, and 5% other phases (*Quick et al.,* 1981a). Neither the black nor the gray breccias in 12013 contain any mare basalt components; apparently 12013 was formed from a very unusual, SiO_2-rich, KREEPy, evolved terrane, probably somewhere in the highlands. Because 12013 appears to be an impact-produced breccia, it is not clear whether the variety of rock types it contains came from a single differentiated intrusion or from a number of unrelated sources (*Quick et al.,* 1981a; see also section 6.3.5).

In addition to the occurrences of K-feldspar in highland samples (KREEPy and granitic rocks), and as a nonstoichiometric phase in some mare basalts, the mineral is also found in an unusual K-rich mare basalt type (very high-K basalt), which has been discovered as clasts in two Apollo 14 breccias (*Shervais et al.,* 1983, 1984b, 1985). These clasts have K_2O > 0.5 wt.% and contain several percent potassium feldspar. *Shervais et al.* (1985) conclude that these basalts have most likely been produced by the partial assimilation of lunar granite crust by a normal low-Ti mare basalt magma on its way to the surface.

Some analyses of lunar potassium feldspars are listed in Table A5.11a. It is obvious that the feldspars can have a significant BaO content (also expressed as *celsian feldspar*). *Quick et al.* (1981a) reported that, in the potassium feldspar in the felsites of sample 12013, the celsian (Cn) content increases with the K:Na ratio in the potassium feldspar, and the composition ranges from 0.9 mol.% Cn at K:Na = 1:1 to 2.9% Cn at K:Na = 3:1.

5.1.6. Comparative Silicate Mineralogy: Earth-Moon

Pyroxenes. A complete discussion of pyroxene minerals from basaltic meteorites, terrestrial basalts, and lunar basalts is given in *BVSP* (1981); the interested reader is referred to that book for more detailed figures and tables. One of the first-order differences between terrestrial and lunar pyroxenes is the abundance of Fe^{3+} in the former and its absence in the latter; this difference reflects the more reducing conditions (lower oxygen partial pressure) in gases on the Moon than on Earth. Some compositional differences between lunar and terrestrial pyroxenes are shown in the "pyroxene quadrilateral" plots of Fig. 5.14.

Lunar pyroxenes, including those from both mare basalts and highland rocks, have great chemical variability. They also differ in several respects from terrestrial pyroxenes. Pyroxenes from terrestrial ocean floor basalts, which are the most abundant basalts on Earth, are more magnesian than those from lunar mare basalts, and the lunar mare basalt pyroxenes are thus displaced compositionally toward the Fe^{2+}-rich side of the pyroxene quadrilateral relative to terrestrial ones. The Mg-rich nature of terrestrial oceanic pyroxenes reflects the high Mg content of the ocean-floor basalt magmas themselves, and this difference implies that the source region in the Earth's mantle is significantly enriched in Mg relative to the source regions for lunar mare basalts.

Other important compositional differences between terrestrial oceanic pyroxenes and mare pyroxenes are seen in elements other than Mg, Fe, and Ca. These include Na, Cr, Fe^{3+}, Al, and Ti. In terrestrial oceanic basalt pyroxenes, the two most important ionic substitutions involving these elements are Fe^{3+}(octahedral) + Al(tetrahedral) and Ti^{4+}(octahedral) + 2A1(tetrahedral) (*Papike and Bence,* 1978). These two substitutions are of roughly equal importance in terrestrial oceanic basalt pyroxenes. However, the low oxygen partial pressures in gases on the Moon preclude the possibility of Fe^{3+} occurring in any mare basalt pyroxenes, and this substitution therefore cannot occur. As a result, lunar pyroxene crystal chemistry and pyroxene-melt interactions are significantly different from those on Earth. In lunar pyroxenes, the most important ionic substitutions involving the same elements are Ti^{4+}(octahedral) + 2A1(tetrahedral), Cr^{3+}(octahedral) + Al(tetrahedral), and Al(octahedral) + Al(tetrahedral).

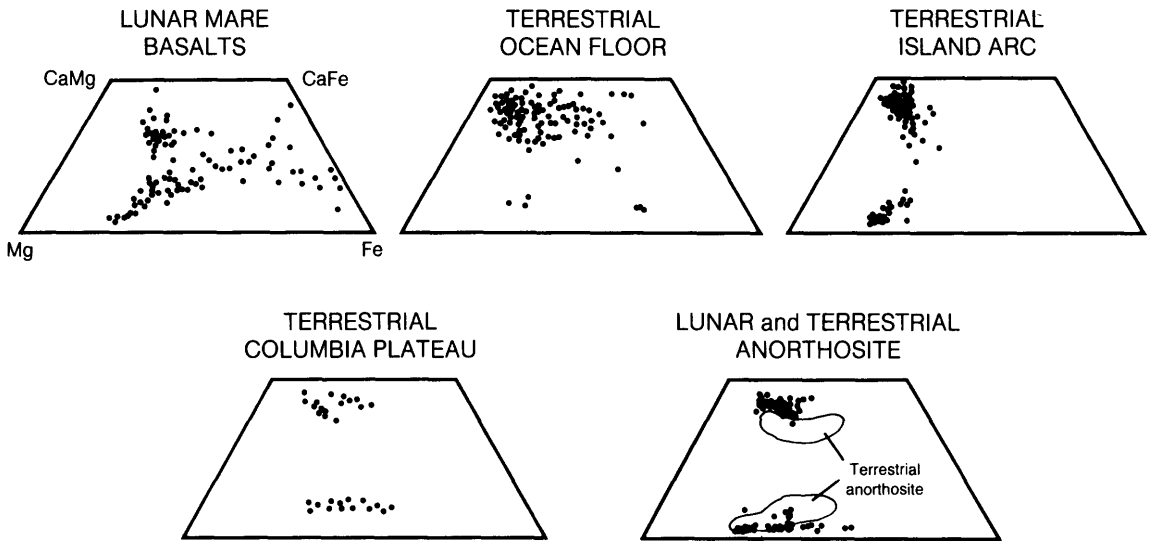

Fig. 5.14. Chemical comparisons between selected suites of lunar and terrestrial pyroxenes, shown on the "pyroxene quadrilateral" part of the compositional triangle $CaSiO_3$ (Ca) — $MgSiO_3$ (Mg) — $FeSiO_3$ (Fe); see Fig. 5.3. Many pyroxenes from lunar mare basalts are more Fe-rich than those from terrestrial lavas. Low-Ca and high-Ca pyroxenes from one group of deep-seated lunar plutonic rocks (*anorthosites*) tend to be more separated in composition than pyroxenes in comparable terrestrial rocks (data from *Ashwal,* 1990). The greater separation between lunar anorthosite pyroxenes may be a result of lower final crystallization temperatures. In the anorthosite diagram, dots (•) indicate lunar pyroxene compositions; fields of pyroxene analyses from terrestrial anorthosites are shown only in outline.

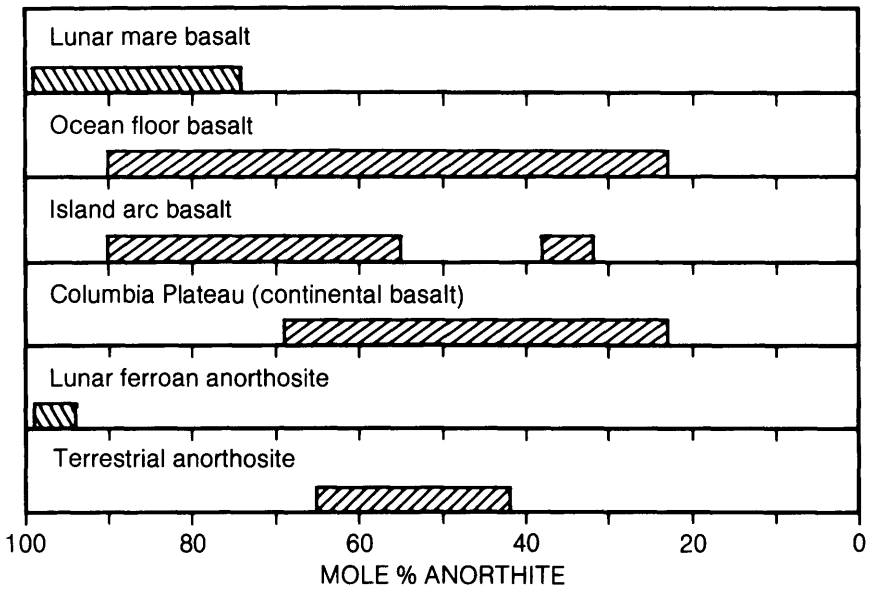

Fig. 5.15. Chemical comparisons between plagioclase feldspar from selected suites of lunar and terrestrial rocks, shown in terms of mol.% anorthite ($CaAl_2Si_2O_8$) in the feldspar. Feldspars from lunar mare basalts are generally more Ca-rich than those from comparable terrestrial volcanic rocks. Feldspars from lunar coarse-crystalline igneous rocks (e.g., ferroan anorthosites; see section 6.3) are far more Ca-rich than those from terrestrial anorthosites.

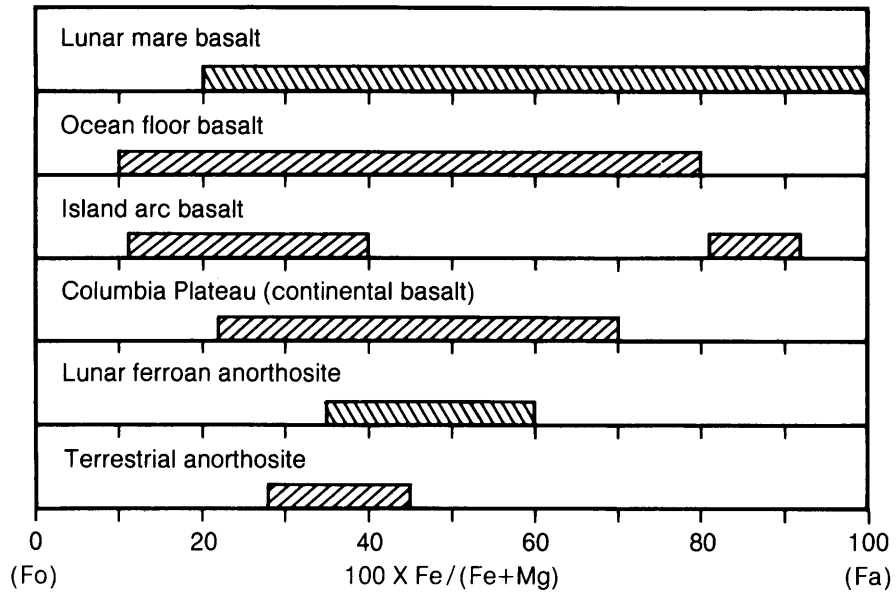

Fig. 5.16. Chemical comparisons between olivines from selected suites of lunar and terrestrial rocks, shown in terms of the atomic ratio Fe/(Fe + Mg) in the olivine. Although there is a high degree of overlap between the terrestrial and lunar populations, the most Fe-rich olivines occur in lunar mare basalts, while terrestrial basalts tend to contain the most Mg-rich ones.

Feldspars. The most significant differences between terrestrial and lunar feldspars (Fig. 5.15) are the striking enrichment of sodium in terrestrial plagioclase feldspars relative to lunar ones and the extreme scarcity of potassium feldspar on the Moon. These conditions reflect the overall depletion of the Moon in alkali elements (e.g., Na, K) relative to the Earth.

Olivines. Comparative lunar and terrestrial olivine compositions are illustrated in Fig. 5.16. Two main differences between terrestrial and lunar olivines are apparent. First, although significant Mg:Fe variation is present in both olivine groups, lunar mare olivines include more iron-rich compositions. Second, the most magnesian terrestrial olivines are more magnesian than the most Mg-rich lunar olivines. As with the lunar pyroxenes, this difference almost certainly reflects the more magnesian composition of the Earth's mantle relative to that of the Moon.

5.2. OXIDE MINERALS

The silicates, such as pyroxene, olivine, and feldspar, are the most abundant minerals in lunar rocks. With minor chemical differences, the common lunar silicate minerals are essentially the same as found on Earth. However, the nonsilicate minerals—especially the oxides—are far more distinctive in lunar rocks. These oxide minerals are likely ores for resource extraction at a lunar base, and they are particularly abundant in some mare basalts (Table 5.2).

As mentioned earlier, several oxide minerals are important constituents of lunar rocks: *ilmenite* ($FeTiO_3$), *spinels* (with extensive chemical variations: $[(Fe,Mg)(Cr,A1,Fe,Ti)_2O_4]$), and *armalcolite* $[(Fe,Mg)Ti_2O_5]$. The less abundant lunar oxide minerals include *rutile* (TiO_2), *baddeleyite* (ZrO_2), and *zirconolite* $[(Ca,Fe)(Zr,REE)(Ti,Nb)_2O_7]$.

The major differences between the oxide minerals in lunar and terrestrial rocks arise from fundamental differences between both the surfaces and the interiors of these two planets. On the Moon, meteoroid impact and shock-metamorphic processes play a major role in altering rocks. These effects are not the same for all minerals. Shock damage and the formation of shock glasses out of minerals (e.g., *maskelynite* from plagioclase feldspar) are observed chiefly in lunar silicate minerals. Oxide minerals also record shock damage (Fig. 4.9a), but another effect of impact on oxide (and sulfide) minerals is to produce small amounts of chemical reduction where these minerals occur as soil particles.

The Moon has no significant atmosphere (see section 3.9). As a result, the Moon has no insulating blanket to (1) retain solar energy and (2) shield it

from cosmic and galactic rays, solar wind, and meteorite infall. Consequently, the surface of the Moon absorbs tremendous solar and cosmic radiation fluxes and undergoes extreme changes in temperature (section 3.5). Meteoroids of all sizes, from kilometers down to submicrometers in size, have for aeons bombarded the lunar surface at very high speeds (about 40,000–250,000 km/hr; Chapter 4). These meteoroid impacts are the only effective weathering and erosion process on the Moon. In addition, the complete lack of any water on the Moon results in the absence of chemical weathering that is so dominant on Earth. As a result, any unmelted and unvaporized meteoroid components, especially the native Fe metal phases, are preserved in the lunar soil. In addition, a steady flux of protons (hydrogen nuclei) and atoms (e.g., helium and carbon) from the solar wind are continually implanted in the uppermost surface of the lunar regolith. These atomic particles, which then become involved as reducing agents during the meteoroid and micrometeoroid impacts that produce shock metamorphism or complete melting, account for one of the distinctive aspects of lunar soil, namely the presence of slaggy, composite particles (*agglutinates*) that contain myriad minute Fe° grains (i.e., native Fe metal).

In addition to the different surface environments of the Earth and Moon, the original conditions of formation of lunar rocks, most notably the volcanic ones, are different from those on Earth in three main aspects: (1) higher temperatures of formation; (2) lower oxygen partial pressures during formation; and (3) complete absence of water. These factors combine to produce oxide minerals on the Moon that are very different from those found on Earth. The temperatures at which igneous rocks melt and crystallize are much higher on the Moon than on Earth because of the absence of water, a chemical species that has a major effect in lowering the melting temperatures (*fluxing*) of these melts. This temperature differential is not large, generally about 100°–150°C for melting temperatures of about 1200°C, and this difference alone would not produce any major changes between terrestrial and lunar magmas.

In contrast, the differences in oxygen partial pressure between the Earth and Moon (Fig. 5.17) lead to pronounced differences in mineralogy (*Sato et al.,* 1973; *Sato,* 1978; *Haggerty,* 1978b). As in the case of the silicate minerals, the low oxygen partial pressure prevents any completely oxidized iron (Fe^{3+}) from forming in the oxide minerals as well. Indeed, oxygen partial pressures on the Moon are so low that native iron (Fe°) is stable with FeO (the mineral *wüstite*—Wu in Fig. 5.17). As a result, metallic iron (Fe°) is ubiquitous in lunar samples of all kinds. Other elements in lunar minerals are also present in unusually low oxidation states (e.g., Ti^{3+}, Co^{2+}, Cr^{2+}, P^{3-}) in comparison to terrestrial minerals.

The oxide minerals, although less abundant than silicates in lunar rocks, are of great significance because they retain signatures of critical conditions of formation (e.g., limited availability of oxygen) from the rocks in which they occur. Whereas most of the silicate minerals differ little from those on Earth, the opaque oxide phases reflect the reducing, anhydrous conditions that prevailed during their formation. By combining analyses of lunar oxide minerals with the results of laboratory experiments on their synthetic equivalents, the temperature and oxygen pressure conditions during formation of lunar rocks can be estimated (Fig. 5.17; see *Sato et al.,* 1973; *Usselman and Lofgren,* 1976).

Because their oxygen is more weakly bonded than in silicate minerals, oxide minerals are obvious and important potential feedstocks for any future production of lunar oxygen and metals. On Earth, similar oxide minerals commonly occur in economically recoverable quantities called *ore deposits.* However, most of these deposits, and the minerals in them, have formed from *hydrothermal* waters (100°-300°C or hotter). The Moon has little if any water, and the presence of similar hydrothermal ore deposits on the Moon is not probable. However, there are other means of concentrating oxide minerals into exploitable ores. *Crystal settling* of dense minerals (e.g., chromite, ilmenite, and minerals containing the platinum-group elements) is possible within silicate magmas, if the magma remains liquid for a long enough time. On Earth, such accumulations are normally found in *layered intrusions.* These bodies form from large masses of magma that have been emplaced into crustal rocks without reaching the Earth's surface. Under such conditions, cooling is slower, and physical separation processes—which may include convection as well as settling—have time to act. Well-known examples of ore deposits resulting from these processes occur in the Stillwater Anorthosite Complex (Montana) and the Bushveld Igneous Complex (South Africa). Can similar deposits form in the very different environment of the Moon?

The accumulation of dense oxide minerals as they crystallize from a magma depends on their *settling velocity* in the less dense silicate melt. The higher the settling velocity, the further the minerals can fall before the melt solidifies, and the more chance they have to accumulate. The settling velocity in the melt can be approximated by *Stokes' Law,* which relates settling velocity (v) to other parameters. For spheres, Stokes' Law is

$$v = (2/9)gr^2[(\rho_s - \rho_l)/\eta]$$

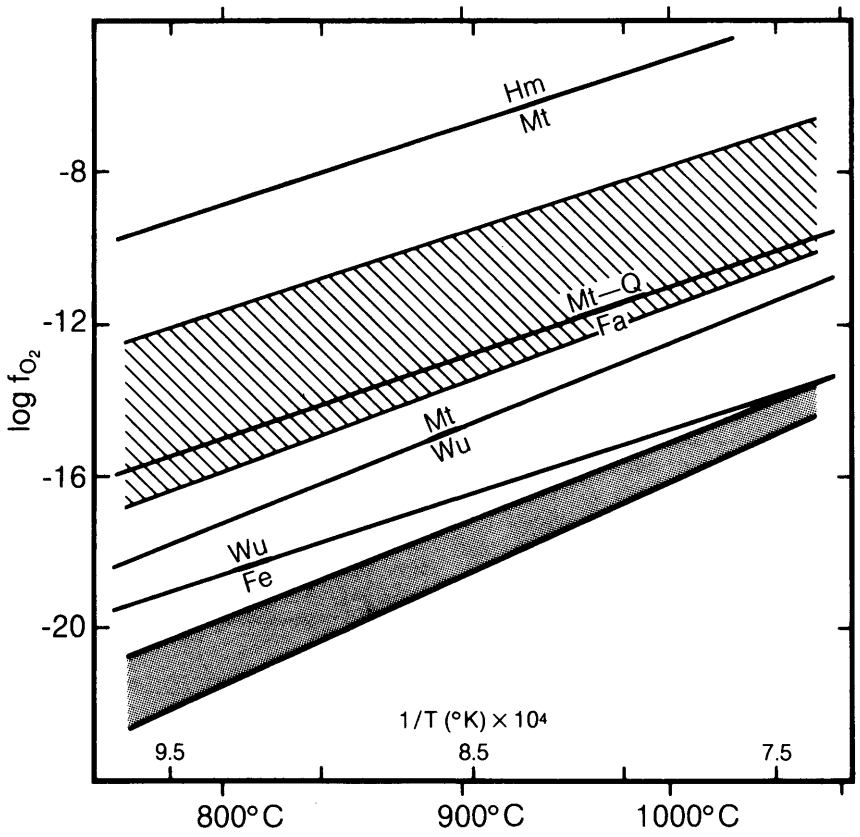

Fig. 5.17. Stability regions for various Fe-bearing minerals, shown as a function of *oxygen fugacity* (fO_2) and temperature (T). Oxygen fugacity is the actual thermodynamic chemical potential of oxygen in a gas mixture, which, because of nonideal gas behavior, is not adequately represented by partial pressure. Minerals shown are metallic iron (Fe), wüstite (Wu)($Fe_{1-x}O$), magnetite (Mt)(Fe_3O_4), the Fe-olivine fayalite (Fa)(Fe_2SiO_4), quartz (Q)(SiO_2), and hematite (Hm)(Fe_2O_3). Mineral assemblages become more oxidized in going from the bottom to the top of the diagram. The fO_2-T region for terrestrial volcanic activity, estimated from the minerals in terrestrial rocks, is shown as a zone marked by diagonal lines and includes the relatively oxidized fayalite/(quartz + magnetite) boundary. The equivalent region for lunar basalts (gray zone) is located entirely below the iron/wüstite boundary. Note that the minerals containing Fe^{3+} (Mt and Hm) are not stable in the lunar region, and that Fe metal is stable in lunar rocks.

where g is the acceleration of gravity, r is the radius of the sphere, ρ_s and ρ_l, are the densities of solid and melt respectively, and η is the viscosity of the melt. The most important factors to be considered in comparing lunar and terrestrial environments are the acceleration due to gravity (g), which directly affects v, and the viscosity (η) of the silicate melt, which affects v inversely. The acceleration due to gravity on the Moon's surface is about 160 cm/sec^2, compared to 980 cm/sec^2 on Earth. This factor will produce a sixfold lesser settling velocity in lunar magmas if all other factors are equal. However, this effect is countered by the fact that the viscosity of an average lunar basaltic melt is 10 to 100 times less than that of a terrestrial basaltic magma. This viscosity difference results from two circumstances: (1) viscosity decreases with temperature and, as noted above, the average crystallization temperatures of lunar basalts are 100°-150°C higher than terrestrial basalts; and (2) typical lunar basalts are considerably higher in FeO and lower in Al_2O_3 than their terrestrial counterparts, making them less viscous at any given temperature. These effects combine to greatly lower the viscosities of lunar magmas. The reduction in viscosity (1/10 to 1/100 × Earth magmas) overwhelms the effect of lower lunar gravity (1/6 × Earth), and crystals will have greater settling velocities on the Moon. It is therefore

possible that layered ore deposits similar to or even larger than those on Earth may occur on the Moon (see *Taylor and Lu,* 1990).

The following discussions of individual oxide minerals have drawn upon ideas and data from many references that provide detailed information about the subject, especially *BVSP* (1981), *Frondel* (1975), *Levinson and Taylor* (1971), *LAPST* (1985), *Papike and Vaniman* (1978), *Papike et al.* (1976), *Smith* (*1974*), *Smith and Steele* (1976), and *S. R. Taylor* (1975, 1982).

5.2.1. Ilmenite

Ilmenite, with the ideal formula $FeTiO_3$, is the most abundant oxide mineral in lunar rocks. The amount of ilmenite in these rocks is a function of the bulk composition of the magma from which the ilmenite crystallized (*Rutherford et al.,* 1980; *Norman and Ryder,* 1980; *Campbell et al.,* 1978); the higher the TiO_2 content of the original magma, the higher the ilmenite content of the rock. Ilmenite forms as much as 15-20% by volume of many Apollo 11 and 17 mare basalts (*McKay and Williams,* 1979). However, the volume percentages of ilmenite in mare basalts vary widely across the Moon as indicated by the range of TiO_2 contents in samples from different lunar missions (Table 5.2 and Fig. 5.18).

The ilmenite crystal structure is hexagonal (Fig. 5.19) and consists of alternating layers of Ti-and Fe-containing octahedra. Most lunar ilmenite contains some Mg substituting for Fe (Table A5.11), which arises from the solid solution that exists between ilmenite ($FeTiO_3$) and $MgTiO_3$, the mineral *geikielite.* Other elements are present only in minor to trace amounts (i.e., <1%); these include Cr, Mn, Al, and V. In addition, ZrO_2 contents of up to 0.6% have

TABLE 5.2. Summary of modal data (vol.%) for mare basalts (after *BVSP,* 1981, p. 255).

	Oxide Minerals	Pyroxene	Feldspar	Olivine
A-17 high Ti	24.4	47.7	23.4	4.6
A-11 high K	20.6	57.5	21.7	0.1
A-17 low K	15.1	51.6	33.3	-
A-11 low K	14.6	50.9	32.2	2.3
A-12 ilmenite	9.3	61.1	25.9	3.6
A-12 pigeonite	9.1	68.4	21.1	1.4
A-12 olivine	7.1	53.5	19.2	20.2
L-16 aluminous	7.1	51.5	41.2	0.1
A-15 olivine	5.5	63.3	24.1	7.0
A-15 pigeonite	3.7	62.5	33.8	-
A-14 aluminous	3.2	53.8	43.0	-
L-24 ferrobasalt	1.8	48.6	39.1	10.4
L-24 ferrobasalt	1.4	60.2	34.2	4.2
A-17 VLT	1.0	61.7	31.9	5.4

Modal data normalized to 100% for the four phases considered, in Apollo (A) and Luna (L) samples. Ordered from top to bottom in terms of decreasing modal content of opaque oxide minerals.

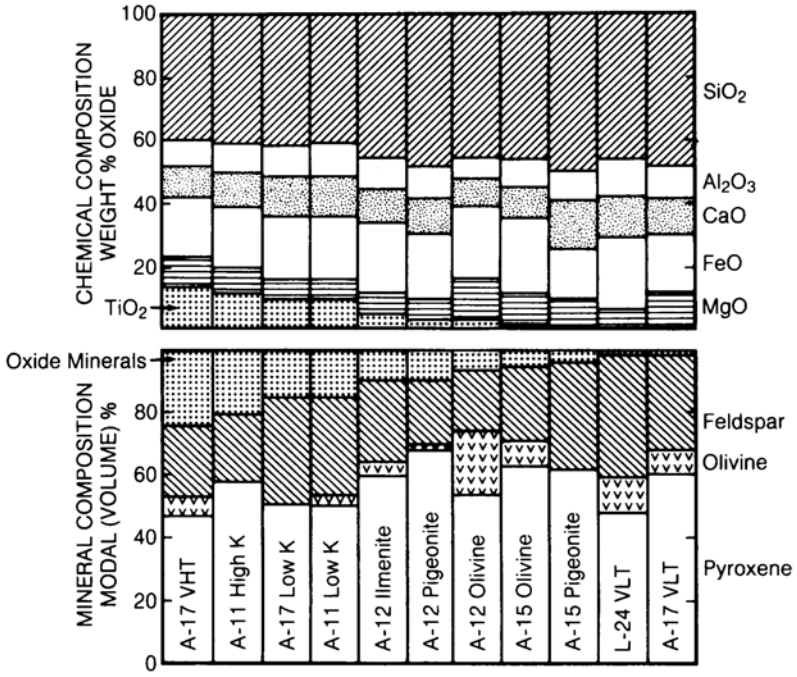

Fig. 5.18. Variations in major-element chemistry and modal (vol.%) mineral content in a range of lunar mare basalts. Analyses are arranged from left to right in order of decreasing TiO_2 (or oxide mineral) content (adapted from *BVSP,* 1981).

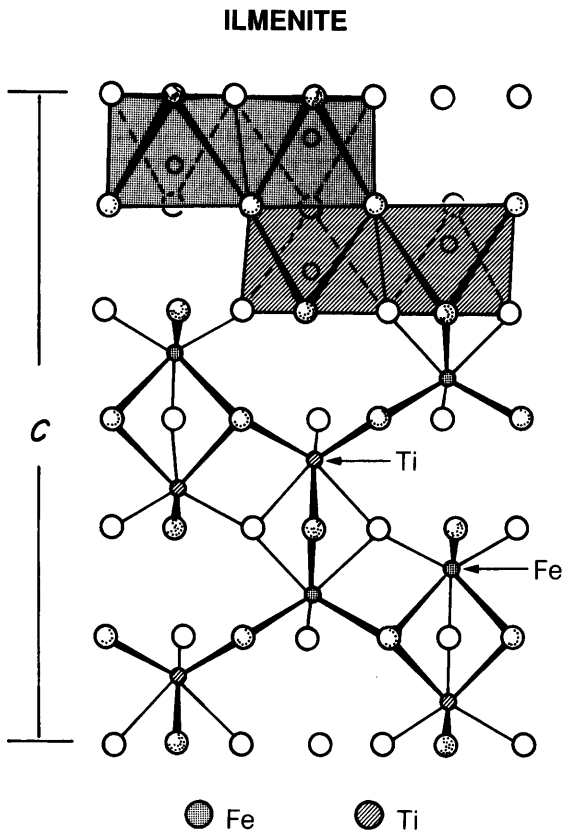

Fig. 5.19. Crystal structure of ilmenite, composed of octahedra defined by oxygen atoms, which contain Fe^{2+}, Ti^{4+}, and other cations. The unit-cell dimension along the *c*-axis is shown as *c* (after *Papike et al.,* 1976). The patterns used to distinguish Fe from Ti sites apply to both octahedra (upper part of structure) and cations (lower part of structure).

been reported from ilmenites in Apollo 14 and 15 basalts (*El Goresy et al.,* 1971a,b; *Taylor et al.,* 1973b). In fact, the partitioning of ZrO_2 between ilmenite and coexisting ulvöspinel (Fe_2TiO_4) has been experimentally determined (*Taylor and McCallister,* 1972) and has been used as both a geothermometer (to deduce temperatures during crystallization) and as a cooling-rate indicator (*Taylor et al.,* 1975, 1978; *Uhlmann et al.,* 1979). Although terrestrial ilmenite almost always contains some Fe^{3+}, lunar ilmenite contains none, a result of the more reducing magmatic conditions within the Moon. Table A5.12 lists representative ilmenite compositions from a wide range of lunar rock types.

The compositions of lunar ilmenites plot along the $FeTiO_3$-$MgTiO_3$ join; variation from $FeTiO_3$ is often expressed in weight percentage of MgO (Fig. 5.20). The appreciable MgO contents of many lunar ilmenites (>3% MgO) are similar to terrestrial ilmenites that formed at high pressure in rocks called *kimberlites* (kimberlites come from deep in the Earth's mantle and are the igneous rocks that often contain diamonds). It was originally thought that the high Mg content in some lunar ilmenites was produced, as in terrestrial kimberlites, by high pressures of formation. In general, the ilmenites with the highest Mg contents tend to come from relatively high-Mg rocks; ilmenite composition correlates with the bulk composition of the rock and therefore reflects magmatic chemistry rather than pressure. In detail, the distribution of Mg between ilmenite and coexisting silicate minerals in a magma is related to the timing of ilmenite crystallization relative to the crystallization of the other minerals. This *crystallization sequence is* itself a function of cooling rate and other factors, most notably the oxygen partial pressure (*Usselman et al.,* 1975). However, it is doubtful that the Mg contents in ilmenite all represent equilibrium conditions, because ilmenite compositions can vary significantly, even within distances of a few millimeters, within a single rock (Fig. 5.21).

Ilmenite commonly occurs in mare basalts as bladed crystals up to a few millimeters long. It typically forms near the middle of the crystallization sequence, where it is closely associated with pyroxene. It also forms later in the sequence and at lower temperatures, where it is associated with native Fe and troilite. In Apollo 17 rocks, ilmenite is frequently associated with armalcolite (see section 5.2.3) and occurs as mantles on armalcolite crystals (e.g., *El Goresy et al.,* 1974; *Haggerty,* 1973a; *Williams and Taylor,* 1974). In these instances, ilmenite has possibly formed by the reaction of earlier armalcolite with the melt during crystallization.

The stability curve of pure ilmenite as a function of temperature and oxygen pressure is significantly different from that of ulvöspinel (*Taylor et al.,* 1973b), the spinel phase with which it is commonly associated (Fig. 5.22), implying that the two minerals did not crystallize together. The data suggest that, in these mineral assemblages, ilmenite has formed by solid-state reduction (oxygen loss) of this high-Ti spinel at temperatures below their melting points (*subsolidus reduction,* see section 5.2.2). Rare grains of ilmenite also contain evidence for subsolidus reduction of ilmenite to rutile (TiO_2) + native Fe; other grains show reduction to chromite ($FeCr_2O_4$) + rutile + native Fe.

Ilmenite as a source of oxygen. The production of oxygen on the Moon from lunar materials is a major goal for a lunar base (*National Commission on Space,* 1986). *McKay and Williams* (1979), *Williams*

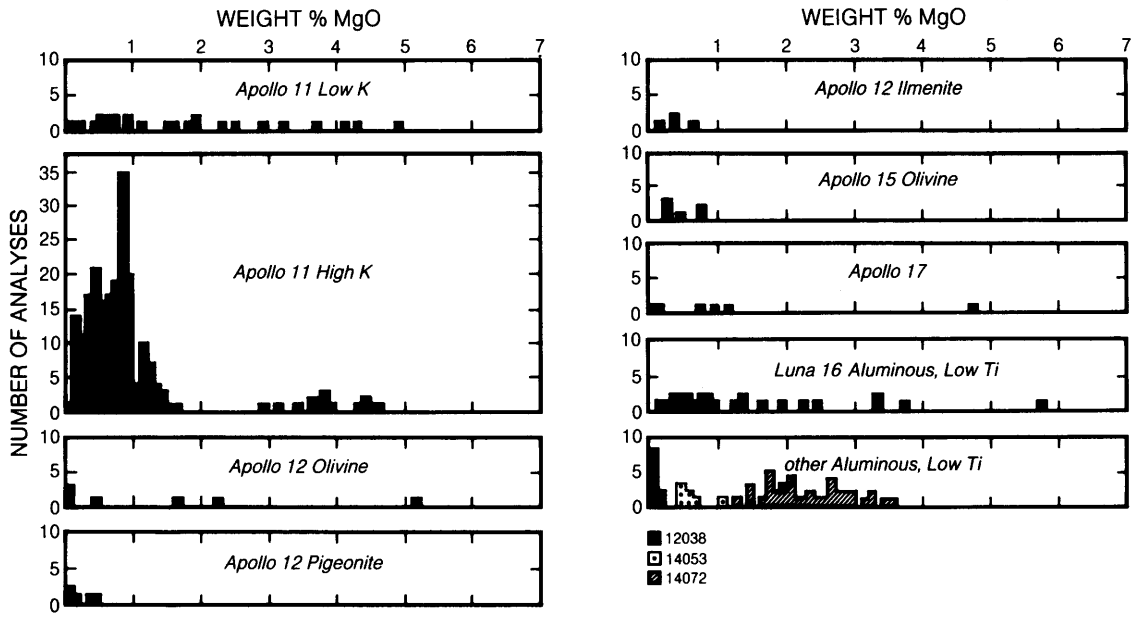

Fig. 5.20. MgO contents (wt.%) of ilmenites in mare basalt samples from various lunar sites (adapted from *Papike et al.,* 1976). The terms "low K," "high K," "olivine," "pigeonite," "ilmenite," and "aluminous, low-Ti" are modifiers used to describe various basalt chemical types (for example, olivine basalts are relatively Mg-rich, pigeonite basalts are relatively Si-rich, and ilmenite basalts are relatively Ti-rich within the general group of low-Ti mare basalts from Apollo 12; see section 6.1 and Table A5.1 for more information on mare basalt types).

and Erstfeld (1979), *Williams et al.* (1979), and *Rao et al.* (1979) first suggested that ilmenite might usefully be reduced to rutile + Fe with the release of oxygen. The lowest curve below 1150°C in Fig. 5.22 represents the conditions for the reaction of interest

$$FeTiO_3 = TiO_2 + Fe + 1/2O_2$$

This reaction could ideally produce 10.5 wt.% O_2 from a given mass of ilmenite. The reaction could be carried out by using hydrogen to reduce the ilmenite. The hydrogen might be obtained from the indigenous solar-wind protons (hydrogen nuclei) that are implanted in the lunar soil and in the ilmenite grains within it (*Blanford,* 1982; *Kiko et al.,* 1979). Preliminary studies have shown the feasibility of this type of oxygen production (*Williams,* 1985; *Gibson and Knudsen,* 1985).

Another possible source of oxygen is the spinel phase, ulvöspinel (Fe_2TiO_4), according to the reaction

$$Fe_2TiO_4 = TiO_2 + 2Fe + O_2$$

This reaction would ideally produce 14.3 wt.% O_2 from a given mass of ulvöspinel. Ulvöspinel is a very abundant mineral (several weight percent) in many mare basalts, particularly those from the Apollo 12, 15, and 17 sites. However, the composition of ulvöspinel is quite variable (see section 5.2.2 below), and this variability could introduce complications into its use for oxygen production.

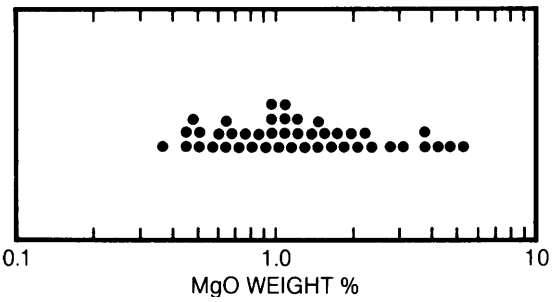

Fig. 5.21. Variations in the MgO (wt.%) content of ilmenites from one sample of lunar mare basalt (sample 12018; see also Fig. 5.26). Each dot represents one analysis. The ilmenite MgO content varies over a wide range, between 0.3% and 6% (adapted from *El Goresy et al.,* 1971b).

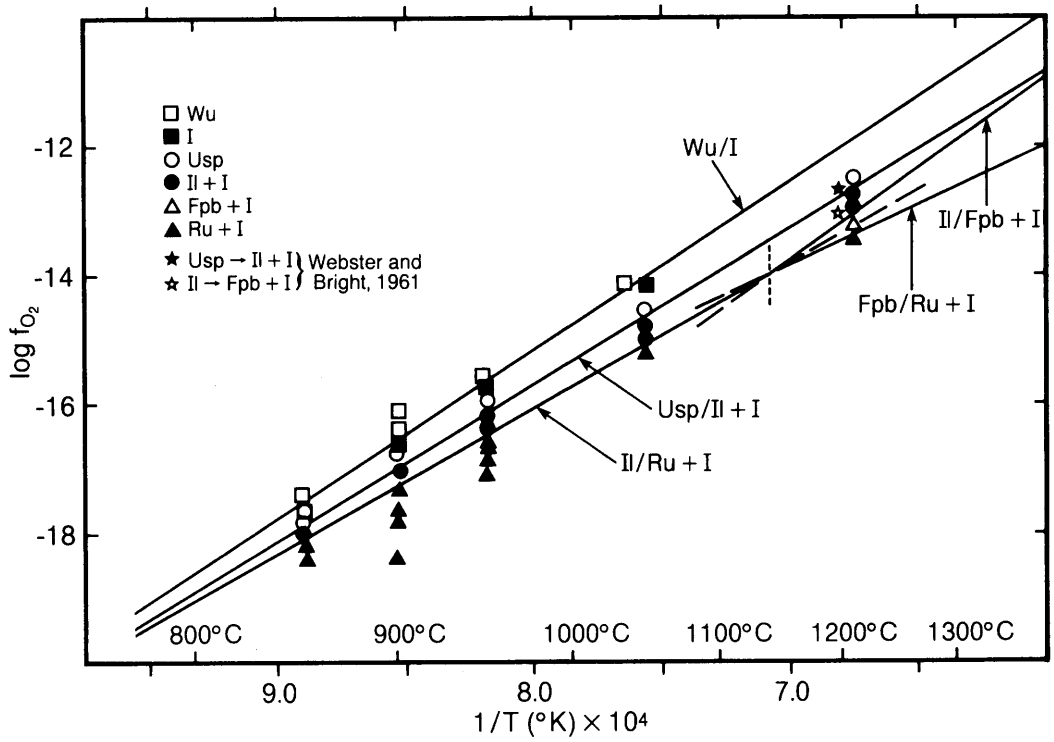

Fig. 5.22. Stability relations of several Fe- and Ti-bearing minerals, shown as a function of oxygen fugacity (fO_2) and temperature (T). The diagram shows possible reactions in the Fe-Ti-O system (adapted from *Taylor et al., 1972*). Abbreviations: Wu = wüstite; I = iron; Usp = ulvöspinel; 11= ilmenite; Fpb = ferropseudobrookite; Ru = rutile. In labeling the curves, the oxidized side of the reaction (upper side of the curve) is listed before the reduced part (lower side of the curve), e.g., Wu/1 ($Fe_{1-x}O$/Fe). The labels for each curve thus show (oxidized side of the reaction)/(reduced side of the reaction). In going from reduced conditions (bottom) to oxidizing ones (top), at temperatures below 1150°C, the sequence of reactions is rutile + iron + oxygen = ilmenite; ilmenite + iron + oxygen = ulvöspinel; and iron + oxygen = wüstite. At higher temperatures, the mineral ferropseudobrookite appears in the sequence.

5.2.2. Spinels

Spinel is the name for a group of minerals, all with cubic crystal symmetry, that have extensive solid solution within the group. Spinels are the second most abundant opaque mineral on the Moon, second only to ilmenite, and they can make up as much as 10% of the volume of certain basalts, most notably those from the Apollo 12 and 15 sites. The general structural formula for these minerals is $^{IV}A^{VI}B_2O_4$, where IV and VI refer to four-cornered (tetrahedral) and six-cornered (octahedral) polyhedra of oxygen atoms.

The basic spinel structure is a cubic array of oxygen atoms. Within the array, the tetrahedral A-sites (black dots in Fig. 5.23) are occupied by one-third of the cations, and the octahedral B-sites (vertical-line shading) are occupied by the remaining two-thirds of the cations. In a *normal spinel* structure the divalent cation, such as Fe^{2+}, occupies only the tetrahedral sites, and the two different sites each contain only one type of cation (e.g., $FeCr_2O_4$). If the divalent cation occurs in one-half of the B-sites, the mineral is referred to as an *inverse spinel* [e.g., $Fe(Fe,Ti)_2O_4$]. In lunar spinels, the divalent cations (usually Fe^{2+} or Mg^{2+}) occupy either the A- or both A- and B-sites (i.e., there are both normal and in-verse lunar spinels), and higher-charge cations (such as Cr^{3+}, Al^{3+}, Ti^{4+}) are restricted to the B-sites.

The relations of the various members of the spinel group can be displayed in a diagram known as the *Johnston compositional prism* (Fig. 5.24). The end members represented include *chromite,* $FeCr_2O_4$; *ulvöspinel,* $FeFeTiO_4$ (commonly written as Fe_2TiO_4,

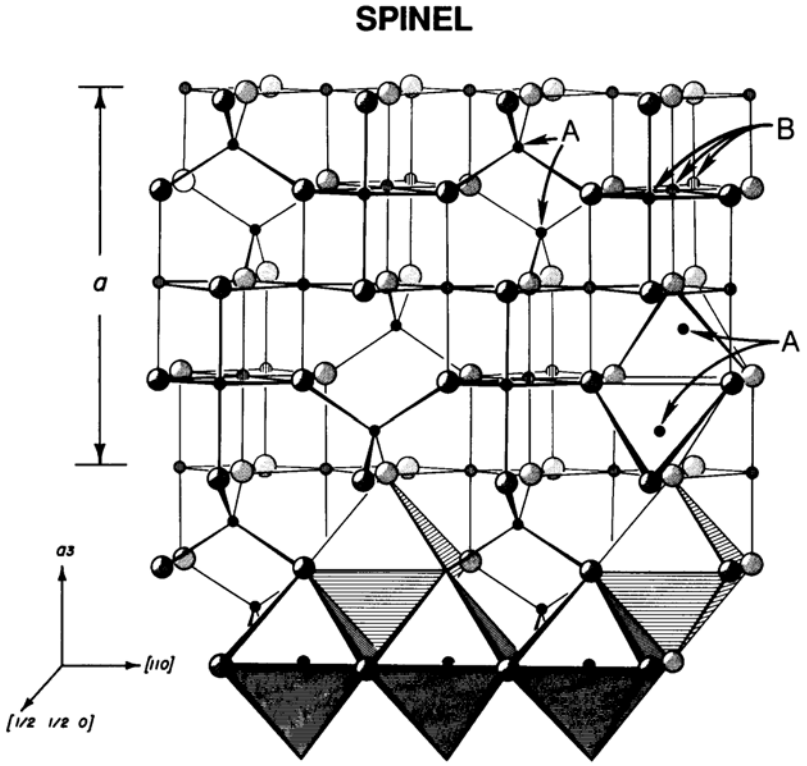

Fig. 5.23. Crystal structure of spinel, composed of a cubic-close-packed array of oxygen atoms. This structure provides two interstitial sites, ^{IV}A (a tetrahedral site coordinated with four oxygens) and ^{VI}B (an octahedral site coordinated with six oxygens). Both A and B can accommodate a wide variety of cations. In this diagram, the A-sites are indicated by small black dots, and the B-sites by somewhat larger shaded spheres. The largest shaded spheres are oxygen atoms. The edge of the cubic unit cell is shown as *a*. The three axes at the lower left indicate reference crystallographic directions for orienting the figure (modified from *Papike et al.,* 1976).

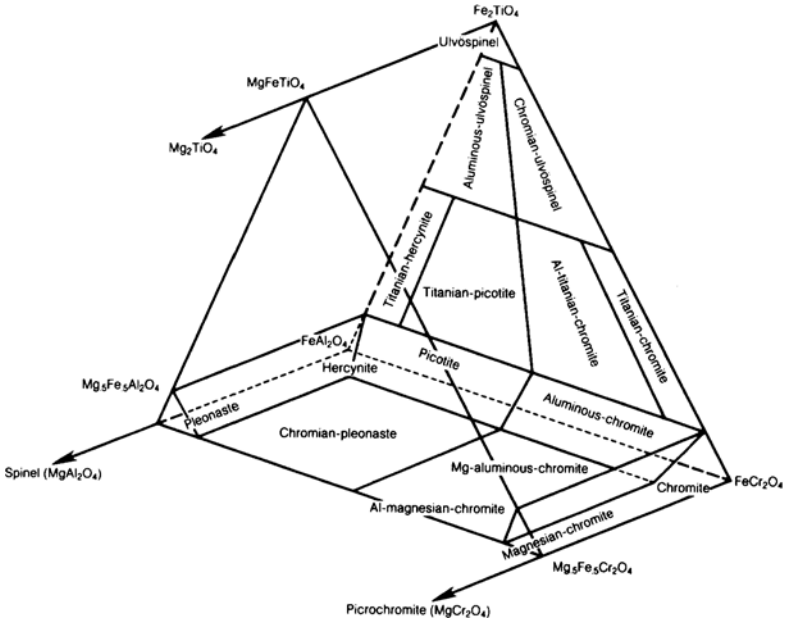

Fig. 5.24. Compositional diagram (modified Johnston prism) showing names used for different chemical varieties of spinels (adapted from *Haggerty,* 1972a). Fe-rich end-member compositions used in this diagram are *chromite* ($FeCr_2O_4$), *ulvöspinel* (Fe_2TiO_4 or $FeFeTiO_4$), and *hercynite* ($FeAl_2O_4$). The prism is filled in with mineral names only in that half where Fe/Mg proportions are >1; the more Mg-rich spinels are relatively rare, but compositions closer to *spinel* (*sensu stricto;* $MgAl_2O_4$) than to hercynite occur in some highland rocks (Table A5.13, columns 56 and 57).

but this is an inverse spinel with Fe^{2+} in both A- and B-sites); *hercynite,* $FeAl_2O_4$; and *spinel* (*sensu stricto*), $MgAl_2O_4$. Intermediate compositions among these end members are designated by using appropriate modifiers (e.g., *chromian ulvöspinel* or *titanian chromite*). Some common solid solution compositions also have distinct names, such as *pleonaste* for compositions between $MgAl_2O_4$ and $FeAl_2O_4$. Figure 5.25 is a set of modified Johnston compositional prisms that show the compositional ranges in lunar spinels.

As shown in Fig. 5.25, most lunar spinels have compositions generally represented within the three-component system: $FeCr_2O_4$ — $FeFeTiO_4$ — $FeAl_2O_4$, and their compositions can be represented on a flat triangular plot. The addition of Mg as another major component provides a third dimension to this system; the compositions are then represented as points within a limited Johnston compositional prism in which the Mg-rich half (Mg > Fe) is deleted because most lunar spinels are Fe-rich (e.g., *Agrell et al,* 1970; *Busche et al.,* 1972; *Dalton et al.,* 1974;

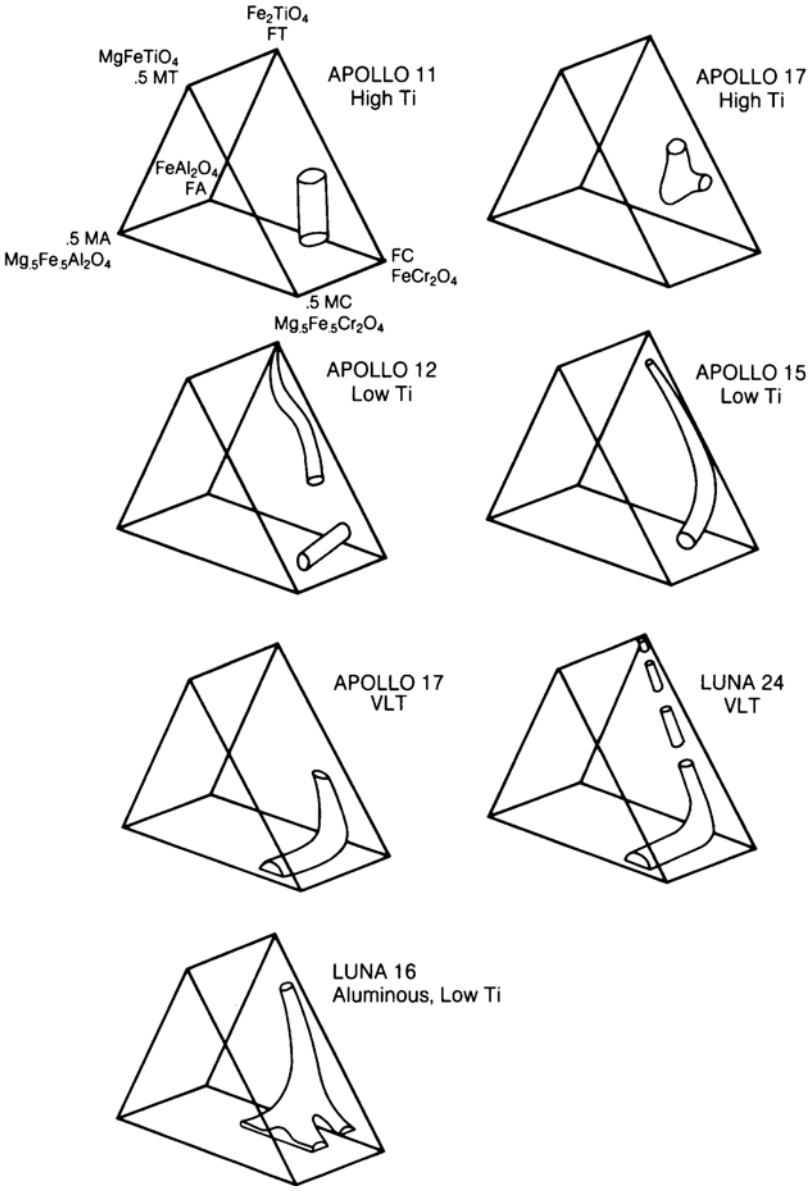

Fig. 5.25. Diagrams showing ranges of chemical variation of lunar spinels in mare basalt samples from individual Apollo and Luna landing sites. Each diagram is a modified Johnston prism, showing only that half for Fe/Mg > 1 (see Fig. 5.24); the mare basalt spinels consist mostly of early-formed chromite varieties and late-crystallizing ulvöspinel. Note the wide variation in spinel compositions between sites and often within a single site (modified from *Haggerty,* 1978a).

El Goresy et al., 1971b, 1976; *Haggerty,* 1971a, 1972b,c, 1973b, 1978a; *Nehru et al.,* 1974, 1976; *Taylor et al.,* 1971). As is apparent from Figs. 5.24 and 5.25, most lunar spinel compositions fall between chromite and ulvöspinel. The principal cation substitutions in these lunar spinels can be represented by $Fe^{2+} + Ti^{4+} = 2\ (Cr,Al)^{3+}$. Other cations commonly present include V, Mn, and Zr. Representative compositions are given in Table A5.13.

Spinels are ubiquitous in lunar mare basalts, where they occur in various textures and associations. These spinels are invariably zoned chemically. Such zoning occurs particularly in Apollo 12 and 15 rocks, in which chromite is usually the first mineral to crystallize from the melt. As the chromite crystals continue to grow, their TiO_2 and FeO contents increase, and their Al_2O_3, MgO, and Cr_2O_3 contents decrease, with the overall composition moving toward that of ulvöspinel (Fig. 5.25; Table A5.13). In most of the basalts that contain both titanian chromites and chromian ulvöspinels, the latter phase occurs as overgrowths and rims surrounding the chromite crystals. (Some individual ulvöspinel grains also occur as intermediate to late-stage crystallization products.)

When observed using a reflected-light microscope, the ulvöspinel in these composite crystals appears as tan to brown rims about the bluish chromite. The contact between the two is commonly sharp, indicating a discontinuity in the compositional trend from core to rim (Fig. 5.25). This break probably records a cessation in growth, followed later by renewed crystallization in which the earlier chromite grains acted as nuclei for continued growth of ulvöspinel (*Cameron,* 1971). Some rocks (e.g., 12018; Fig. 5.26) contain spinel grains with diffuse contacts that are also reflected in gradational changes in the composition of the solid solution. These textures could result from continuous crystallization of the spinel or from later reequilibration by solid-state diffusion within the crystal (*Taylor et al.,* 1971).

Although most abundant in mare basalts, spinels also occur in highland rocks such as anorthosites, anorthositic gabbros, troctolites, and impact mix-

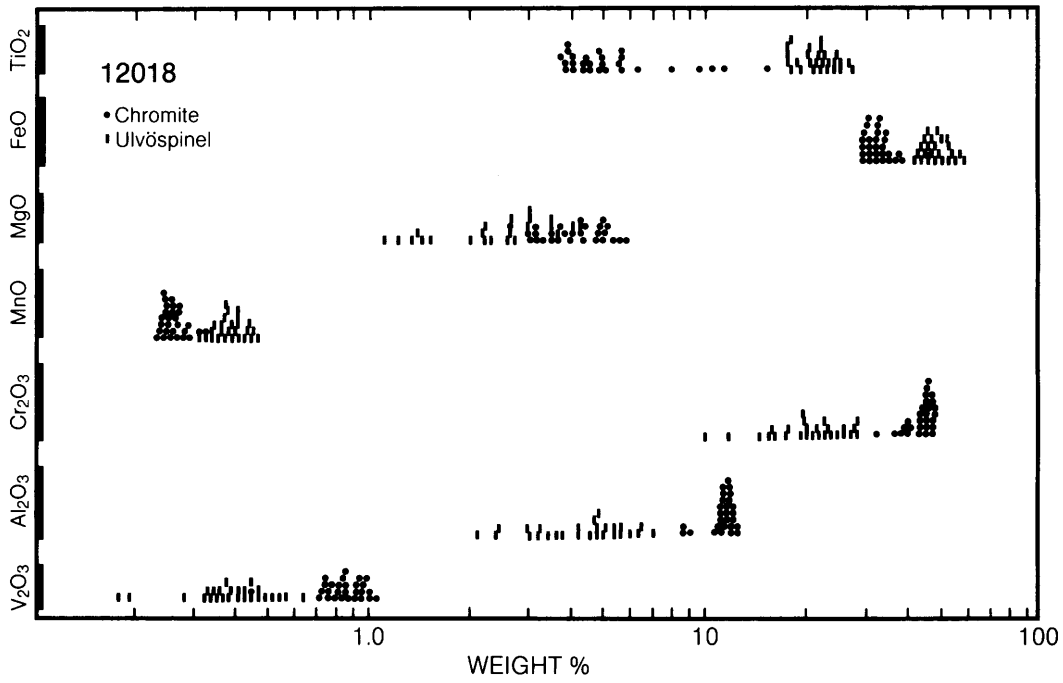

Fig. 5.26. Distribution of chemical compositions (oxide wt.%) of chromites and ulvöspinels in Apollo 12 low-Ti mare basalt 12018 (see also Fig. 5.21) (adapted from *El Goresy et al.,* 1971b). The diagram shows individual analyses for chromite (dots) and ulvöspinel (small bars) in wt.% abundance of several oxide constituents (V_2O_3, Al_2O_3, etc.). In major oxide content, chromites (high Cr_2O_3) are readily distinguished from ulvöspinels (high TiO_2 and FeO). Chromites also have relatively high contents of the minor oxides Al_2O_3, MgO, and V_2O_3, but are lower in MnO. Note that the ulvöspinels compositions are less tightly clustered than the chromites (i.e., the ulvöspinels are more chemically zoned).

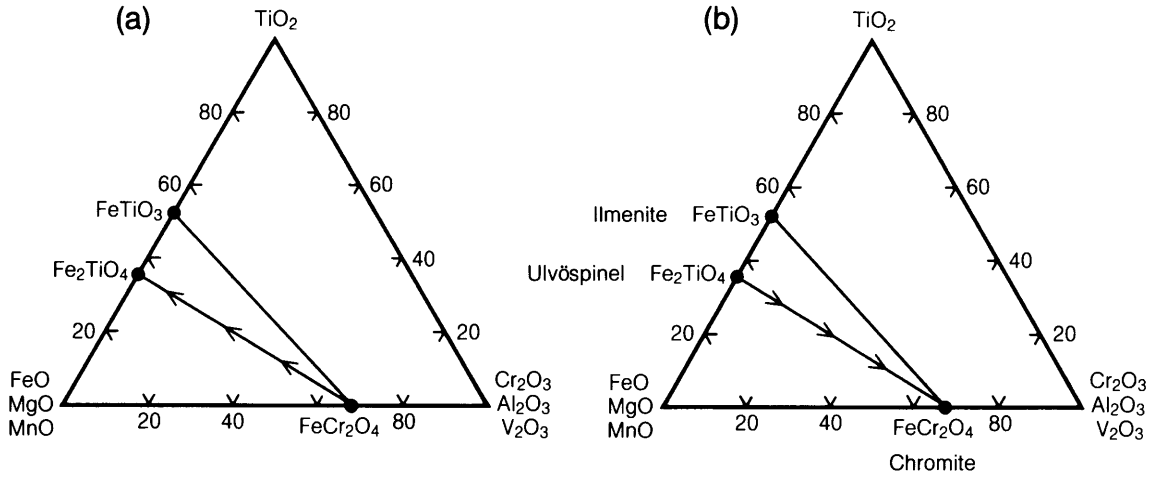

Fig. 5.27. Stability relations between ulvöspinel (Fe_2TiO_4) and chromite ($FeCr_2O_4$) during **(a)** crystallization and **(b)** reduction during cooling of the solid rock (the example here is an Apollo 14 impact melt). During crystallization, spinels change in composition from chromite toward ulvöspinel. As the spinels are reduced when the rock cools, the ulvöspinel breaks down to form ilmenite ($FeTiO_3$) and Fe metal, while that portion that retains the spinel structure reverts to a more chromite-rich composition (adapted from *El Goresy et al.,* 1972).

tures of these rock types (e.g., *Haselton and Nash,* 1975; see sections 6.3 and 6.4). The spinels in anorthositic (plagioclase-rich) highland rocks tend to be chromite with lesser amounts of MgO, Al_2O_3, and TiO_2 (Table A5.13). However, certain highland rocks, notably the olivine-feldspar types (*troctolites*), contain pleonaste spinel. The composition of this spinel is slightly more Fe- and Cr-rich than an ideal composition precisely between the end members $MgAl_2O_4$ and $FeAl_2O_4$ (Fig. 5.25). This spinel is not opaque; under the microscope, it stands out because of its pink color, high index of refraction, and isotropic character in cross-polarized light.

Subsolidus reduction. Crystals that originally form from a melt may continue to change while the rock is solid but still hot. Such *subsolidus reactions* can occur at temperatures significantly below the melting point. In terrestrial rocks, the oxygen pressure is relatively high during such changes, and terrestrial subsolidus reactions generally involve oxidation. However, in lunar rocks and soils, evidence for *subsolidus reduction* is extremely common. Lunar ulvöspinel grains are often reduced to ilmenite + native Fe; more rarely, ilmenite is reduced to rutile + native Fe or to chromite + rutile + native Fe (*El Goresy et al.,* 1971a, 1972; *Haggerty,* 1971b, 1972a,d, 1977; *McCallister and Taylor,* 1973; *Taylor et al.,* 1971). The causes of this late-stage reduction of ulvöspinel are speculative, but the effects have been quite pervasive (*Brett,* 1975; *Haggerty,* 1978b; *Sato,* 1978). In a few rocks (e.g., 14053, 14072), the Ti-rich ulvöspinel is reduced to a mixture of Ti-poor spinel + titanian chromite + ilmenite + native Fe (*El Goresy et al.,* 1972; *Haggerty,* 1972a).

Compositional changes of the spinel during later subsolidus reduction are the opposite of those observed during primary crystallization (*El Goresy et al.,* 1972; *Haggerty,* 1972c; *Taylor et al.,* 1971). During normal crystallization of spinel from a melt, the spinel typically begins as chromite and changes its composition toward ulvöspinel as growth continues (Fig. 5.27a). The net effect of later subsolidus reduction on the ulvöspinel is to form ilmenite + native Fe; the residual components enrich the remaining spinel so that its composition moves back toward chromite (Fig. 5.27b). The secondary generation of native Fe during these subsolidus reactions is of some importance. It provides evidence for the reducing nature of the reaction. It also increases the Fe metal content of the rock involved. Spinel grains in the lunar soil also readily undergo reduction when shock metamorphosed by impacting micrometeoroids. This reduction is possibly caused by the presence in the soil of implanted solar-wind particles, notably the elements hydrogen and carbon, which create a reducing environment when heated to high temperatures during impact.

5.2.3. Armalcolite

Armalcolite is named after the Apollo 11 astronauts (ARMstrong, ALdrin, and COLlins). It was first recognized as a new mineral in samples from the

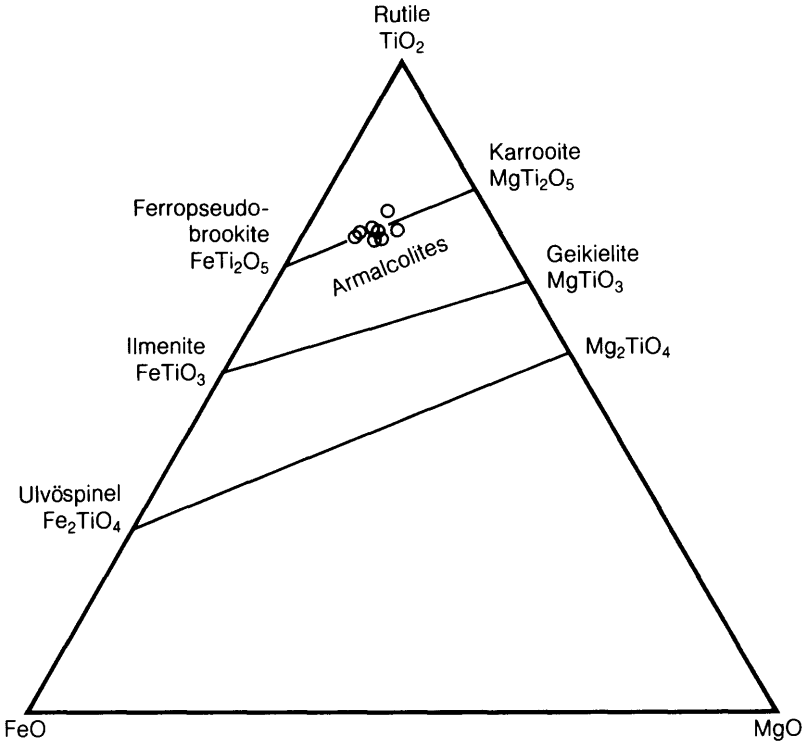

Fig. 5.28. Triangular compositional plot of the system FeO — MgO — TiO_2 (in wt.%), showing armalcolite compositions, which plot along the join $FeTi_2O_5$ — $MgTi_2O_5$ (adapted from *Anderson et al.,* 1970).

Apollo 11 site, where it is a minor constituent in Ti-rich basalts (*Anderson et al.,* 1970). Its composition is strictly defined as $(FeO_5Mg0_5)Ti_2O_5$, but the name is also used in a broader sense to describe *solid solutions* whose compositions vary between $FeTi_2O_5$ and $MgTi_2O_5$ (Fig. 5.28).

Armalcolite has a crystal structure like that of the mineral *ferropseudobrookite* ($FeTi_2O_5$; Fig. 5.29). Titanium is restricted to the M2 site, and Mg, Al, and Fe occupy the M1 site. Detailed chemical analyses of armalcolite, with careful consideration of the ionic charge balance required within the crystal structure, have shown that appreciable Ti is present as Ti^{3+} rather than Ti^{4+} (Fig. 5.30; *Wechsler et al.,* 1976). *Kesson and Lindsley* (1975) examined the effects of Ti^{3+}, Al^{3+}, and Cr^{3+} on the stability of armalcolite, and later work showed that the Ti^{3+} content can be used to deduce the *fugacity* (effective partial pressure in terms of thermodynamic chemical potential) of oxygen during crystallization (*Stanin and Taylor,* 1979, 1980). The presence of reduced Ti (Ti^{3+}) as well as Ti^{4+} in lunar armalcolites, due to the strongly reducing lunar environment, serves to distinguish between the lunar mineral from the armalcolites subsequently identified on Earth (*Cameron and Cameron,* 1973), in which all Ti occurs as Ti^{4+}.

The occurrence of armalcolite is restricted to rocks with high TiO_2 content that have also cooled rapidly. This rapid cooling (*quenching*) *is* essential to prevent early-formed armalcolite from reacting with the remaining liquid to form magnesian ilmenite. There are three distinct compositional types of armalcolite in lunar samples (*Haggerty,* 1973a; Fig. 5.31). The first and most abundant type is *Fe-Mg armalcolite* ("A" in Fig. 5.31), and it is represented by intermediate compositions in the solid solution series $FeTi_2O_5$-$MgTi_2O_5$ (Table A5.14). This variety is the typical armalcolite observed in the high-Ti Apollo 11 and 17 basalts, although it is also found in basalt samples from all missions. Two varieties of this type have been characterized by their appearance in reflected-light microscopy as gray- vs. tan-colored; *Haggerty* (1973b) referred to these as ortho- and para-armalcolite respectively. They have overlapping compositions (*Papike et al.,* 1974; *Williams and Taylor,* 1974) and appear to be present in a range of different textures. The most common type is the gray variety, which occurs with rims of high-Mg ilmenite, especially in Apollo 17 samples. There were suggestions that these two varieties had different crystal structures, but the crystal structures have since been shown to be identical (*Smyth,* 1974).

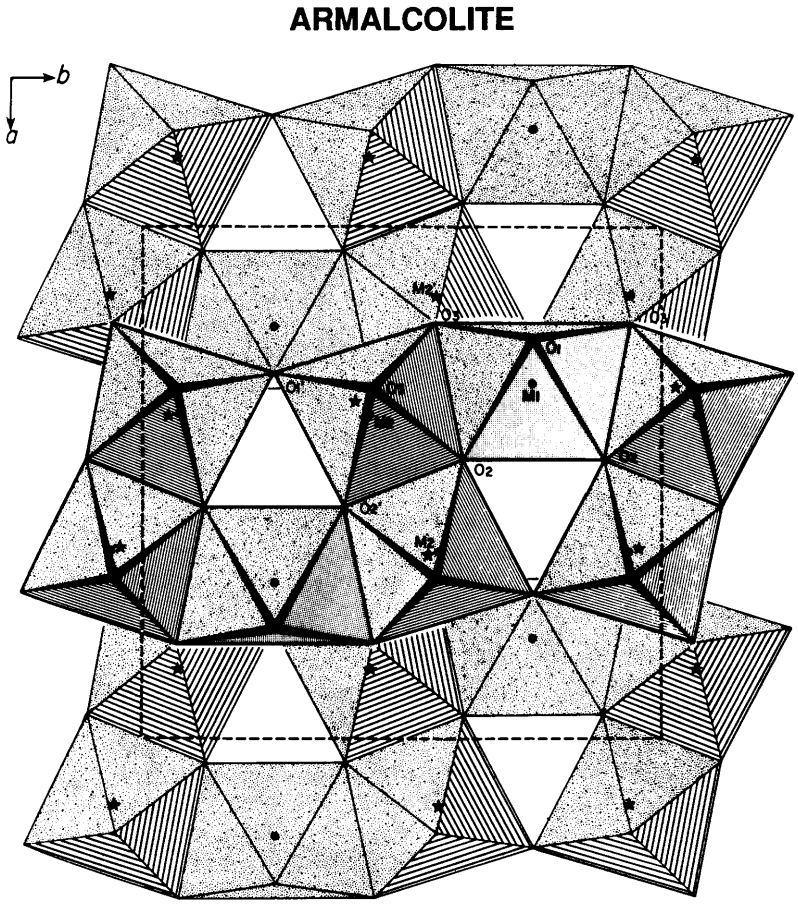

Fig. 5.29. Crystal structure of armalcolite, composed of octahedra defined by oxygen atoms. The octahedra are strongly deformed, and the oxygens do not approach close packing. Cations occur within the octahedra at M-sites. Dots indicate M1 sites, which contain Fe and Mg; stars represent M2 sites, which contain Ti. Directions of *a* and *b* crystallographic axes are shown at upper left, and dashed lines indicate the unit cell (adapted from the pseudobrookite structure of *Wechsler et al.,* 1976).

The second compositional type of armalcolite is characterized by high contents of ZrO_2 (3.8-6.2 wt.%), Cr_2O_3 (4.3-11.5 wt.%), and CaO (3.0-3.5 wt.%). This has been called *Cr-Zr-Ca-armalcolite* ("C-Z-A" in Fig. 5.31). The third type is intermediate in composition between the first type, Fe-Mg armalcolite, and the second type, Cr-Zr-Ca armalcolite. It has been called *Zr-armalcolite* ("Z-A" in Fig. 5.31) and has distinctive amounts of ZrO_2 (2.0-4.4 wt.%), Y_2O_3 (0.15-0.53 wt.%), and Nb_2O_5 (0.26-0.65 wt.%). Detailed descriptions and analyses of these various types of armalcolite are given in Table A5.14 and by *Haggerty* (1973a).

5.2.4. Other Oxides

The only other oxide minerals of significant abundance in lunar rocks and soils are *rutile* (TiO_2) and *baddeleyite* (ZrO_2); representative compositions

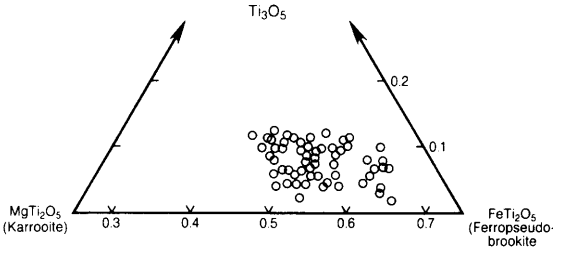

Fig. 5.30. Compositions of armalcolites (in mol.%) from lunar mare basalts, plotted on a triangular composition diagram in the system $MgTi_2O_5$ — $FeTi_2O_5$ — $Ti^{3+}{}_2Ti^{4+}O_5$. Compositions are calculated from electron microprobe chemical analyses. Note that the compositions are all displaced from the $MgTi_2O_5$ — $FeTi_2O_5$ join, indicating that significant amounts of Ti are present in the reduced form of Ti^{3+} (adapted from *Wechsler et al.,* 1976).

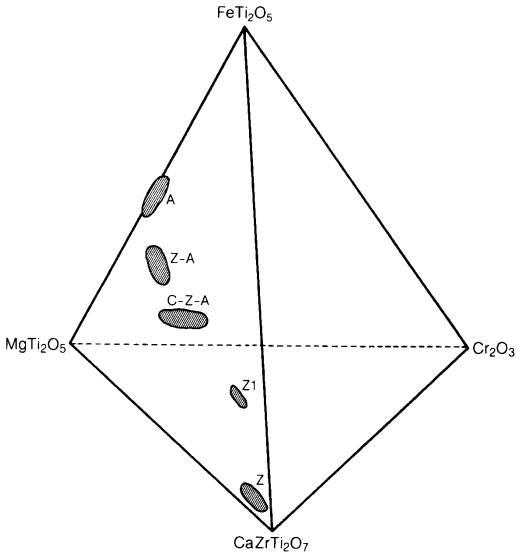

Fig. 5.31. Compositional tetrahedron (in wt.%) showing compositions of different varieties of lunar armalcolites (adapted from *Haggerty, 1973*). Normal armalcolites (A) lie along the line between $MgTi_2O_5$ and $FeTi_2O_5$. Zr-armalcolites (Z-A) and Cr-Zr-Ca armalcolites (C-Z-A) are displaced toward the high-Cr and high-Zr apices. "Phase Z1" is a possible new mineral from the Apollo 15 site, and (Z) indicates the mineral *zirconolite*.

of these phases are given in Table A5.15. Rutile is generally associated with ilmenite, and it occurs most commonly as a reaction product from the reduction of ilmenite and/or armalcolite. Primary rutile occurs as discrete euhedral grains, also typically associated with ilmenite. Rutile in this association often contains Nb, Cr, Ta, and lanthanide elements (*Marvin,* 1971; *Hlava et al.,* 1972; *El Goresy and Ramdohr,* 1975; Table A5.15). Baddeleyite is common in certain Apollo 14 clast-poor impact melt rocks (e.g., 14310, 14073; section 6.4) where it is associated with schreibersite [$(Fe,Ni,Co)_3P$; *El Goresy et al.,* 1971a]. Although these two minerals were originally thought to be indigenous to the Moon, it is now thought probable that the high Zr and P contents of these baddeleyite- and schreibersite-bearing rocks arise from meteoritic contamination that was incorporated into the original melts, which were produced by large meteoroid impact events.

Although rare on the Moon and not truly an oxide, the compound FeOOH has been found and often described as "rust" in lunar rocks from every mission, particularly those from Apollo 16 (*El Goresy et al.,* 1973a,b; *Taylor et al.,* 1973a). It has been conclusively shown that this phase, the mineral *akaganeite* (β-FeOOH), is the product of contamination of the lunar rocks by terrestrial water vapor, which caused the oxyhydration of indigenous *lawrencite,* $FeCl_2$, to form this water-bearing phase (*Taylor et al.,* 1973a). Therefore, to date, no evidence for indigenous water has been found in any lunar minerals.

5.3. SULFIDE MINERALS

Sulfur is a relatively volatile element (section 8.7.7) that plays a dual role on the Moon: in the gases that drove lunar pyroclastic eruptions (section 4.2.1), and in the gases released during impact heating. For a planet with a surface otherwise poor in volatile elements, the Moon has a fair amount of sulfur. Lunar mare basalts, for instance, have about twice as much sulfur as do typical terrestrial basalts. On the Moon, this sulfur is present in sulfide (S) minerals; the low oxygen partial pressures in the lunar environment apparently do not permit the formation of sulfate (SO_4) minerals.

5.3.1. Troilite

Troilite (FeS) is the most common sulfide mineral in lunar rocks. Although it almost always forms less than 1% by volume of any lunar rock, troilite is ubiquitous. It is commonly associated with native Fe, ilmenite, and spinel. The chemical composition of troilite is essentially that of FeS with less than 1 wt.% of all other components (Table A5.16).

Based on study of a small number of early Apollo samples, *Skinner* (1970) proposed that lunar troilite was always associated with native Fe in textures that result from crystallization at the 988°C *eutectic* point where both FeS and Fe form simultaneously. The formation of an immiscible sulfide melt late in the crystallization of a silicate magma preceded this eutectic crystallization. Some lunar troilite has undoubtedly formed in this way. However, other troilite occurrences are void of native Fe and require precipitation directly from the S-saturated silicate melt.

The most common occurrence of troilite is as an accessory phase in mare basalts, where it is usually a late-stage crystallization product. Such primary troilite forms when the original bulk composition of the melt, in particular the sulfur content, is appropriate. Secondary troilite forms later, in the solid rocks, in cases where the partial pressure of sulfur increases rapidly and sulfurizes native Fe during the high-temperature shock metamorphism produced by meteoroid impacts. Some Apollo 16 rocks, notably 66095, contain troilite that most likely formed as a direct result of this remobilization of sulfur during meteoroid impact.

5.3.2. Other Sulfides

Other sulfide minerals positively identified in lunar rocks include *chalcopyrite* ($CuFeS_2$), *cubanite* ($CuFe_2S_3$), *pentlandite* [$(Fe,Ni)_9S_8$], *mackinawite* ($Fe_{1+x}S$), and *sphalerite* [(Zn,Fe)S]. All these minerals are so rare as to be only geologic curiosities, and they have only minor applications in determining the origins of the rocks that contain them.

The Cu-bearing phases have only been found as small grains (<10-15 μm) in some Apollo 12 basalts (*Taylor and Williams,* 1973) and in small cavities (vugs) in two Apollo 17 breccias, where chalcopyrite is associated with pentlandite (*Carter et al.,* 1975). Pentlandite has also been reported from an Apollo 14 breccia (*Ramdohr,* 1972). Mackinawite was identified as small (<5 μm) grains in certain Apollo 12 basalts (*El Goresy et al.,* 1971b; *Taylor et al.,* 1971). Sphalerite (with 28 mol.% FeS in solution with ZnS) was observed in some Apollo 16 breccias, notably 66095 (Table A5.16; *El Goresy et al.,* 1973; *Taylor et al.,* 1973a), where it was probably formed as a result of the mobilization of Zn and S during impact-produced shock metamorphism. It is only present as small grains (<20 μm) and in minor quantities (<0.01 vol.%).

5.4. NATIVE FE

Native iron metal, Fe°, is only rarely found in terrestrial rocks. However, in lunar rocks it is a ubiquitous minor phase, largely because of the low oxygen partial pressures during original crystallization of lunar magmas (Fig. 5.17) and during subsequent meteoroid impacts.

Native Fe occurs in lunar rocks as three different minerals with different crystal structures. These minerals occur in various proportions and form intricate textures, either from exsolution during cooling or from later subsolidus reequilibration. These three minerals also have different chemical compositions, involving varying amounts of solid solution between Fe and Ni. *Kamacite* (alpha-type iron) has a body-centered cubic crystal structure and contains 0-6 wt.% Ni. *Taenite* (gamma-type iron) has a face-centered cubic crystal structure and contains 6-50% Ni. *Tetrataenite* has a tetragonal crystal structure and is essentially FeNi, with 50±2% Ni.

In lunar samples, kamacite is the most abundant metal phase and taenite the second most abundant. Tetrataenite is only rarely observed, and that which occurs is most likely due to meteoritic contamination. These minerals are apparently formed by four different processes: (1) normal igneous crystallization; (2) subsolidus reduction of oxides (see section 5.2.2), or of troilite and olivine (this process has occurred in rocks 14053 and 14072); (3) reduction of the FeO component in impact-produced silicate melts in the soil; and (4) meteoroid contamination. Effects of the first and second processes are readily apparent and were easily recognized in the first returned samples. The meteoroid metal component is to be expected because of the large flux of impacting bodies onto the lunar surface. However, the discovery that abundant native Fe could be produced in the soils during impact melting was unexpected. At first, the observation of significant Fe metal in the lunar soils presented a quandary: Was the metal produced by a surface process or was it simply meteoroid contamination? The resolution of this question, and the recognition that Fe metal in the lunar soil comes from several sources, are discussed in more detail in section 5.4.3.

5.4.1. Meteoritic Contamination

It is important to determine how much of the FeNi metal found in the lunar soil is actually extralunar in origin, having been brought in as a component of the meteoroids that have bombarded the Moon over geologic time. Unfortunately, making this distinction is a major problem, and the results to date are controversial. An early method of distinguishing between lunar and meteoroid metal was based on Ni and Co contents. Figure 5.32 shows a plot of Co vs. Ni contents for native Fe metal. The "meteoritic field" is a region originally designated as unique to metal from meteoroids (*Goldstein and Yakowitz,* 1971). However, these boundaries were established with earlier data, obtained by others, on the whole-rock compositions of iron meteorites, and these data were incorrectly presented as indicative of meteoroid metal as a whole (for further discussion, see *Misra and Taylor,* 1975a,b). Most meteorites are stony, not iron, and the metal they contain can vary widely from the bulk composition of iron meteorites.

As a result of newer data, it is now clear that these earlier boundaries are no longer valid for distinguishing between lunar and meteoroid metal and that there is extensive overlap between the two. If the composition of metal lies within the "meteoritic" field in Fig. 5.32, this does not imply that it is of meteoroid origin; it may have an indigenous lunar origin. Nor does a composition of Fe metal outside this area mean that it is lunar in origin. The Ni and Co contents of native Fe metal can vary considerably, from 0% to over 50% Ni and from 0% to 8% Co. For example, Fig. 5.33 shows the range of compositional variation (*Misra and Taylor,* 1975a) in several Apollo 16 highland samples. Of all lunar samples, it is reasonable to suppose that the older highland rocks contain the greatest amount of introduced meteoroid metal; however, determination

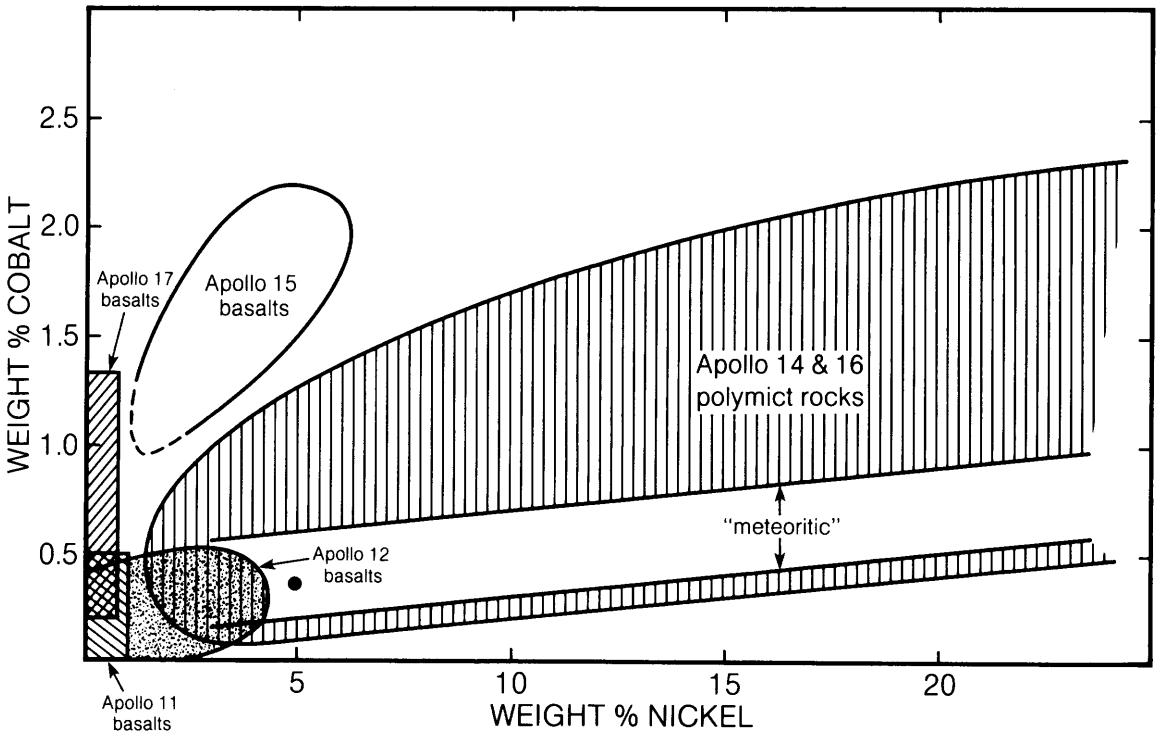

Fig. 5.32. Plot of Co and Ni contents (in wt.%) of the Fe metal phase occurring in mare basalts (*pristine* rocks) and breccias (*polymict* rocks) from different Apollo landing sites. The region for metal from the Apollo 14 and 16 polymict rocks is from *Ryder et al.* (1980). The solid circle at about 5% Ni represents the average composition of chondritic meteorites. The region labeled "meteoritic" was established by early work on iron meteorites (*Goldstein and Yakowitz,* 1971) and is used here only for reference. Later work has shown that the compositions of meteoritic metal can extend far beyond this region (see text for discussion).

of the exact amount is not possible by using the "meteoritic" range of Fig. 5.32. For example, it would appear that many of these rocks do not contain any lunar metal, if the criteria of *Goldstein and Yakowitz* (1971) are used. Based upon other chemical criteria, this is not likely.

The best means of determining the meteoroid contribution to the metal contents of lunar soils and breccias is through use of the rarer *siderophile* (i.e., readily soluble in molten iron) elements, other than Ni (*Ganapathy et al.,* 1970; *Pearce and Chou,* 1976; *Reed and Taylor,* 1974; *Wlotzka et al.,* 1973). These elements, which tend to concentrate in Fe-metal minerals, especially during melting processes, include Au, Pt, Ir, Os, Mo, and Ge. Because lunar rocks contain relatively small amounts of these elements compared to meteoroid FeNi metal, estimates can be made about the quantity of meteoroid material in a soil or breccia (see sections 6.4 and 8.6). It has been determined, for example, that the average Apollo 16 soil contains about 2% input from chondritic meteoroids. In addition, the siderophile content of a sample, particularly the amount of iridium (Ir), has been successfully used as a criterion for distinguishing between *pristine* and meteorite-contaminated lunar rocks (sections 6.3 and 6.4).

5.4.2. Native Fe in Lunar Rocks

One of the surprising findings from the first-returned lunar samples, Apollo 11 mare basalts, was the presence of native Fe metal grains in every sample (e.g., *Reid et al.,* 1970). These metal grains were produced by the crystallization of normal igneous melts under reducing conditions. Subsequently, native Fe metal was identified in all returned lunar rocks. The amount of metal varies between samples as well as between sites, but is always less than 1% by volume. Representative analyses of metals are listed in Table A5.17. In the mare basalts, native Fe makes up only a small portion of the opaque (i.e., "black" in transmitted-light microscopy)

mineral content, which is mostly formed of the oxide minerals ilmenite and spinel. However, in some highland rocks such as the Apollo 16 breccias, native Fe is virtually the only opaque mineral present (*Misra and Taylor,* 1975a,b). Some cubic Fe crystals have grown in the open spaces of breccias, apparently from Fe-rich vapor (*Clanton et al.,* 1973).

Although there are substantial variations in the compositions of native Fe among the samples from a single landing site, some differences between sites can still be recognized (Fig. 5.32). Native Fe from Apollo 11 basalts is usually low in Ni (<1%) and Co (<0.5%); metals from the Apollo 17 samples are similar but may have higher Co content. Metals from Apollo 12 and 15 basalts have compositions with 0-30% Ni and 0-6% Co. The high-Ni and high-Co content metals in these basalts are rare, however, and the majority of lunar metal compositions fall within the areas shown in Fig. 5.32. Such correlations should be treated with caution, however, because major differences in metal composition can exist even within a single sample. Native Fe enclosed within early-formed olivine crystals can contain 30% Ni, whereas that in the later-crystallized parts of the rock can be virtually pure Fe (i.e., <0.2% Ni). The metal in breccias from the Apollo 14 and 16 sites is difficult to distinguish from meteoroid metal and has wide-ranging compositions similar to those reported for meteorites (i.e., 0% to more than 50% Ni; 0-8% Co).

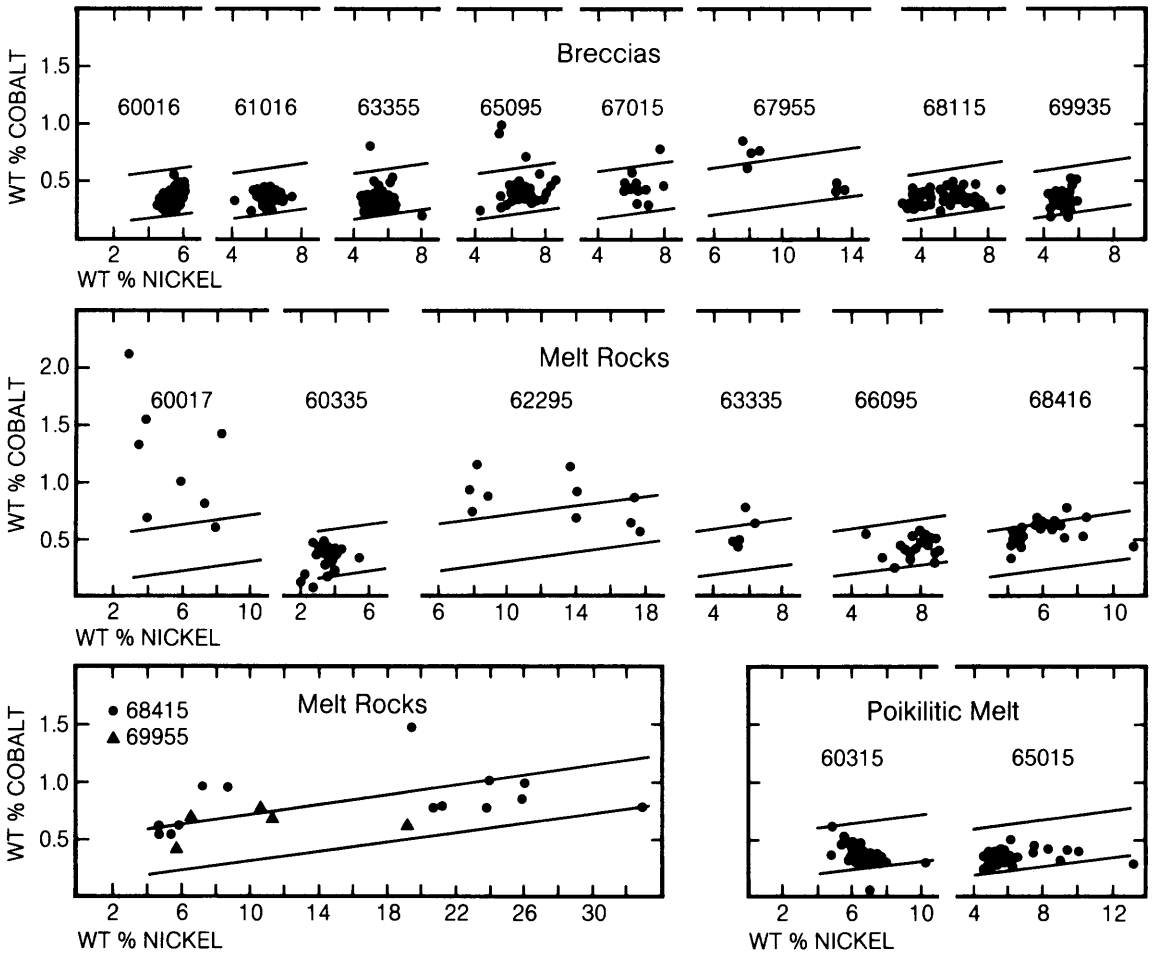

Fig. 5.33. Plots of Ni vs. Co contents (wt.%) of Fe metal grains in Apollo 16 rocks (adapted from *Misra and Taylor,* 1975a). The samples include fragmental rocks (*breccias*), relatively fine-grained crystallized clast-poor impact *melt rocks,* and coarsely crystalline (*poikilitic*) clast-poor impact melt rocks. The parallel diagonal lines outline the "meteoritic" region of *Goldstein and Yakowitz* (1971) and are used here only for reference (see text for discussion).

5.4.3. Native Fe in Lunar Soil

The lunar soil consists of comminuted rocks and minerals. Therefore, any mineral occurring in the rocks can become part of the soil (*Taylor,* 1988). In particular, the native Fe metal grains now observed in the soil can have formed originally by normal crystallization of a silicate melt or by later subsolidus reduction of other minerals (e.g., oxides in the cooling magma). In addition, a large amount of metal can be contributed by impacting meteoroids. As a result of these diverse sources, the compositions of lunar Fe metal vary from essentially pure Fe to virtually any composition in the range reported for meteoritic metal. The compositions of metal grains larger than a few micrometers (i.e., those large enough for *electron microprobe* analysis), when taken as a whole for a given soil, tend to center around a bulk composition of Ni = 5-6% and Co = 0.3-0.5%; these values are the same as the average compositions of metal in chondrite meteorites (Fig. 5.32).

However, magnetic studies of the lunar soil indicate that a significant amount of Fe metal is present as much smaller particles, well below 0.1 μm in size. *Tsay et al.* (1971) noticed that the ferromagnetic resonance (FMR) signal for *single-domain* Fe (i.e., from grains 40 to 330 Å in size) in the lunar soil was an order of magnitude greater than that from associated rock samples (see review article by *Taylor and Cirlin,* 1986). These studies indicated that there is considerably more Fe metal in the lunar soils than in the rocks from which they were derived, that much of it is very fine-grained (<300 Å), and that it is not meteoroid metal. Since the soils are composed of disaggregated rock material, what is inherently different between the lunar rocks and soils? That is, where did this additional Fe metal come from? It must be produced by a process involved in the formation of the lunar soil itself.

There are two principal processes at work in forming lunar soils: (1) simple *disaggregation,* or the breaking of rocks and their minerals into smaller particles; and (2) *agglutination,* the welding together of rock and mineral fragments by the glass produced by melting due to small meteoroid impacts (the glass-welded particles are called *agglutinates;* see section 7.1.3). These two processes compete to decrease and increase, respectively, the grain size of soil particles (*Morris,* 1977, 1980).

The agglutinates contain much of the fine-grained, single-domain Fe metal particles in the soil. The majority of the metal grains in the agglutinates are from 100-200 Å in size, well within the single-domain size range of 40-330 Å for metallic Fe. The composition of most of these minute Fe particles is >99% Fe with only trace amounts of Ni and Co (*Mehta and Goldstein,* 1979). By contrast, metal grains that are larger than a few micrometers across have higher Ni, Co, and P contents; these may be finely disseminated particles of meteoroid metal. Further details are contained in numerous studies characterizing the nature of the native Fe in lunar soils from various missions (e.g., *Axon and Goldstein,* 1973; *Goldstein and Axon,* 1973; *Goldstein and Blau,* 1973; *Hewins and Goldstein,* 1974, 1975; *Ivanov et al.,* 1973; *Mehta et al.,* 1979; *Misra and Taylor,* 1975a,b).

What is the origin of this abundant single-domain metallic iron? As originally discussed by *Tsay et al.* (1971), and reiterated later by others (e.g., *Housley et al.,* 1973), the soil particles at the surface before the impact are exposed to the solar wind, and they are effectively saturated with solar-wind-implanted protons (hydrogen nuclei) and carbon atoms in the outer 0.1 μm of their surface. When the soil is melted by a small micrometeoroid impact, these elements produce an extremely reducing environment, which causes reduction of the Fe^{2+} in the agglutinate melt to Fe°. This Fe metal then precipitates as myriad tiny Fe° spheres disseminated throughout the quenched melt, i.e., in the agglutinate glass. This *autoreduction* process is responsible for producing the additional Fe° that occurs in agglutinate particles. Unfortunately, although this additional Fe metal is abundant in the soil, it is extremely fine-grained and may be too fine for easy concentration and beneficiation to produce iron metal as a resource. Possibly, heat treatment to produce Fe metal grain coarsening could make agglutinates into a more desirable feedstock for resource applications.

5.5. PHOSPHATE MINERALS

Lunar rocks and soils generally contain about 0.5 wt.% P_2O_5, most of which is contained in the phosphate minerals *whitlockite* [ideally $Ca_3(PO_4)_2$] and *apatite* [ideally $Ca_5(PO_4)_3(OH,F,Cl)$; *Friel and Goldstein,* 1977], which occur in very minor amounts in most lunar rocks. Whitlockite and apatite generally form crystals with hexagonal cross-sections. Apatite crystals with two well-shaped pyramidal ends (*doubly-terminated*), thought to be vapor-deposited, have been found in gas-formed cavities within lunar rocks.

As is the case for most minor lunar minerals, the phosphates occur as late-stage crystallization products in mare basalts. However, they are more abundant, and crystallize earlier, in certain KREEPy (K, rare earth element, and P-rich) highland samples. Phosphates are also commonly found in association with metal particles (*Friel and Goldstein,* 1977); in such occurrences they have probably formed by the oxidation of phosphorus out of the metal (*Friel and Goldstein,* 1976, 1977).

Of the two major lunar phosphates, whitlockite is more abundant and has higher rare earth element (REE; La to Lu) contents. As Table A5.18 shows, lunar whitlockite can also contain significant amounts of FeO, MgO, Na_2O, and Y_2O_3, as well as the REEs (especially the light REEs, La_2O_3, Ce_2O_3, Nd_2O_3). It is also U-enriched; crystals from the Apollo 12 basalts contain ~100 ppm U (*Lovering and Wark,* 1971). These compositions contrast sharply with terrestrial and meteoritic whitlockites, which contain only trace amounts of rare earth elements (*Albee and Chodos,* 1970). Table A5.18 also shows that lunar whitlockites have a fairly wide range of Fe:Mg ratios. On the other hand, the REE contents do not vary so widely, especially in whitlockites from KREEP-rich basalts (e.g., *Simon and Papike,* 1985). These data suggest the existence of a fairly uniform KREEP component across the Moon (*Warren and Wasson,* 1979; *Warren,* 1985).

As shown by the formula given above, apatite contains one OH, F, or Cl position per formula unit, and in terrestrial apatites the OH content may be quite high relative to F and Cl. However, the general lack of water in lunar samples causes lunar apatites to have low OH contents, and analyses indicate that they are Cl- and F-rich. Some nearly pure fluorapatites have been found on the Moon (e.g., *Fuchs,* 1970), containing over 3 wt.% F out of a possible maximum of 3.8%. This F-rich end member (also found in human teeth) is the harder and more durable of apatite variants. The analyses in Table A5.18 also show that some "chlorofluorapatites" have also been found. Chlorine-rich apatites are typically characteristic of high-temperature rocks (*Albee and Chodos,* 1970) and meteorites (*Fuchs,* 1969; *Dodd,* 1981).

There are other major- and trace-element differences between lunar and terrestrial apatites. Lunar apatites have higher Si, Y, and REE contents. The ionic exchanges involved in producing these compositions are largely Si^{4+} for P^{5+}, balanced by REE^{3+} and Y^{3+} for Ca^{2+} (*Fuchs,* 1970).

Both whitlockite and apatite are important REE carriers in lunar rocks, and they are enriched in REE relative to their terrestrial counterparts. The lunar whitlockites have higher REE contents than lunar apatites (e.g., La, Ce, Nd; Table A5.18). At least some of this difference between apatite and whitlockite can be attributed to different crystal/liquid *distribution coefficients* (K_d: the ratio between the amount of an element in a mineral crystallizing from a melt and the amount of the same element in the melt itself). Experimental work by *Dickinson and Hess* (1983) shows K_ds of about 9.5 for the distribution of light REE (Ce-Sm) in the system whitlockite/melt, compared to K_ds of about 2.5-5 for apatite/melt. The apatite distribution coefficients can approach and even exceed those of whitlockite in Si-rich liquids (*Watson and Green,* 1981; *Dickinson and Hess,* 1983), but Si-rich liquids are rare on the Moon.

APPENDIX

Compositions of Lunar Minerals

Numerous analyses have been made of lunar minerals. Almost all of the analyses made have been done by electron microprobe, a technique of microanalysis that allows accurate determinations of mineral compositions from samples as small as 5-10 μm. Elements with atomic number equal to or greater than F are routinely determined by this technique; oxygen abundances are assumed based on the relative abundances of the heavier elements. All the data in this appendix were collected by electron microprobe.

These appendix tables provide for each mineral analysis (1) the measured element abundance in weight percent, recalculated as an oxide if it is known to occur with oxygen in the mineral structure, and (2) the cation molecular proportions of the analysis (where the mineral consists of an oxygen framework, these cation abundances are calculated in terms of a given number of oxygens). For most of the silicate minerals, the ratios of certain major cations are also listed; these ratios determine the positions of plotted points in several of the diagrams in section 5.1.

References are provided for each analysis, to provide more detailed information should the reader need it. An indication of the rock type (or soil) from which the analysis was obtained is also listed, based on the categories of rock types described in Chapter 6. These rock types are listed in Table A5.1. For the mare basalts, ranges of host rock chemistry are given in parentheses (Table A5.1) where chemical composition is an important part of the mare rock classification. For highland rocks, features of mineral, glass, and fragmental makeup are listed, for these are more important in rock classification.

TABLE A5.1. Listing of rock types and corresponding abbreviations for Chapter 5 mineral chemistry tables.

Rock Type	Table Symbol
Mare Basalts (see section 6.1 for more detail)	
High-Ti (>9% TiO_2)	
Apollo 11	
high-K (>0.3% K_2O)	A-11 HK
low-K (<0.11% K_2O)	A-11 LK
Apollo 17	A-17
Low-Ti (1.5-9% TiO_2)	
Apollo 12	
pigeonite (<10% MgO, <5% TiO_2)	A-12 pig
olivine (>10% MgO, <5% TiO_2)	A-12 ol
ilmenite (<10% MgO, >5% TiO_2)	A-12 ilm
Apollo 15	
pigeonite (<10% MgO, <5% TiO_2)	A-15 pig
olivine (>10% MgO, <5% TiO_2)	A-15 ol
Aluminous, Low-Ti (>10% Al_2O_3, 2-5% TiO_2)	
Luna 16	L-16 Al
Apollo 14	A-14 Al
Very-High-K (>0.6% K_2O)	VHK
Very Low-Ti (<1.5% TiO_2)	
Apollo 17	A-17 VLT
Luna 24	L-24 VLT
Highland Igneous and Monomict Rocks (section 6.3)	
KREEP rocks (high K, rare earths, and P)	KREEP
Ferroan Anorthosites (Low-Na plagioclase, low-Mg pyroxene)	Fan
Mg-rich Rocks (variable plagioclase, high-Mg pyroxene)	Mg rock
Alkali Anorthosites (relatively high-Na plagioclase)	Alk an
Granite (or felsite) (K-feldspar, silica minerals)	Granite
Highland Polymict Rocks (see section 6.4)	
Fragmental Breccias (mainly fragments)	Frag br
Glassy Melt Breccias (glass with some fragments)	Glassy br
Crystalline Melt Breccias (crystallized melt with some fragments)	Cryst br
Clast-poor Impact Melt Rocks (crystallized melt with rare fragments)	Melt rock
Granulitic Breccias (recrystallized)	Gran br
Dimict Breccias (two rock types joined)	Dimict
Regolith Breccias (compressed soil)	Reg br
Soil (single crystals in soil, from unknown rock types)	Soil

TABLE A5.2. Pyroxene analyses from mare basalts.

	High-Ti Basalts															
	Apollo 17						Apollo 11 High-K						Apollo 11 Low-K			
	1.	2.	3.	4.	5.	6.	7.	8.	9.	10.	11.	12.	13.	14.	15.	16.
Chemical Composition (Weight Percent)																
SiO_2	44.50	48.50	52.10	50.40	49.20	53.80	50.60	44.10	49.90	45.20	49.80	46.10	46.60	47.00	49.32	47.09
Al_2O_3	7.70	2.73	1.64	2.50	3.93	0.96	3.40	1.43	2.56	0.88	2.79	1.09	5.25	1.85	3.17	0.86
TiO_2	6.00	2.20	1.33	1.78	3.37	0.78	2.76	1.06	2.47	0.72	2.39	0.79	3.74	1.41	2.49	0.72
Cr_2O_3	0.98	0.52	0.50	0.71	1.00	0.31	0.0	0.06	0.58	0.06	0.61	0.09	0.60	0.29	0.45	0.06
FeO	8.10	19.10	16.70	13.10	9.55	18.40	12.00	45.80	11.10	43.90	11.80	42.80	9.60	28.00	10.95	41.07
MnO	0.28	0.50	0.30	0.29	0.0	0.0	0.0	0.59	0.18	0.59	0.25	0.58	0.25	0.53	0.08	0.67
MgO	12.00	10.70	20.40	15.40	16.10	22.80	16.60	1.72	15.90	1.40	16.40	2.24	14.40	7.20	14.80	2.29
CaO	20.70	16.00	6.80	15.80	17.40	3.68	15.20	3.52	16.50	6.12	15.50	6.57	18.80	12.60	17.95	8.04
Na_2O	0.19	0.17	0.0	0.09	0.0	0.0	0.10	0.03	0.0	0.0	0.12	0.0	0.0	0.0	0.0	0.0
Total	100.45	100.42	99.77	100.07	100.55	100.73	100.66	98.31	99.19	98.87	99.66	100.26	99.24	98.88	99.21	100.80
Cation Formula Based on 6 Oxygens (Ideal Pyroxene = 4 Cations per 6 Oxygens)																
Si	1.668	1.873	1.934	1.891	1.820	1.967	1.868	1.923	1.877	1.952	1.866	1.947	1.762	1.908	1.861	1.965
^{iv}Al	0.332	0.124	0.066	0.109	0.171	0.033	0.132	0.074	0.114	0.045	0.123	0.053	0.234	0.089	0.139	0.035
Total tet*	2.000	1.997	2.000	2.000	1.991	2.000	2.000	1.997	1.991	1.997	1.989	2.000	1.996	1.997	2.000	2.000
Ti	0.169	0.064	0.037	0.050	0.094	0.021	0.077	0.035	0.070	0.023	0.067	0.025	0.106	0.043	0.071	0.023
^{vi}Al	0.008	0.0	0.006	0.002	0.0	0.008	0.016	0.0	0.0	0.0	0.0	0.001	0.0	0.0	0.002	0.007
Cr	0.029	0.016	0.015	0.021	0.029	0.009	0.0	0.002	0.017	0.002	0.018	0.003	0.018	0.009	0.013	0.002
Fe	0.254	0.617	0.519	0.411	0.295	0.562	0.371	1.671	0.349	1.585	0.370	1.512	0.304	0.950	0.345	1.433
Mn	0.009	0.016	0.009	0.009	0.0	0.0	0.0	0.022	0.006	0.022	0.008	0.021	0.008	0.018	0.003	0.024
Mg	0.670	0.616	1.129	0.861	0.887	1.242	0.913	0.112	0.891	0.090	0.916	0.141	0.812	0.436	0.832	0.142
Ca	0.831	0.662	0.271	0.635	0.690	0.144	0.601	0.165	0.665	0.283	0.622	0.297	0.762	0.548	0.726	0.359
Na	0.014	0.013	0.0	0.007	0.0	0.0	0.007	0.003	0.0	0.0	0.009	0.0	0.0	0.0	0.0	0.0
Total Cations	3.984	4.001	3.986	3.996	3.986	3.986	3.985	4.007	3.989	4.002	3.999	4.000	4.006	4.001	3.992	3.990
Cation Ratios: Ca : Mg : Fe and Fe/(Fe+Mg)																
Ca	47.4	34.9	14.1	33.3	36.8	7.4	31.9	8.4	34.9	14.5	32.6	15.2	40.6	28.3	38.1	18.6
Mg	38.2	32.5	58.9	45.1	47.4	63.7	48.4	5.7	46.8	4.6	48.0	7.2	43.2	22.5	43.7	7.4
Fe	14.5	32.6	27.0	21.6	15.8	28.9	19.7	85.8	18.3	80.9	19.4	77.5	16.2	49.1	18.2	74.1
Fe/(Fe+Mg)	0.27	0.50	0.31	0.32	0.25	0.31	0.29	0.94	0.28	0.95	0.29	0.91	0.27	0.69	0.29	0.91

TABLE A5.2. (continued).

	Low-Ti Basalts																	
	Apollo 12 Ilmenite		Apollo 12 Pigeonite						Apollo 12 Olivine				Apollo 15 Pigeonite					
	17.	18.	19.	20.	21.	22.	23.	24.	25.	26.	27.	28.	29.	30.	31.	32.	33.	34.
Chemical Composition (Weight Percent)																		
SiO_2	49.00	47.32	50.30	45.00	53.51	45.23	51.50	46.80	52.10	49.40	45.60	51.77	54.01	41.43	52.40	43.20	51.50	48.20
Al_2O_3	3.46	1.41	3.06	2.15	0.66	0.54	2.05	0.83	1.21	0.90	1.27	1.51	0.63	10.10	1.89	9.66	2.77	1.43
TiO_2	2.13	1.14	0.89	1.41	0.35	0.73	0.68	0.89	0.63	1.29	0.99	1.08	0.19	2.96	0.36	3.99	0.63	1.11
Cr_2O_3	0.97	0.18	1.38	0.09	0.74	0.05	0.93	0.09	0.52	0.13	0.0	0.37	0.77	0.02	1.04	0.66	1.06	0.45
FeO	13.31	30.28	17.10	43.10	16.69	46.54	16.90	37.80	19.20	25.70	41.90	16.34	15.76	27.68	16.90	20.10	14.50	30.20
MnO	0.24	0.43	0.36	0.51	0.29	0.56	0.37	0.56	0.38	0.44	0.52	0.32	0.28	0.39	0.0	0.0	0.0	0.0
MgO	15.64	2.64	21.60	0.41	24.26	0.34	21.90	3.80	21.40	11.10	0.29	15.34	26.26	3.90	23.90	8.58	14.20	7.41
CaO	14.44	16.24	4.54	7.69	2.61	6.43	5.10	8.90	4.59	10.50	9.16	13.99	2.02	10.98	2.62	13.80	14.70	10.80
Na_2O	0.05	0.01	0.0	0.0	0.0	0.03	0.0	0.0	0.0	0.0	0.0	0.01	0.00	0.09	0.03	0.05	0.03	0.03
Total	99.24	99.65	99.23	100.36	99.11	100.45	99.43	99.67	100.03	99.46	99.73	100.73	99.92	97.55	99.14	100.04	99.39	99.63
Cation Formula Based on 6 Oxygens (Ideal Pyroxene = 4 Cations per 6 Oxygens)																		
Si	1.853	1.943	1.879	1.910	1.973	1.947	1.916	1.953	1.940	1.948	1.945	1.941	1.96	1.70	1.935	1.676	1.941	1.941
^{iv}Al	0.147	0.057	0.121	0.090	0.027	0.027	0.084	0.041	0.053	0.042	0.055	0.059	0.03	0.30	0.065	0.324	0.059	0.059
Total tet*	2.000	2.000	2.000	2.000	2.000	1.974	2.000	1.994	1.993	1.990	2.000	2.000	1.99	2.00	2.000	2.000	2.000	2.000
Ti	0.061	0.035	0.025	0.045	0.010	0.024	0.019	0.028	0.018	0.038	0.032	0.030	0.00	0.09	0.010	0.116	0.018	0.034
^{vi}Al	0.008	0.012	0.013	0.018	0.001	0.0	0.006	0.0	0.0	0.0	0.009	0.007	0.00	0.19	0.017	0.117	0.064	0.008
Cr	0.029	0.006	0.041	0.003	0.022	0.002	0.027	0.003	0.015	0.004	0.0	0.011	0.02	0.00	0.030	0.020	0.032	0.014
Fe	0.421	1.040	0.534	1.530	0.515	1.675	0.526	1.319	0.598	0.848	1.495	0.512	0.48	0.95	0.522	0.652	0.457	1.017
Mn	0.008	0.015	0.011	0.018	0.009	0.020	0.012	0.020	0.012	0.015	0.019	0.010	0.01	0.01	0.0	0.0	0.0	0.0
Mg	0.882	0.162	1.202	0.026	1.333	0.022	1.214	0.236	1.188	0.652	0.018	0.857	1.42	0.24	1.315	0.496	0.798	0.445
Ca	0.585	0.715	0.182	0.350	0.103	0.297	0.203	0.398	0.183	0.444	0.419	0.562	0.08	0.48	0.104	0.574	0.594	0.466
Na	0.004	0.001	0.0	0.0	0.0	0.003	0.0	0.0	0.0	0.0	0.0	0.001	0.00	0.01	0.002	0.004	0.002	0.002
Total Cations	3.998	3.986	4.008	3.990	3.993	4.017	4.007	3.998	4.007	3.991	3.992	3.990	4.000	3.970	4.000	3.979	3.965	3.986
Cation Ratios: Ca : Mg : Fe and Fe/(Fe+Mg)																		
Ca	31.0	37.3	9.5	18.4	5.3	14.9	10.5	20.4	9.3	22.8	21.7	29.1	4.0	28.7	5.3	33.3	32.1	24.2
Mg	46.7	8.4	62.7	1.4	68.3	1.1	62.5	12.1	60.3	33.6	1.0	44.4	71.7	14.4	67.8	28.8	43.2	23.1
Fe	22.3	54.3	27.8	80.3	26.4	84.0	27.1	67.5	30.4	43.6	77.4	26.5	24.2	56.9	26.9	37.9	24.7	52.8
Fe/(Fe+Mg)	0.32	0.87	0.31	0.98	0.28	0.99	0.30	0.85	0.33	0.57	0.99	0.37	0.25	0.80	0.28	0.57	0.36	0.70

TABLE A5.2. (continued).

	Low-Ti Basalts				Aluminous, Low-Ti Basalts						Very Low-Ti Basalts					
	Apollo 15 Olivine				Luna 16		Apollo 14		VHK		Luna 24		Apollo 17			
	35.	36.	37.	38.	39.	40.	41.	42.	43.	44.	45.	46.	47.	48.	49.	50.
Chemical Composition (Weight Percent)																
SiO_2	51.80	49.90	51.40	47.00	49.24	46.28	51.30	45.32	51.21	51.90	49.13	44.95	50.45	48.28	53.09	45.76
Al_2O_3	2.88	1.66	2.15	1.16	3.03	0.98	1.73	1.68	1.97	1.64	3.76	0.88	5.13	2.91	1.45	1.04
TiO_2	0.90	1.21	0.83	0.92	2.48	1.16	0.84	1.62	0.83	1.45	0.89	0.76	0.39	1.26	0.20	1.19
Cr_2O_3	0.86	0.22	0.75	0.0	0.59	0.10	0.73	0.02	0.72	0.42	0.89	0.00	1.53	0.17	0.73	0.06
FeO	14.50	25.80	13.60	36.60	13.27	38.67	18.60	30.32	19.07	15.17	16.95	43.35	17.42	31.81	17.45	42.54
MnO	0.0	0.0	0.0	0.0	0.28	0.55	0.0	0.30	0.47	0.37	0.28	0.54	0.30	0.43	0.27	0.58
MgO	16.30	11.40	16.80	5.59	13.22	3.13	21.20	0.57	20.21	11.67	11.68	0.12	19.86	11.01	23.60	0.82
CaO	12.80	10.60	14.40	7.81	18.01	8.75	4.37	18.24	5.37	18.16	16.87	7.88	6.10	5.93	3.63	8.58
Na_2O	0.0	0.0	0.0	0.0	0.09	0.01	0.02	0.07	–	–	0.00	0.00	0.00	0.00	0.00	0.00
Total	100.04	100.79	99.93	99.08	100.21	99.63	98.79	98.14	99.85	100.78	100.45	98.48	101.18	101.80	100.42	100.57
Cation Formula Based on 6 Oxygens (Ideal Pyroxene = 4 Cations per 6 Oxygens)																
Si	1.928	1.935	1.921	1.948	1.86	1.94	1.928	1.913	1.915	1.956	1.875	1.955	1.853	1.887	1.945	1.938
^{iv}Al	0.072	0.065	0.079	0.052	0.14	0.05	0.072	0.084	0.086	0.044	0.125	0.045	0.147	0.113	0.055	0.052
Total tet*	2.000	2.000	2.000	2.000	2.000	1.99	2.000	1.997	2.000	2.000	2.000	2.000	2.000	2.000	2.000	1.990
Ti	0.025	0.035	0.023	0.029	0.07	0.04	0.024	0.051	0.023	0.041	0.026	0.025	0.011	0.037	0.006	0.038
^{vi}Al	0.054	0.011	0.015	0.005	0.0	0.0	0.005	0.0	0.001	0.029	0.044	0.000	0.075	0.021	0.007	0.000
Cr	0.025	0.007	0.022	0.0	0.02	0.003	0.022	0.001	0.021	0.013	0.027	0.000	0.044	0.005	0.021	0.002
Fe	0.451	0.837	0.425	1.269	0.42	1.36	0.585	1.070	0.596	0.478	0.541	1.577	0.535	1.040	0.535	1.506
Mn	0.0	0.0	0.0	0.0	0.009	0.002	0.0	0.011	0.014	0.012	0.009	0.020	0.009	0.014	0.008	0.021
Mg	0.904	0.659	0.936	0.345	0.74	0.20	1.187	0.036	1.126	0.656	0.664	0.008	1.087	0.641	1.288	0.052
Ca	0.510	0.440	0.577	0.347	0.73	0.40	0.176	0.825	0.215	0.733	0.690	0.367	0.240	0.248	0.142	0.389
Na	0.0	0.0	0.0	0.0	0.006	0.001	0.001	0.006	–	–	0.000	0.000	0.000	0.000	0.000	0.000
Total Cations	3.969	3.989	3.998	3.995	3.995	3.996	4.000	3.997	3.996	3.962	4.001	3.997	4.001	4.006	4.007	3.998
Cation Ratios: Ca : Mg : Fe and Fe/(Fe+Mg)																
Ca	27.4	22.8	29.8	17.7	38.6	20.4	9.0	42.7	11.3	39.3	36.2	18.6	12.8	12.8	7.2	20.0
Mg	48.5	34.0	48.3	17.6	39.2	10.2	61.0	1.9	57.5	35.1	34.9	0.4	58.1	33.0	65.6	2.7
Fe	24.2	43.2	21.9	64.7	22.2	69.4	30.0	55.4	31.2	25.6	28.9	81.0	29.1	54.2	27.2	77.4
Fe/(Fe+Mg)	0.33	0.56	0.31	0.79	0.36	0.87	0.33	0.97	0.35	0.42	0.45	0.99	0.33	0.62	0.29	0.97

"Total tet" = sum of Si and Al in tetrahedral sites; in ideal pyroxenes, this number = 2. Some Al (listed as ^{vi}Al) may also occur in octahedral sites.
Analyses #1 and 2 are from sample 74275 (*Hodges and Kushiro,* 1974); #3 and 4 are from sample 70017 (*Hodges and Kushiro,* 1974); #5 and 6 are from sample 70035 (*Papike et al.,* 1974); #7 is from sample 10022 (*Smith et al.,* 1970); #8 is from sample 10022 (*Kushiro and Nakamura,* 1970); #9 and 10 are from sample 10017 (*Kushiro and Nakamura,* 1970); #11 and 12 are from sample 10024 (*Kushiro and Nakamura,* 1970); #13 and 14 are from sample 10045 (*Brown et al.,* 1970); #15 is from sample 10058 (*Agrell et al.,* 1970b); #16 is from sample 10058 (*Hollister and Hargraves,* 1970); #17 and 18 are from sample 12063 (*Hollister et al.,* 1971); #19 and 20 are from sample 12052 (*Bence et al.,* 1970); #21 and 22 are from sample 12065 (*Hollister et al.,* 1971); #23 is from sample 12021 (*Dence et al.,* 1971); #24 is from sample 12021 (*Boyd and Smith,* 1971); #25 to 27 are from sample 12020 (*Kushiro et al.,* 1971); #28 is from sample 12040 (*Newton et al.,* 1971); #29 and 30 are from sample 15597 (*Weigand and Hollister,* 1973); #31 and 32 are from sample 15499 (*Bence and Papike,* 1972); #33 and 34 are from sample 15058 (*Bence and Papike,* 1972); #35 and 36 are from sample 15016 (*Bence and Papike,* 1972); #37 and 38 are from sample 15555 (*Bence and Papike,* 1972); #39 and 40 are from sample Luna 16 B-1 (*Albee et al.,* 1972); #41 is from sample 14053 (*Bence and Papike,* 1972); #42 is from sample 14053 (*Gancarz et al.,* 1971); #43 is from sample 14305 (*Shervais et al.,* I985b); #44 is from sample 14168 (*Shervais et al.,* 1985b); #45 and 46 are from sample 24174 (*Laul et al.,* 1978b); #47 and 48 are from sample 70009 (*Vaniman and Papike,* 1977c); #49 and 50 are from sample 70008 (*Vaniman and Papike,* 1977c).

TABLE A5.3. Pyroxene analyses from clast-poor melt rocks, crystalline melt breccias, and KREEP rocks.

	Melt Rocks							Cryst Melt Breccias				Melt Rocks					
	1.	2.	3.	4.	5.	6.	7.	8.	9.	10.	11.	12.	13.	14.	15.	16.	17.
Chemical Composition (Weight Percent)																	
SiO_2	54.3	52.8	49.8	53.2	52.0	53.1	49.4	53.6	51.8	53.4	51.1	54.6	53.5	45.2	53.2	49.3	54.8
Al_2O_3	4.1	1.6	0.9	1.1	2.1	4.5	1.6	1.8	2.4	1.7	2.8	2.0	0.81	1.3	3.7	2.6	0.89
TiO_2	0.32	0.50	1.1	0.23	0.69	0.36	1.3	1.1	1.6	1.2	1.7	0.34	0.40	1.5	0.74	2.5	0.36
Cr_2O_3	0.76	0.68	0.01	0.63	0.89	0.61	0.26	0.87	0.87	0.54	0.81	0.53	0.38	0.08	0.67	0.37	0.54
FeO	9.8	14.9	26.4	13.2	11.3	10.4	25.3	10.9	6.4	13.1	13.1	11.2	18.0	41.2	11.4	15.9	11.9
MnO	0.09	0.21	0.38	0.19	0.18	0.16	0.36	0.21	0.15	0.20	0.26	0.28	0.30	0.45	0.23	0.28	0.19
MgO	30.3	21.7	9.9	27.3	18.1	28.3	11.3	29.1	17.3	26.2	24.1	30.0	22.3	4.4	28.2	11.6	28.8
CaO	2.1	8.2	11.6	2.2	14.7	2.5	11.7	2.8	20.4	4.2	5.2	1.6	5.0	4.6	2.6	17.5	2.6
Na_2O	0.00	0.00	0.00	0.00	0.10	0.00	0.00	0.00	0.10	0.00	0.00	0.00	0.10	0.10	0.00	0.10	0.00
Total	101.77	100.59	100.09	98.05	100.06	99.93	101.22	100.38	101.02	100.54	99.07	100.55	100.79	98.83	100.74	100.15	100.08
Cation Formula Based on 6 Oxygens (Ideal Pyroxene = 4 Cations per 6 Oxygens)																	
Si	1.882	1.932	1.958	1.952	1.924	1.883	1.916	1.905	1.888	1.919	1.879	1.927	1.962	1.911	1.881	1.872	1.955
^{iv}Al	0.118	0.068	0.042	0.047	0.076	0.117	0.074	0.075	0.103	0.072	0.120	0.073	0.035	0.065	0.119	0.116	0.037
Total tet*	2.000	2.000	2.000	1.999	2.000	2.000	1.990	1.980	1.991	1.991	1.999	2.000	1.997	1.976	2.000	1.988	1.992
Ti	0.008	0.014	0.033	0.006	0.019	0.009	0.037	0.030	0.044	0.033	0.047	0.011	0.014	0.060	0.025	0.089	0.009
^{vi}Al	0.050	0.003	0.000	0.000	0.015	0.070	0.000	0.000	0.000	0.000	0.000	0.010	0.000	0.000	0.035	0.000	0.000
Cr	0.020	0.020	0.000	0.018	0.026	0.017	0.008	0.024	0.024	0.015	0.023	0.015	0.011	0.003	0.019	0.011	0.015
Fe	0.284	0.456	0.869	0.403	0.351	0.309	0.819	0.324	0.194	0.394	0.402	0.330	0.552	1.456	0.337	0.505	0.355
Mn	0.002	0.006	0.013	0.006	0.006	0.005	0.012	0.006	0.005	0.006	0.008	0.008	0.009	0.016	0.007	0.009	0.005
Mg	1.567	1.186	0.582	1.491	0.998	1.498	0.655	1.541	0.945	1.405	1.317	1.578	1.219	0.277	1.486	0.657	1.533
Ca	0.078	0.323	0.491	0.084	0.582	0.095	0.487	0.107	0.797	0.160	0.205	0.060	0.196	0.208	0.099	0.712	0.098
Na	0.000	0.000	0.000	0.000	0.008	0.000	0.000	0.000	0.006	0.000	0.000	0.000	0.007	0.005	0.000	0.007	0.000
Total Cations	4.009	4.008	3.988	4.007	4.005	4.003	4.008	4.012	4.006	4.004	4.001	4.012	4.005	4.001	4.008	3.978	4.007
Cation Ratios: Ca : Mg : Fe and Fe/(Fe+Mg)																	
Ca	4.0	16.4	25.1	4.3	30.1	5.0	24.7	5.4	41.1	8.2	10.6	3.1	10.0	10.7	5.1	38.0	4.9
Mg	81.1	60.2	29.8	75.1	51.5	78.6	33.2	77.9	48.6	71.5	68.2	80.1	62.0	14.3	77.3	35.0	77.0
Fe	14.9	23.4	45.1	20.6	18.4	16.4	42.1	16.7	10.3	20.3	21.2	16.8	28.0	75.0	17.5	27.0	18.1
Fe/(Fe+Mg)	0.15	0.28	0.60	0.21	0.26	0.17	0.56	0.17	0.17	0.22	0.23	0.17	0.31	0.84	0.18	0.43	0.19

TABLE A5.3. (continued).

	Cryst Melt Breccias						KREEP						
	18.	19.	20.	21.	22.	23.	24.	25.	26.	27.	28.	29.	30.
Chemical Composition (Weight Percent)													
SiO_2	54.1	50.3	53.9	50.4	55.1	50.7	53.4	51.8	49.5	53.5	51.5	49.2	48.3
Al_2O_3	2.9	3.6	2.4	2.7	1.8	4.9	3.0	1.9	1.1	1.6	1.5	2.6	1.4
TiO_2	0.79	3.0	0.56	2.2	0.54	1.8	0.6	0.85	0.82	0.51	0.97	2.0	0.91
Cr_2O_3	0.83	0.72	0.64	0.48	0.60	0.17	0.92	0.85	0.27	0.79	0.92	1.00	0.37
FeO	9.0	6.6	10.5	10.5	10.9	14.7	11.7	19.0	30.8	14.1	20.4	13.4	32.3
MnO	0.15	0.21	0.13	0.14	0.16	0.20	0.09	0.25	0.49	0.20	0.34	0.24	0.52
MgO	30.9	16.6	29.5	15.3	30.2	14.4	28.9	23.0	11.0	26.9	19.6	13.0	8.8
CaO	1.5	19.5	1.5	18.2	1.7	14.4	1.40	2.2	6.2	1.7	5.1	17.9	8.9
Na_2O	0.00	0.2	0.00	0.10	0.00	0.20	0.00	0.00	0.00	0.00	0.00	0.00	0.00
Total	100.17	100.73	99.13	100.02	101.00	101.47	100.01	99.85	100.18	99.30	100.33	99.34	101.50
Cation Formula Based on 6 Oxygens (Ideal Pyroxene = 4 Cations per 6 Oxygens)													
Si	1.901	1.842	1.923	1.881	1.932	1.871	1.901	1.920	1.958	1.941	1.930	1.878	1.920
^{iv}Al	0.099	0.156	0.077	0.118	0.068	0.129	0.099	0.081	0.042	0.059	0.066	0.116	0.066
Total tet*	2.000	1.998	2.000	1.999	2.000	2.000	2.000	2.001	2.000	2.000	1.996	1.994	1.986
Ti	0.021	0.082	0.015	0.062	0.014	0.050	0.016	0.024	0.025	0.014	0.028	0.058	0.027
^{vi}Al	0.019	0.000	0.025	0.000	0.007	0.084	0.026	0.000	0.009	0.009	0.000	0.000	0.000
Cr	0.023	0.021	0.018	0.014	0.017	0.005	0.026	0.025	0.008	0.023	0.027	0.030	0.011
Fe	0.265	0.202	0.314	0.327	0.321	0.454	0.348	0.588	1.019	0.429	0.639	0.427	1.072
Mn	0.004	0.006	0.004	0.004	0.004	0.007	0.003	0.008	0.016	0.006	0.011	0.008	0.017
Mg	1.616	0.906	1.567	0.854	1.580	0.794	1.533	1.269	0.649	1.454	1.092	0.740	0.523
Ca	0.058	0.766	0.057	0.729	0.065	0.568	0.054	0.088	0.263	0.065	0.204	0.732	0.380
Na	0.000	0.013	0.000	0.005	0.000	0.016	0.000	0.000	0.000	0.000	0.000	0.000	0.000
Total Cations	4.006	3.994	4.000	3.994	4.008	3.978	4.006	4.003	3.989	4.000	3.997	3.989	4.016
Cation Ratios: Ca : Mg : Fe and Fe/(Fe+Mg)													
Ca	3.0	40.7	2.9	38.1	3.3	31.2	2.8	4.5	13.5	3.3	10.5	38.4	19.1
Mg	83.1	48.2	80.7	44.6	80.2	43.6	79.1	65.0	33.3	74.4	56.1	38.8	26.2
Fe	13.9	11.1	16.4	17.3	16.5	25.2	18.1	30.5	53.2	22.3	33.4	22.8	54.7
Fe/(Fe+Mg)	0.14	0.18	0.17	0.28	0.17	0.36	0.19	0.32	0.61	0.23	0.37	0.37	0.67

* "Total tet" = sum of Si and Al in tetrahedral sites; in ideal pyroxenes, this number = 2. Some Al (listed as ^{vi}Al) may also occur in octahedral sites.

Analyses #1 to 3 are from sample 67559; #4 and 5 are from sample 68416; #6 and 7 are from sample 63549; #8 and 9 are from sample 60335; #10 and 11 are from sample 66095; #12 to 14 are from sample 14276; #15 and 16 are from sample 14310; #17 is from sample 64455; #18 and 19 are from sample 60315; #20 and 21 are from sample 62235; #22 and 23 are from sample 77135; #24 to 26 are from sample 15386; #27 to 30 are from sample 15434 (all analyses by V*animan and Papike*, 1980).

TABLE A5.4. Pyroxene analyses from ferroan anorthosites and Mg-rich rocks.

	Ferroan Anorthosites										Mg-rich Rocks								
											Norite					Troctolite		Dunite	
	1.	2.	3.	4.	5.	6.	7.	8.	9.	10.	11.	12.	13.	14.	15.	16.	17.	18.	19.
Chemical Composition (Weight Percent)																			
SiO_2	52.88	53.42	52.71	53.00	53.00	52.40	51.80	51.80	53.60	51.38	54.39	54.18	53.31	55.3	53.91	55.9	53.48	56.05	54.13
Al_2O_3	0.51	0.68	0.28	0.75	0.51	0.87	0.35	0.73	0.45	1.32	1.02	1.02	1.10	1.30	0.99	1.5	1.00	0.96	1.22
TiO_2	0.26	0.36	0.17	0.45	0.24	0.48	0.20	0.42	0.18	0.42	0.26	0.29	0.66	0.20	0.27	0.4	0.53	0.28	0.11
Cr_2O_3	0.20	0.19	0.11	0.21	0.09	0.24	0.08	0.11	0.19	0.25	0.65	0.67	0.64	0.51	0.67	0.6	0.72	0.26	1.11
FeO	25.22	9.70	24.18	9.01	22.60	8.90	27.70	12.40	22.40	10.40	12.80	12.89	4.80	12.35	12.57	7.4	2.87	6.94	2.71
MnO	0.52	0.24	0.54	0.23	0.62	0.29	0.66	0.39	0.53	0.23	0.20	0.23	0.15	0.25	0.22	0.1	0.06	0.15	0.11
MgO	20.26	13.83	20.36	14.47	21.90	14.90	18.60	13.20	22.40	14.60	29.35	29.50	16.77	28.7	29.25	32.7	18.11	32.29	18.40
CaO	1.02	22.14	1.33	22.33	0.80	21.50	1.30	20.80	0.87	21.50	1.47	1.19	22.29	1.56	1.46	1.5	23.44	2.24	22.50
Na_2O	–	0.03	–	0.01	0.00	0.00	0.00	0.00	0.00	0.00	–	–	–	–	–	–	0.02	0.01	0.05
Total	100.87	100.59	99.68	100.46	99.76	99.58	100.69	99.85	100.62	100.10	100.14	99.97	99.72	100.17	99.34	100.1	100.23	99.18	100.34
Cation Formula Based on 6 Oxygens (Ideal Pyroxene = 4 Cations per 6 Oxygens)																			
Si	1.98	1.98	1.99	1.97	1.984	1.962	1.974	1.963	1.985	1.930	1.944	1.940	1.958	1.967	1.942	1.945	1.946	1.967	1.959
^{iv}Al	0.02	0.02	0.01	0.03	0.016	0.038	0.016	0.033	0.015	0.058	0.044	0.044	0.042	0.033	0.042	0.055	0.043	0.033	0.041
Total tet*	2.00	2.00	2.00	2.00	2.000	2.000	1.990	1.996	2.000	1.988	1.988	1.984	2.000	2.000	1.984	2.000	1.989	2.000	2.000
Ti	0.01	0.01	0.01	0.01	0.007	0.014	0.006	0.012	0.005	0.012	0.008	0.008	0.018	0.005	0.008	0.010	0.014	0.007	0.003
^{vi}Al	0.00	0.01	0.00	0.00	0.006	0.000	0.000	0.000	0.005	0.000	0.000	0.000	0.006	0.021	0.000	0.006	0.000	0.007	0.011
Cr	0.01	0.01	0.00	0.01	0.003	0.007	0.002	0.003	0.006	0.007	0.018	0.020	0.018	0.015	0.020	0.017	0.021	0.007	0.032
Fe	0.79	0.30	0.76	0.28	0.707	0.279	0.883	0.393	0.694	0.327	0.382	0.386	0.148	0.366	0.378	0.215	0.087	0.203	0.082
Mn	0.02	0.01	0.02	0.01	0.020	0.009	0.021	0.013	0.017	0.007	0.006	0.008	0.004	0.008	0.006	0.002	0.002	0.004	0.003
Mg	1.13	0.77	1.15	0.80	1.222	0.831	1.056	0.746	1.236	0.817	1.562	1.574	0.918	1.520	1.570	1.697	0.981	1.687	0.991
Ca	0.04	0.88	0.05	0.89	0.032	0.862	0.053	0.845	0.035	0.865	0.056	0.046	0.878	0.060	0.056	0.056	0.914	0.084	0.872
Na	–	–	–	–	0.000	0.000	0.000	0.000	0.000	0.000	–	–	–	–	–	–	0.002	0.001	0.003
Total Cations	4.00	3.99	3.990	4.00	3.997	4.002	4.011	4.008	3.998	4.023	4.020	4.026	3.990	3.995	4.022	4.003	4.010	4.000	3.997
Cation Ratios: Ca : Mg : Fe and Fe/(Fe+Mg)																			
Ca	2.0	45.1	2.5	45.2	1.6	43.7	2.7	42.6	1.8	43.1	2.82	2.28	45.16	3	2.81	2.8	46.1	4.2	44.8
Mg	57.7	39.5	58.7	40.6	62.3	42.1	53.0	37.6	62.9	40.7	78.08	78.47	47.25	78	78.31	86.2	49.5	85.5	50.9
Fe	40.3	15.4	38.8	14.2	36.1	14.1	44.3	19.8	35.3	16.3	19.11	19.25	7.59	19	18.88	10.9	4.4	1.03	4.2
Fe/(Fe+Mg)	0.41	0.28	0.40	0.26	0.37	0.25	0.46	0.35	0.36	0.29	0.20	0.20	0.14	0.19	0.19	0.11	0.08	0.11	0.08

* "Total tet" = sum of Si and Al in tetrahedral sites; in ideal pyroxenes, this number = 2. Some Al (listed as ^{vi}Al) may also occur in octahedral sites.

Analyses #1 to 4 are from sample 15415 (*Hargraves and Hollister,* 1972); #5 and 6 are from sample 60015 (*Dixon and Papike,* 1975); #7 and 8 are from sample 60025 (*Dixon and Papike,* 1975); #9 and 10 are from sample 61016 (*Dixon and Papike,* 1975); #11 to 13 are from sample 78235 (*McCallum and Mathez,* 1975); #14 is from sample 78235 (*Sclar and Bauer,* 1975); #15 is from sample 78238 (*McCallum and Mathez,* 1975); #16 is from sample 76535 (*Smyth,* 1975); #17 is from sample 76535 (*Dymek et al.,* 1975a); #18 and 19 are from sample 72415 (*Dymek et al.,* 1975a).

TABLE A5.5. Plagioclase analyses from mare basalts.

	High-Ti Basalts						Low-Ti Basalts			Aluminous, Low-Ti			Very Low-Ti Basalts			
	Apollo 17		Apollo 11 High-K		Apollo Low-K		A-12 Ilmenite	A-12 Pigeonite	A-15 Olivine	L-16 Al	A-14 Al	VHK	Luna 24		A-17 VLT	
	1.	2.	3.	4.	5.	6.	7.	8.	9.	10.	11.	12.	13.	14.	15.	16.
Chemical Composition (Weight Percent)																
SiO_2	46.9	48.6	49.80	48.30	45.72	46.30	48.10	44.50	46.70	45.18	45.10	44.09	45.54	45.52	45.03	47.01
Al_2O_3	34.5	31.7	30.50	32.40	34.53	34.00	32.00	35.20	31.80	33.87	33.90	35.18	34.31	33.96	34.93	32.67
FeO	0.28	0.63	0.81	0.51	0.30	0.99	1.17	0.81	2.62	0.54	0.29	0.25	0.92	1.32	0.90	1.34
MgO	0.26	0.22	0.25	0.22	0.07	0.30	0.08	0.08	1.16	0.16	0.0	–	0.06	0.00	0.26	0.15
CaO	17.4	17.0	15.80	16.60	18.64	17.10	17.50	19.20	17.30	18.80	18.80	19.54	18.89	17.20	19.42	18.48
Na_2O	1.34	1.55	1.95	1.84	0.70	1.05	0.40	0.58	0.88	0.86	0.88	0.55	0.65	1.02	0.46	0.71
K_2O	0.05	0.02	0.25	0.19	0.01	0.09	0.20	0.02	0.06	0.06	0.03	0.03	0.00	0.15	0.03	0.12
Total	100.73	99.72	99.36	100.06	99.97	99.83	99.45	100.39	100.52	99.47	99.00	99.64	100.37	99.17	101.03	100.48
Cation Formula Based on 8 Oxygens (Ideal Plagioclase = 5 Cations per 8 Oxygens)																
Si	2.141	2.237	2.295	2.216	2.108	2.136	2.222	2.056	2.160	2.100	2.105	2.048	2.100	2.121	2.067	2.165
^{iv}Al	1.853	1.721	1.657	1.753	1.877	1.849	1.743	1.917	1.734	1.850	1.865	1.927	1.865	1.866	1.891	1.774
Total tet*	3.994	3.958	3.952	3.969	3.985	3.985	3.965	3.973	3.894	3.950	3.970	3.975	3.965	3.987	3.958	3.939
Fe	0.011	0.024	0.031	0.020	0.012	0.038	0.045	0.031	0.101	0.020	0.011	0.009	0.036	0.052	0.034	0.052
Mg	0.018	0.015	0.017	0.015	0.005	0.021	0.006	0.006	0.080	0.010	0.000	–	0.004	0.000	0.018	0.010
Ca	0.850	0.836	0.780	0.816	0.921	0.845	0.866	0.950	0.857	0.930	0.940	0.972	0.933	0.859	0.955	0.912
Na	0.119	0.138	0.174	0.164	0.063	0.094	0.036	0.052	0.079	0.080	0.080	0.049	0.058	0.092	0.041	0.063
K	0.003	0.001	0.015	0.011	0.001	0.005	0.012	0.001	0.004	0.004	0.002	0.001	0.000	0.009	0.002	0.007
Total Cations	4.995	4.972	4.969	4.995	4.987	4.988	4.930	5.013	5.015	4.994	5.003	5.006	4.996	4.999	5.008	4.983
Cation Ratio Fe/(Fe+Mg), and Molecular Proportion of Orthoclase (Or), Albite (Ab), and Anorthite (An)																
Fe/(Fe+Mg)	0.38	0.62	0.65	0.57	0.71	0.65	0.89	0.85	0.56	0.67	1.00	1.00	0.90	1.00	0.65	0.84
Or	0.3	0.1	1.5	1.1	0.1	0.5	1.3	0.1	0.4	0.4	0.2	0.1	0.0	9.6	0.2	0.7
Ab	12.2	14.1	18.0	16.6	6.4	10.0	3.9	5.2	8.4	7.9	7.8	4.8	5.8	0.9	4.1	6.4
An	87.5	85.7	80.5	82.3	93.5	89.5	94.8	94.7	91.2	91.7	92.0	95.1	94.2	89.5	95.7	92.9

* "Total tet" = sum of Si and Al, both of which must be in the 4 tetrahedral sites per 8 oxygens.

Analyses #1 and 2 are from sample 75083 (*Papike et al.,* 1974); #3 is from sample 10022 (*Kushiro and Nakamura,* 1970); #4 is from sample 10024 (*Crawford,* 1973); #5 is from sample 10045 (*Agrell et al.,* 1970b); #6 is from sample 10050 (*Appleman et al.,* 1971); #7 is from sample 12063 (*Crawford,* 1973); #8 is from sample 12021 (*Crawford,* 1973); #9 is from sample 15016 (*S. R. Taylor et al.,* 1973a); #10 is from sample Luna 16 B-1 (*Albee et al.,* 1972); #11 is from sample 14053 (*Kushiro et al.,* 1972); #12 is from sample 14305 (*Shervais et al.,* 1985b); #13 and 14 are from sample 24174 (*Laul et al.,* 1978b); #15 and 16 are from sample 70008 (*Vaniman and Papike,* 1977c).

TABLE A5.6. Plagioclase analyses from highland clast-poor melt rocks, crystalline melt breccias, and KREEP rocks.

	Melt Rocks						Cryst Melt Breccias				Melt Rocks						Cryst Melt Breccias					KREEP			
	1.	2.	3.	4.	5.	6.	7.	8.	9.	10.	11.	12.	13.	14.	15.	16.	17.	18.	19.	20.	21.	22.	23.	24.	25.
Chemical Composition (Weight Percent)																									
SiO_2	44.5	47.6	43.9	45.4	43.5	44.4	44.6	45.8	43.8	45.5	44.7	47.4	43.8	46.4	45.4	45.9	44.9	45.8	45.5	44.2	45.8	47.3	49.5	47.1	51.3
Al_2O_3	36.4	33.3	36.7	35.7	36.1	35.7	35.9	34.3	36.1	35.4	34.7	33.4	36.1	34.0	36.3	32.7	34.5	34.3	35.4	35.9	35.3	34.0	30.8	32.5	30.8
FeO	0.10	0.52	0.15	0.46	0.07	0.11	0.12	0.18	0.15	0.30	0.21	0.39	0.15	0.06	0.06	0.26	0.27	0.22	0.27	0.18	0.26	0.19	0.38	0.16	0.48
MgO	0.00	0.00	0.05	0.07	0.00	0.07	0.01	0.07	0.00	0.15	0.12	0.14	0.19	0.29	0.36	0.37	0.00	0.00	0.11	0.00	0.00	0.19	0.10	0.17	0.08
CaO	20.0	17.3	20.2	18.1	19.4	18.8	19.3	17.9	19.7	18.7	19.5	17.2	19.2	17.1	18.5	19.0	19.0	18.7	18.6	19.7	18.7	17.1	15.9	17.1	14.7
Na_2O	0.26	1.6	0.27	0.97	0.29	0.56	0.40	0.92	0.39	0.71	0.49	1.6	0.51	1.4	0.69	0.78	0.66	0.88	0.91	0.28	0.98	1.4	2.2	1.5	2.4
K_2O	0.01	0.10	0.01	0.09	0.00	0.01	0.03	0.06	0.01	0.12	0.05	0.29	0.05	0.21	0.02	0.09	0.06	0.25	0.07	0.07	0.09	0.08	0.34	0.11	0.33
Total	101.27	100.42	101.28	100.79	99.36	99.65	100.36	99.23	100.15	100.88	99.77	100.42	100.00	99.46	101.33	99.10	99.39	100.15	100.86	100.33	101.13	100.26	99.22	98.64	100.09
Cation Formula Based on 8 Oxygens (Ideal Plagioclase = 5 Cations per 8 Oxygens)																									
Si	2.031	2.181	2.009	2.078	2.022	2.053	2.051	2.123	2.024	2.082	2.073	2.173	2.026	2.143	2.062	2.142	2.087	2.112	2.082	2.039	2.090	2.163	2.285	2.191	2.334
^{IV}Al	1.962	1.796	1.980	1.926	1.981	1.949	1.948	1.874	1.968	1.909	1.897	1.804	1.968	1.851	1.946	1.796	1.891	1.864	1.909	1.952	1.896	1.834	1.676	1.783	1.650
Total tet*	3.993	3.977	3.989	4.004	4.003	4.002	3.999	3.997	3.992	3.991	3.970	3.977	3.994	3.994	4.008	3.938	3.978	3.976	3.991	3.991	3.986	3.997	3.961	3.974	3.984
Fe	0.004	0.020	0.006	0.018	0.003	0.004	0.005	0.007	0.006	0.012	0.008	0.015	0.006	0.002	0.002	0.010	0.011	0.009	0.010	0.007	0.010	0.007	0.015	0.006	0.018
Mg	0.000	0.000	0.003	0.005	0.000	0.005	0.001	0.005	0.000	0.010	0.008	0.010	0.013	0.020	0.024	0.026	0.000	0.000	0.008	0.000	0.000	0.013	0.007	0.012	0.006
Ca	0.977	0.850	0.991	0.888	0.970	0.934	0.953	0.888	0.976	0.916	0.969	0.845	0.952	0.846	0.899	0.949	0.946	0.924	0.912	0.971	0.914	0.840	0.787	0.855	0.719
Na	0.023	0.139	0.024	0.086	0.026	0.050	0.036	0.084	0.035	0.063	0.142	0.046	0.125	0.060	0.071	0.060	0.079	0.081	0.025	0.086	0.121	0.196	0.133	0.210	0.003
K	0.001	0.006	0.001	0.005	0.000	0.001	0.002	0.003	0.000	0.007	0.003	0.017	0.003	0.012	0.001	0.005	0.003	0.014	0.004	0.004	0.005	0.005	0.020	0.007	0.019
Total Cations	4.998	4.992	5.014	5.006	5.002	4.996	4.996	4.984	5.009	4.999	5.002	5.006	5.014	4.999	4.994	4.999	4.998	5.002	5.006	4.998	5.001	4.983	4.986	4.987	4.956
Cation Ratio Fe/(Fe+Mg), and Molecular Proportion of Orthoclase (Or), Albite (Ab), and Anorthite (An)																									
Fe/(Fe+Mg)	1.00	1.00	0.66	0.79	1.00	0.44	0.83	0.58	1.00	0.55	0.50	0.61	0.21	0.10	0.09	0.28	1.00	1.00	0.56	1.00	1.00	0.35	0.68	0.34	0.76
Or	0.10	0.60	0.10	0.50	0.00	0.10	0.10	0.30	0.00	0.70	0.30	1.70	0.30	1.30	0.10	0.50	0.30	1.40	0.40	0.40	0.50	0.50	2.00	0.70	2.00
Ab	2.30	14.00	2.40	8.80	2.60	5.10	3.60	8.50	3.50	6.40	4.30	14.20	4.60	12.70	6.30	6.90	5.90	7.80	8.10	2.50	8.60	12.50	19.60	13.30	22.10
An	97.60	85.40	97.60	90.70	97.40	94.80	96.20	91.20	96.50	92.90	95.40	84.10	95.10	86.00	93.60	92.60	93.80	90.80	91.50	97.10	90.90	87.00	78.40	86.00	75.90

"Total tet" = sum of Si and Al, both of which must be in the 4 tetrahedral sites per 8 oxygens.

Analyses #1 and 2 are from sample 67559; #3 and 4 are from sample 68415; #5 and 6 are from sample 63549; #7 and 8 are from sample 60335; #9 and 10 are from sample 66095; #11 and 12 are from sample 14276; #13 and 14 are from sample 14310; #15 is from sample 64455; #16 is from sample 62295; #17 and 18 are from sample 62235; #19 is from sample 65015; #20 and 21 are from sample 77135; #22 and 23 are from sample 15386; #24 and 25 are from sample 15434 (all analyses from *Vaniman and Papike,* 1980).

TABLE A5.7. Plagioclase analyses from ferroan anorthosites and Mg-rich rocks.

	Ferroan Anorthosites								Mg-rich Rocks						
									Norite				Troctolite		
	1.	2.	3.	4.	5.	6.	7.	8.	9.	10.	11.	12.	13.	14.	15.
Chemical Composition (Weight Percent)															
SiO_2	44.19	43.92	44.6	44.6	43.4	43.9	43.2	42.8	44.72	45.25	46.48	45.27	43.40	44.1	44.21
Al_2O_3	35.77	36.24	35.2	36.0	35.2	35.7	36.6	35.6	35.15	34.85	32.75	35.18	35.41	35.3	35.89
FeO	0.16	0.09	0.20	0.18	0.19	0.16	0.08	0.10	0.10	0.15	1.21	0.10	0.18	0.04	0.10
MgO	0.00	–	0.06	0.07	0.04	0.04	0.00	0.00	0.08	0.10	1.51	0.08	0.11	–	0.07
CaO	19.66	19.49	20.0	19.5	19.5	19.2	19.6	18.9	19.24	18.73	17.77	18.79	19.22	18.7	19.60
Na_2O	0.22	0.26	0.35	0.38	0.42	0.45	0.25	0.33	0.57	0.59	0.71	0.66	0.58	0.43	0.29
K_2O	–	–	0.01	0.03	0.00	0.01	0.00	0.00	0.09	0.10	0.09	0.14	0.08	0.07	0.05
Total	100.00	100.00	100.4	100.8	98.8	99.5	99.7	97.7	99.95	99.77	100.52	100.22	98.98	98.64	100.21
Cation Formula Based on 8 Oxygens (Ideal Plagioclase = 5 Cations per 8 Oxygens)															
Si	2.04	2.03	2.057	2.046	2.034	2.040	2.002	2.024	2.068	2.093	2.137	2.083	2.033	2.063	2.04
^{iv}Al	1.95	1.97	1.915	1.947	1.947	1.956	1.999	1.984	1.917	1.900	1.775	1.908	1.952	1.943	1.950
Total tet*	3.99	4.00	3.972	3.993	3.981	3.996	4.001	4.008	3.985	3.993	3.912	3.991	3.985	4.006	3.991
Fe	0.01	0.00	0.008	0.007	0.007	0.006	0.003	0.004	0.004	0.006	0.047	0.004	0.007	0.002	0.004
Mg	0.00	–	0.004	0.005	0.003	0.003	0.000	0.000	0.005	0.005	0.104	0.005	0.008	–	0.005
Ca	0.97	0.97	0.987	0.959	0.981	0.955	0.973	0.957	0.953	0.928	0.876	0.927	0.964	0.937	0.970
Na	0.02	0.02	0.031	0.034	0.038	0.041	0.023	0.030	0.051	0.053	0.063	0.059	0.052	0.038	0.026
K	–	–	0.001	0.002	0.000	0.000	0.000	0.000	0.005	0.006	0.005	0.008	0.004	0.004	0.003
Total Cations	4.99	4.99	5.003	5.000	5.010	5.001	5.000	4.999	5.003	4.991	5.007	4.994	5.020	4.987	4.999
Cation Ratio Fe/(Fe+Mg), and Molecular Proportion of Orthoclase (Or), Albite (Ab), and Anorthite (An)															
Fe/(Fe+Mg)	1.00	1.00	0.67	0.58	0.70	0.67	1.00	1.00	0.44	0.54	0.31	0.44	0.47	1.00	0.44
Or	–	–	0.05	0.2	0.0	0.0	0.0	0.00	0.5	0.6	0.6	0.9	0.4	0.4	0.3
Ab	2.0	2.0	3.0	3.4	3.7	4.1	2.3	3.0	5.1	5.4	6.7	5.9	5.1	3.9	2.6
An	98.0	98.0	96.9	96.4	96.3	95.9	97.7	97.0	94.4	94.0	92.7	93.2	94.5	95.7	97.1

* "Total tet" = sum of Si and Al, both of which must be in the 4 tetrahedral sites per 8 oxygens.

Analyses #1 and 2 are from sample 15415 (*Hargraves and Hollister,* 1972); #3 and 4 are from sample 60015 (*Dixon and Papike,* 1975); #5 is from sample 60025 (*Dixon and Papike,* 1975); #6 is from sample 61016 (*Dixon and Papike,* 1975); #7 and 8 are from sample 65315 (*Dixon and Papike,* 1975); #9 to 11 are from sample 78235 (*McCallum and Mathez,* 1975); #12 is from sample 78238 (*McCallum and Mathez,* 1975); #13 is from sample 12033,66 (*Marvin and Walker,* 1985); #14 is from sample 76255 (*J. L. Warner et al.,* 1976a,b); #15 is from sample 76535 (*Dymek et al.,* 1975a).

TABLE A5.8. Olivine analyses from mare basalts.

	High-Ti Basalts						Low-Ti Basalts								Very Low-Ti Basalts					
	Apollo 17		A-11 HK		A-11 LK		A-12 ilm		A-12 pig	A-12 ol		A-15 ol	VHK		Luna 24		Apollo 17			
	1.	2.	3.	4.	5.	6.	7.	8.	9.	10.	11.	12.	13.	14.	15.	16.	17.	18.	19.	20.
Chemical Composition (Weight Percent)																				
SiO_2	37.60	37.53	37.50	37.50	38.60	29.20	38.08	30.60	34.10	37.80	35.40	29.70	37.46	33.50	33.37	29.93	37.24	34.99	37.98	37.71
Al_2O_3	0.02	0.01	0.04	0.05	0.00	0.30	0.02	0.00	0.32	0.00	0.00	0.06	–	–	0.20	0.29	0.17	0.20	0.18	0.21
FeO	28.44	27.44	26.20	25.50	25.40	68.70	22.15	65.30	39.60	21.10	33.80	64.80	24.71	49.79	48.61	67.15	28.25	39.35	23.06	23.43
MgO	34.66	35.93	35.80	36.50	34.90	0.50	38.86	3.54	23.70	39.20	30.10	3.80	37.39	15.75	17.88	0.97	35.23	26.42	37.94	38.30
MnO	0.31	0.28	0.22	0.30	0.36	1.10	0.24	0.00	0.52	0.24	0.36	0.66	0.36	0.71	0.45	0.74	0.28	0.42	0.29	0.26
Cr_2O_3	0.19	0.13	0.21	0.21	0.28	0.02	0.35	0.00	0.24	0.44	0.11	0.04	–	–	0.12	0.10	0.39	0.15	0.55	0.67
CaO	0.33	0.29	0.28	0.33	0.31	0.26	0.27	0.65	0.59	0.30	0.36	0.40	0.23	0.32	0.48	1.03	0.28	0.29	0.41	0.39
Na_2O	0.01	0.00	0.00	0.00	0.00	0.00	0.01	0.00	0.00	0.00	0.00	0.00	–	–	–	0.00	–	–	–	–
Total	101.56	101.61	100.25	100.39	99.85	100.08	99.98	100.09	99.07	99.08	100.13	99.46	100.15	100.07	101.11	100.21	101.84	101.82	100.41	100.97
Cation Formula Based on 4 Oxygens (Ideal Olivine = 3 Cations per 4 Oxygens)																				
Si	0.993	0.986	0.993	0.989	1.020	0.987	0.992	1.005	0.984	0.990	0.978	0.987	0.986	1.006	0.985	0.996	0.981	0.975	0.989	0.980
Al	0.001	0.000	0.001	0.002	0.000	0.012	0.001	0.000	0.011	0.000	0.000	0.002	–	–	0.007	0.011	0.005	0.006	0.006	0.006
Fe	0.628	0.603	0.580	0.562	0.561	1.942	0.483	1.794	0.956	0.462	0.781	1.800	0.544	1.251	1.200	1.870	0.622	0.917	0.502	0.509
Mg	1.364	1.407	1.413	1.435	1.374	0.025	1.509	0.173	1.020	1.530	1.240	0.188	1.468	0.705	0.786	0.048	1.382	1.097	1.473	1.483
Mn	0.007	0.006	0.005	0.007	0.008	0.031	0.005	0.000	0.013	0.005	0.008	0.019	0.007	0.018	0.011	0.021	0.006	0.010	0.006	0.006
Cr	0.004	0.003	0.004	0.004	0.006	0.001	0.007	0.000	0.005	0.009	0.002	0.001	–	–	0.003	0.002	0.008	0.003	0.011	0.014
Ca	0.009	0.008	0.008	0.009	0.009	0.009	0.008	0.023	0.018	0.008	0.011	0.014	0.006	0.009	0.015	0.037	0.008	0.009	0.012	0.011
Na	0.001	0.000	0.000	0.000	0.000	0.000	0.001	0.000	0.000	0.000	0.000	0.000	–	–	–	0.000	–	–	–	–
Total Cations	3.007	3.013	3.004	3.008	2.978	3.007	3.006	2.995	3.007	3.004	3.020	3.011	3.011	2.989	3.007	2.985	3.012	3.017	2.999	3.009
Cation Ratio Fe/(Fe+Mg)																				
Fe/(Fe+Mg)	0.32	0.30	0.29	0.28	0.29	0.99	0.24	0.91	0.48	0.23	0.39	0.91	0.27	0.64	0.60	0.97	0.31	0.46	0.25	0.26

Analysis #1 is from sample 70215 (*Dymek et aL,* 1975); #2 is from sample 71055 (*Dymek et al.,* 1975); #3 is from sample 10022 (*Kushiro and Nakumura,* 1970); #4 is from sample 10020 (*Haggerty et al.,* 1970); #5 is from sample 10045 (*Brown et al.,* 1970); #6 is from sample 10044 (*Smith et al.,* 1970); #7 is from sample 12022 (*Weill et al.,* 1971); #8 is from sample 12063 (*El Goresy et al.,* 1971b); #9 is from sample 12052 (*Bence et al.,* 1970); #10 is from sample 12009 (*Butler,* 1972); #11 is from sample 12035 (*Butler,* 1972); #12 is from sample 15555 (*Roedder and Weiblen,* 1972). #13 and 14 are from sample 14305 (*Shervais et al.,* 1985b); #15 and 16 are from sample 24174 (*Laul et al.,* 1978b); #17 and 18 are from sample 70008 (*Vaniman and Papike,* 1977c); #19 is from sample 70007 (*Vaniman and Papike,* 1977c); #20 is from sample 70008 (*Vaniman and Papike,* 1977c).

TABLE A5.9. Olivine analyses from highland clast-poor melt rocks and crystalline melt breccias.

	Melt Rocks				Cryst Melt Breccias				Melt Rocks				Cryst Melt Breccias							
	1.	2.	3.	4.	5.	6.	7.	8.	9.	10.	11.	12.	13.	14.	15.	16.	17.	18.	19.	20.
Chemical Composition (Weight Percent)																				
SiO_2	36.5	38.2	37.4	36.1	39.3	38.9	38.8	38.0	31.9	39.0	39.1	38.2	38.4	37.8	38.8	38.4	38.8	35.8	39.5	37.7
Al_2O_3	0.11	0.06	0.02	0.22	0.06	0.10	0.11	0.13	0.44	0.16	0.10	0.11	0.17	0.14	0.15	0.17	0.14	0.54	0.26	0.08
FeO	34.1	25.4	28.8	33.3	15.8	18.0	20.2	22.2	58.3	17.4	20.1	21.4	22.0	26.6	21.4	22.8	22.2	33.7	18.5	26.2
MgO	30.5	37.6	34.5	30.4	44.6	42.0	41.2	39.2	8.4	43.0	41.4	40.0	39.7	35.5	40.6	39.3	38.3	29.5	43.1	36.3
MnO	0.28	0.33	0.28	0.36	0.18	0.21	0.27	0.20	0.55	0.14	0.19	0.22	0.27	0.42	0.21	0.25	0.15	0.31	0.14	0.25
Cr_2O_3	0.09	0.10	0.07	0.12	0.21	0.22	0.20	0.12	0.02	0.09	0.08	0.03	0.10	0.06	0.21	0.20	0.07	0.07	0.20	0.04
CaO	0.40	0.16	0.16	0.26	0.12	0.13	0.17	0.22	0.30	0.15	0.16	0.11	0.15	0.19	0.23	0.19	0.26	0.24	0.39	0.23
Total	101.98	101.85	101.23	100.76	100.27	99.56	100.95	100.07	99.91	99.94	101.13	100.07	100.79	100.71	101.60	101.31	99.92	100.16	102.09	100.80
Cation Formula Based on 4 Oxygens (Ideal Olivine = 3 Cations per 4 Oxygens)																				
Si	0.986	0.989	0.991	0.986	0.989	0.995	0.990	0.987	1.004	0.992	0.994	0.989	0.989	0.996	0.988	0.988	1.006	0.983	0.987	0.992
Al	0.004	0.002	0.001	0.007	0.002	0.003	0.003	0.004	0.016	0.005	0.003	0.003	0.005	0.004	0.004	0.005	0.004	0.017	0.008	0.003
Fe	0.771	0.550	0.638	0.759	0.332	0.385	0.430	0.482	1.535	0.369	0.427	0.463	0.472	0.586	0.456	0.490	0.481	0.774	0.387	0.576
Mg	1.229	1.451	1.363	1.234	1.673	1.604	1.566	1.519	0.394	1.630	1.569	1.543	1.522	1.395	1.540	1.506	1.480	1.207	1.607	1.421
Mn	0.006	0.007	0.006	0.008	0.004	0.004	0.006	0.004	0.015	0.003	0.004	0.004	0.006	0.009	0.004	0.005	0.003	0.007	0.003	0.005
Cr	0.002	0.002	0.001	0.002	0.004	0.004	0.004	0.002	0.000	0.002	0.002	0.001	0.002	0.001	0.004	0.004	0.001	0.002	0.004	0.001
Ca	0.012	0.004	0.005	0.008	0.003	0.004	0.005	0.006	0.010	0.004	0.004	0.003	0.004	0.005	0.006	0.005	0.007	0.007	0.010	0.006
Total Cations	3.010	3.005	3.005	3.004	3.007	2.999	3.004	3.004	2.974	3.005	3.003	3.006	3.000	2.996	3.002	3.003	2.982	2.997	3.006	3.004
Cation Ratio Fe/(Fe+Mg)																				
Fe/(Fe+Mg)	0.38	0.27	0.32	0.38	0.17	0.20	0.22	0.24	0.80	0.19	0.22	0.23	0.24	0.30	0.23	0.25	0.24	0.39	0.19	0.29

Analysis #1 is from sample 67559; #2 and 3 are from sample 68415; #4 is from sample 68416; #5 to 7 are from sample 60335; #8 is from sample 66095; #9 is from sample 14310; #10 and 11 are from sample 64455; #12 is from sample 62295; #13 and 14 are from sample 60315; #15 and 16 are from sample 62235; #17 and 18 are from sample 65015; #19 and 20 are from sample 77135 (all analyses from *Vaniman and Papike,* 1980).

TABLE A5.10. Olivine analyses from ferroan anorthosites and Mg-rich rocks.

	Ferroan Anorthosites		Mg-rich Rocks					
			Troctolite			Dunite		
	1.	2.	3.	4.	5.	6.	7.	8.
	Chemical Composition (Weight Percent)							
SiO_2	37.1	35.59	40.3	39.9	40.85	40.24	40.13	39.84
Al_2O_3	0.08	0.0	0.0	–	0.0	<0.01	0.05	0.00
FeO	31.8	34.58	12.3	12.0	11.0	12.29	13.00	13.13
MgO	30.9	30.11	47.96	47.1	48.45	47.65	48.14	48.30
MnO	–	0.42	0.16	0.1	0.11	0.13	0.15	0.17
Cr_2O_3	–	0.05	0.02	<0.02	0.04	0.04	0.05	0.05
CaO	0.06	0.03	0.03	<0.02	0.09	0.13	0.13	0.08
Na_2O	–	–	–	–	0.05	–	0.06	0.02
Total	99.94	100.78	100.77	99.10	100.59	100.48	101.71	101.59
	Cation Formula Based on 4 Oxygens (Ideal Olivine = 3 Cations per 4 Oxygens)							
Si	1.009	0.979	0.991	0.994	1.000	0.993	0.980	0.978
Al	0.003	–	–	–	–	–	0.001	–
Fe	0.723	0.795	0.253	0.250	0.225	0.254	0.265	0.269
Mg	1.253	1.235	1.760	1.750	1.768	1.753	1.752	1.768
Mn	–	0.010	0.003	0.001	0.002	0.003	0.003	0.003
Cr	–	0.001	0.000	0.000	0.001	0.001	0.001	0.001
Ca	0.002	0.001	0.001	0.000	0.002	0.003	0.003	0.002
Na	–	–	–	–	0.002	–	0.003	0.001
Total Cations	2.990	3.014	3.008	2.995	3.000	3.007	3.008	3.022
	Cation Ratio Fe/(Fe+Mg)							
Fe/(Fe+Mg)	0.37	0.39	0.13	0.12	0.11	0.13	0.13	0.13

Analysis #1 is from sample 67635,2 (*Borchardt et al.,* 1985); #2 is from sample 62237 (*Dymek et al.,* 1975a); #3 is from sample 76535 (*Dymek et al.,* 1975a); #4 is from sample 76535 (*Gooley et al.,* 1974); #5 is from sample 12033 (*Marvin and Walker,* 1985); #6 is from sample 72415 (*Dymek et al.,* 1975a); #7 and 8 are from sample 72415 (*Richter et al.,* 1976).

TABLE A5.11a. Analyses of miscellaneous lunar silicate minerals.

	Zircon					Pyroxferroite			K-Feldspar				Silica Polymorphs			
	Soil	Reg br		Granite		A-11 LK		A-12 pig	Granite	Soil	A-12 pig	A-14 Al	A-11 HK	A-11 LK		
	1.	2.	3.	4.	5.	6.	7.	8.	9.	10.	11.	12.	13.	14.	15.	16.
	Chemical Composition (Weight Percent)															
SiO_2	32.2	35.5	32.11	32.41	32.41	46.92	45.86	45.23	60.93	61.0	57.2	63.49	98.0	98.0	97.6	96.9
Al_2O_3	0.09	1.3	–	0.2	–	0.76	0.36	0.54	22.52	20.5	20.1	19.44	1.56	0.92	1.1	1.03
TiO_2	–	0.2	–	0.19	–	0.74	0.37	0.73	–	–	–	–	0.48	0.27	0.2	–
Cr_2O_3	–	–	–	0.03	–	0.12	0.08	0.05	–	–	–	–	–	–	–	–
FeO	0.32	0.8	–	0.02	0.35	42.48	44.33	46.54	0.13	–	0.35	0.03	0.18	0.05	0.3	0.35
MnO	–	–	–	–	–	0.65	0.76	0.56	–	–	–	–	–	–	–	
MgO	0.18	0.1	–	0.19	–	2.41	0.90	0.34	0.0	–	–	–	–	–	–	–
CaO	–	–	–	0.26	–	6.69	6.56	6.43	3.87	2.07	0.55	0.35	0.34	0.16	0.3	0.52
Na_2O	0.09	–	–	–	–	–	–	0.03	3.46	1.24	0.81	0.74	0.19	0.15	0.0	0.05
K_2O	–	–	–	–	–	–	–	–	7.99	10.9	11.1	14.76	–	–	0.0	0.25
ZrO_2	64.7	61.5	67.23	66.93	63.48	–	–	–	–	–	–	–	–	–	–	–
HfO_2	–	0.6	0.88	–	3.01	–	–	–	–	–	–	–	–	–	–	–
BaO	–	–	–	–	–	–	–	–	1.19	2.73	9.3	0.44	–	–	–	–
Total	97.58	100.0	100.22	100.23	99.25	100.77	99.22	100.45	100.09	98.44	99.41	99.24	100.75	99.55	99.5	99.10
	Cation Compositions Based on Relevant Number of Oxygens															
Si	1.004	1.054	0.986	0.987	1.01	1.965	1.978	1.95	2.788	2.88	2.819	2.954	0.979	0.988	0.986	0.985
Al	0.003	0.045	–	0.007	–	0.038	0.018	0.03	1.215	1.14	1.168	1.064	0.018	0.011	0.013	0.012
Ti	–	0.004	–	0.009	–	0.023	0.012	0.02	–	–	–	–	0.004	0.002	0.002	–
Cr	–	–	–	0.001	–	0.004	0.003	0.00	–	–	–	–	–	–	–	–
Fe	0.008	0.020	–	0.001	0.009	1.488	1.599	1.68	0.005	–	0.014	0.000	0.002	0.000	0.003	0.003
Mn	–	–	–	–	–	0.023	0.028	0.02	–	–	–	–	–	–	–	–
Mg	0.008	0.004	–	0.004	–	0.150	0.058	0.02	–	–	–	–	–	–	–	–
Ca	–	–	–	0.008	–	0.300	0.303	0.30	0.190	0.105	0.029	0.016	0.004	0.002	0.003	0.006
Na	0.005	–	–	–	–	–	–	0.00	0.307	0.113	0.077	0.065	0.004	0.003	–	0.001
K	–	–	–	–	–	–	–	–	0.466	0.656	0.698	0.875	–	–	–	0.003
Zr	0.984	0.890	1.007	0.994	0.962	–	–	–	–	–	–	–	–	–	–	–
Hf	–	0.005	0.008	–	0.027	–	–	–	–	–	–	–	–	–	–	–
Ba	–	–	–	–	–	–	–	–	0.021	0.050	0.180	0.006	–	–	–	–
Total	2.012	2.022	2.001	2.011	2.008	3.991	3.999	4.02	4.992	4.944	4.985	4.980	1.011	1.006	1.007	1.010
No. of Oxygens	4	4	4	4	4	6	6	6	8	8	8	8	2	2	2	2

Analysis #1 is from sample 12070 (*Keil et al.,* 1971); #2 is from sample 12034 (*Anderson and Smith,* 1971); #3 is from sample 12032 (*Brown et al.,* 1971); #4 is from sample 14321 (*Gay et al.,* 1972); #5 is from sample 12013 (*Lunatic Asylum,* 1970); #6 is from sample 10058 (*Agrell et al.,* 1970b); #7 is from sample 10058 (*Brown et al.,* 1972); #8 is from sample 12065 (*Hollister et al.,* 1971); #9 is from sample 12013 (*Drake et al.,* 1970); #10 is from sample 10085 (*Albee and Chodos,* 1970); #11 is from sample 12039 (*Keil et al.,* 1971); #12 is from sample 14305 (*Shervais et al.,* 1985); #13 is from sample 10017 (*Brown et al.,* 1970); #14 is from sample 10058 (*Brown et al.,* 1970); #15 is from sample 10020 (*Dence et al.,* 1970); #16. is from sample 10045 (*Keil et al.,* 1970).

TABLE A5.11b. Tranquillityite analyses from mare basalts.

	A-11 LK					A-12 ol	A-12 pig
	1.	2.	3.	4.	5.	6.	7.
	Chemical Composition (Weight Percent)						
SiO_2	13.66	13.77	13.98	13.75	13.65	13.00	14.7
Al_2O_3	0.87	0.90	0.83	0.85	0.92	0.70	1.71
TiO_2	19.75	20.66	20.01	20.28	19.80	17.50	19.7
Cr_2O_3	0.06	0.19	0.13	0.15	–	–	–
FeO	43.00	42.37	42.90	42.34	42.50	41.78	42.3
MnO	0.36	0.30	0.34	0.30	0.50	0.25	0.22
CaO	1.04	1.11	1.17	1.20	1.20	1.00	1.53
Zr_2O_3	16.96	16.79	16.35	16.87	16.90	17.80	17.3
HfO_2	0.05	0.06	0.04	0.05	0.49	0.60	–
Y_2O_3	2.51	2.73	2.61	2.58	3.50	4.71	1.34
Total	98.26	98.88	98.36	98.37	99.46	97.34	98.80
	Cation Formula Based on 24 Oxygens						
Si	2.859	2.849	2.906	2.860	2.836	2.805	3.009
Al	0.141	0.151	0.094	0.140	0.164	0.178	0.000
Subtotal	3.000	3.000	3.000	3.000	3.000	2.983	3.009
Ti	2.916	2.900	2.870	2.907	2.939	2.839	2.587
Al	0.074	0.069	0.109	0.068	0.061	0.000	0.413
Cr	0.010	0.031	0.021	0.025	0.000	0.000	0.000
Subtotal	3.000	3.000	3.000	3.000	3.000	2.839	3.000
Fe	7.527	7.332	7.458	7.365	7.385	7.538	7.241
Ti	0.193	0.315	0.258	0.265	0.155	0.000	0.446
Mn	0.064	0.053	0.060	0.053	0.088	0.046	0.038
Ca	0.233	0.246	0.261	0.267	0.267	0.231	0.336
Subtotal	8.017	7.946	8.037	7.950	7.895	7.815	8.061
Zr	1.731	1.694	1.657	1.711	1.712	1.873	1.727
Hf	0.003	0.004	0.002	0.003	0.029	0.037	0.000
Y	0.279	0.300	0.288	0.285	0.387	0.540	0.146
Subtotal	2.013	1.998	1.947	1.999	2.128	2.450	1.873
Total cations	16.030	15.944	15.984	15.949	16.023	16.087	15.943

Analyses #1 to 5 are from sample 10047; #6 is from sample 12018; #7 is from sample 12039 (all analyses from *Lovering et al.*, 1971).

TABLE A5.12. Ilmenite analyses from lunar rocks and soils.

	A-11 Soil	A-11 HK				A-11 LK	A-12 ol	A-11 ol	A-12 pig	A-12 ilm	A-12 pig	A-12 ilm
	1.	2.	3.*	4.*	5.	6.	7.	8.	9.	10.	11.	12.
	Chemical Composition (Weight Percent)											
TiO_2	56.30	54.2	52.22	54.53	52.1	53.0	53.8	53.0	52.25	52.34	52.91	53.9
Al_2O_3	1.64	0.17	<0.03	<0.03	—	—	0.02	0.03	0.04	0.28	1.13	0.42
Cr_2O_3	0.34	0.72	0.53	0.53	2.12	0.52	0.51	0.75	0.18	0.24	0.19	0.39
V_2O_3	—	—	—	—	—	—	0.07	0.04	—	—	—	0.04
FeO	32.39	41.7	44.38	44.84	44.4	45.1	40.5	44.1	46.74	45.16	46.30	45.4
MgO	9.63	3.12	1.39	1.14	1.35	0.75	5.14	2.28	0.47	0.39	0.01	0.10
MnO	0.34	0.35	0.15	0.15	0.45	0.45	0.42	0.41	0.30	0.34	0.31	0.36
CaO	0.44	0.03	0.21	0.21	0.01	0.10	—	—	—	—	—	—
ZrO_2	—	—	—	—	—	—	—	—	—	—	—	—
SiO_2	—	0.04	0.09	0.09	0.12	0.23	—	—	—	—	—	—
Total	101.08	100.33	98.97	101.49	100.55	100.15	100.46	100.61	99.98	98.75	100.85	100.61
	Cation Formula Based on 3 Oxygens (Ideal Ilmenite = 2 Cations per 3 Oxygens)											
Ti	0.976	0.997	0.989	1.014	0.974	0.996	0.983	0.985	0.991	1.000	0.988	1.007
Al	0.045	0.002	0.000	0.000	—	—	0.001	0.001	0.001	0.008	0.033	0.012
Cr	0.006	0.014	0.010	0.010	0.042	0.010	0.010	0.015	0.004	0.005	0.004	0.008
V	—	—	—	—	—	—	0.001	0.001	—	—	—	0.001
Fe	0.624	0.853	0.935	0.918	0.923	0.942	0.822	0.912	0.986	0.959	0.962	0.943
Mg	0.331	0.114	0.052	0.042	0.050	0.028	0.186	0.084	0.018	0.015	0.000	0.004
Mn	0.001	0.007	0.003	0.003	0.009	0.009	0.009	0.009	0.006	0.007	0.007	0.008
Ca	0.011	0.001	0.006	0.006	0.000	0.003	—	—	—	—	—	—
Zr	—	—	—	—	—	—	—	—	—	—	—	—
Si	—	0.001	0.002	0.002	0.003	0.006	—	—	—	—	—	—
Total	1.994	1.989	1.997	1.995	2.001	1.994	2.012	2.007	2.006	1.994	1.994	1.983

TABLE A5.12. (continued).

	A-12 ol	Mg Rock (anorth.)	Glassy br	Melt rock	A-14 Al	A-15 ol	A-17 Basalt	Luna 16 Soil		Luna 20 Soil	
	13.	14.	15.	16.	17.	18.	19.	20.	21.	22.	23.
	Chemical Composition (Weight Percent)										
TiO_2	52.7	51.7	59.35	52.66	53.24	50.70	53.1	52.00	50.79	53.7	53.1
Al_2O_3	0.12	0.19	0.60	0.10	0.09	0.09	0.15	0.17	0.28	—	—
Cr_2O_3	0.23	0.58	0.85	0.38	0.35	0.23	0.39	0.58	0.27	0.39	0.16
V_2O_3	0.06	—	—	—	—	—	—	—	—	—	—
FeO	46.7	37.7	34.30	44.62	45.30	46.84	45.7	44.70	48.14	37.1	45.7
MgO	0.09	8.2	3.85	0.83	0.72	0.27	0.72	0.86	0.15	8.0	0.15
MnO	0.37	0.20	—	0.32	0.47	0.52	0.44	0.50	0.45	0.36	0.40
CaO	—	0.31	—	0.12	—	0.16	—	0.11	0.34	0.58	0.04
ZrO_2	—	—	—	—	0.05	—	0.04	—	—	—	—
SiO_2	—	0.30	—	0.39	0.16	0.50	—	0.23	0.45	0.18	—
Total	100.27	99.18	98.95	99.42	100.38	99.31	100.54	99.15	100.87	100.31	99.55
	Cation Formula Based on 3 Oxygens (Ideal Ilmenite = 2 Cations per 3 Oxygens)										
Ti	0.998	0.943	1.062	0.994	0.998	0.970	0.996	0.987	0.960	0.966	1.008
Al	0.004	0.005	0.017	0.003	0.003	0.003	0.004	0.005	0.008	—	—
Cr	0.005	0.011	0.016	0.008	0.007	0.005	0.008	0.012	0.005	0.007	0.003
V	0.000	—	—	—	—	—	—	—	—	—	—
Fe	0.983	0.765	0.682	0.936	0.944	0.997	0.953	0.943	1.012	0.742	0.964
Mg	0.004	0.297	0.136	0.031	0.027	0.010	0.027	0.032	0.006	0.285	0.006
Mn	0.008	0.004	—	0.007	0.010	0.011	0.009	0.011	0.010	0.007	0.009
Ca	—	0.008	—	0.003	—	0.004	—	0.003	0.009	0.015	0.001
Zr	—	—	—	—	0.001	—	0.000	—	—	—	—
Si	—	0.007	—	0.010	0.004	0.013	—	0.006	0.011	0.004	—
Total	2.002	2.040	1.913	1.992	1.994	2.013	1.997	1.999	2.021	2.026	1.991

*Columns 3 and 4 are averages of multiple analyses.

Analysis #1 is from sample 10085 (*Agrell et al.,* 1970b); #2 is from sample 10072 (*Kushiro and Nakamura,* 1970); #3 and 4 are from sample 10057 (*Lovering and Ware,* 1970); #5 is from sample 10017 (*Brown et al.,* 1970); #6 is from sample 10058 (*Brown et al.,* 1970); #7 and 8 are from sample 12018 (*El Goresy et al.,* 1971b); #9 is from sample 12065 (*Cameron,* 1971); #10 is from sample 12022 (*Cameron,* 1971); #11 is from sample 12065 (*Cameron,* 1971); #12 is from sample 12063 (*El Goresy et al.,* 1971b); #13 is from sample 12002 (*El Goresy et al.,* 1971b); #14 is from sample 14258 (*Powell and Weiblen,* 1972); #15 is from sample 14257 (*Klein and Drake,* 1972); #16 is from sample 14310 (*Gancarz et al.,* 1971); #17 is from sample 14053 (*Haggerty,* 1972a); #18 is from sample 15555 (*Haggerty,* 1972a); #19 is from sample 75035 (*Meyer and Boctor,* 1974); #20 and 21 are from Luna 16 soil (*Haggerty,* 1972c); #22 and 23 are from Luna 20 soil (*Brett et al.,* 1973).

TABLE A5.13. Spinel analyses from lunar rocks and soils.

	A-11 LK			A-12 ol	A-12 pig	A-12 ilm	A 12 pig	A-12 ilm			A-12 ol			A-12 ilm		A-12 ol		A-12 pig	
	1.	2.	3.	4.	5.	6.	7.	8.	9.	10.	11.	12.	13.	14.	15.	16.	17.	18.	19.
Chemical Composition (Weight Percent)																			
TiO_2	20.9	21.2	32.8	3.8	4.7	6.27	7.90	9.33	10.8	20.6	22.0	23.7	25.3	24.70	24.8	28.6	29.1	32.0	33.3
Al_2O_3	8.61	4.20	1.56	12.2	12.5	11.0	12.17	10.99	11.0	8.00	4.24	4.03	3.03	5.89	5.18	3.3	2.35	2.3	2.1
Cr_2O_3	23.5	21.9	0.16	49.1	48.8	43.8	41.61	40.07	34.9	24.1	21.7	17.6	16.6	15.59	15.1	11.9	8.71	2.8	1.2
V_2O_3	0.4	—	—	—	—	0.74	—	—	0.92	0.4	0.54	0.42	0.38	—	0.75	—	0.19	0.3	—
FeO	42.1	46.4	65.7	26.8	26.3	33.3	35.98	34.46	37.8	44.4	49.3	51.7	52.8	49.55	51.6	54.1	57.4	63.3	62.8
MgO	4.23	4.74	—	7.8	7.6	3.92	1.26	4.43	3.94	2.6	2.19	0.81	2.01	2.78	2.63	2.7	0.59	0.1	0.1
MnO	0.25	0.50	0.24	—	0.4	0.27	—	0.38	0.20	0.3	0.38	0.53	0.41	0.37	0.39	0.4	1.31	0.3	0.4
CaO	<0.03	0.15	0.10	—	—	—	0.15	0.13	—	—	—	—	—	0.34	—	—	—	—	—
SiO_2	—	0.46	0.13	—	—	—	0.36	0.18	—	—	—	—	—	0.18	—	—	—	—	—
ZrO_2	<0.10	—	—	—	—	—	—	—	—	—	—	—	—	—	—	—	—	—	—
Total	99.99	99.55	100.69	99.70	100.30	99.30	99.43	99.97	99.56	100.40	100.35	98.79	100.53	99.40	100.45	101.0	99.65	101.1	99.9
Cation Formula Based on 4 Oxygens (Ideal Spinel = 3 Cations per 4 Oxygens)																			
Ti	0.541	0.566	0.915	0.096	0.117	0.163	0.205	0.240	0.281	0.537	0.592	0.654	0.685	0.659	0.662	0.764	0.807	0.880	0.924
Al	0.349	0.176	0.068	0.481	0.488	0.449	0.493	0.442	0.446	0.327	0.178	0.174	0.129	0.246	0.217	0.138	0.102	0.100	0.091
Cr	0.638	0.615	0.005	1.299	1.279	1.198	1.138	1.081	0.953	0.660	0.612	0.510	0.473	0.438	0.424	0.334	0.254	0.080	0.035
V	0.011	—	—	—	—	0.021	—	—	0.025	0.012	0.013	0.012	0.011	—	0.021	—	0.006	0.009	—
Fe	1.213	1.378	2.039	0.750	0.729	0.962	1.060	0.984	1.093	1.287	1.478	1.587	1.589	1.471	1.536	1.608	1.770	1.938	1.938
Mg	0.217	0.251	—	0.389	0.375	0.203	0.065	0.225	0.203	0.132	0.117	0.044	0.108	0.147	0.139	0.143	0.032	0.007	0.011
Mn	0.007	0.015	0.008	—	0.011	0.007	—	0.011	0.006	0.008	0.012	0.017	0.013	0.011	0.012	0.012	0.041	0.010	0.013
Ca	0.000	0.006	0.004	—	—	—	0.005	0.005	—	—	—	—	—	0.013	—	—	—	—	—
Si	—	0.016	0.005	—	—	—	0.012	0.006	—	—	—	—	—	0.006	—	—	—	—	—
Zr	0.000	—	—	—	—	—	—	—	—	—	—	—	—	—	—	—	—	—	—
Total	2.976	3.023	3.044	3.015	2.999	3.003	2.978	2.994	3.007	2.963	3.002	2.998	3.008	2.991	3.011	2.999	3.012	3.024	3.012

TABLE A5.13. (continued).

	A-12 pig							A-14 Al						Melt Rocks			A-15 pig		A-15 ol
	20.	21.	22.* core	23.* core	24.* rim	25.* rim	26.* rim	27.	28.	29.	30.	31.	32.	33.	34.	35.	36.	37.	38.
Chemical Composition (Weight Percent)																			
TiO_2	33.6	33.8	4.5	4.8	27.0	29.9	33.3	4.95	3.31	2.79	18.57	22.60	23.0	30.23	32.4	32.3	1.71	2.46	4.10
Al_2O_3	2.3	1.6	12.6	12.5	3.6	2.5	2.1	16.11	20.1	21.74	6.00	4.52	4.38	2.21	2.10	1.33	10.64	10.84	11.76
Cr_2O_3	0.8	0.2	49.2	48.6	14.8	7.1	1.2	39.56	39.1	38.17	26.06	18.99	17.3	4.52	0.97	0.32	54.87	53.30	46.28
V_2O_3	0.3	0.2	—	—	—	—	—	0.70	0.63	0.56	—	—	0.45	—	0.01	0.04	1.33	—	—
FeO	63.1	62.9	27.3	28.0	51.6	59.6	62.8	33.29	31.7	29.24	47.59	48.33	52.0	60.53	62.5	63.5	24.38	26.38	35.21
MgO	0.1	0.0	6.7	6.2	1.8	0.3	0.2	4.02	4.62	5.98	0.70	3.22	1.55	0.87	0.66	0.26	7.23	6.15	2.35
MnO	0.3	0.3	0.4	0.4	0.4	0.4	0.4	0.25	0.24	0.18	0.51	0.74	0.71	0.40	0.44	0.47	0.27	0.41	0.44
CaO	—	—	—	—	—	—	—	—	—	—	0.04	0.13	—	0.07	—	—	0.05	—	0.03
SiO_2	—	—	—	—	—	—	—	—	—	—	0.31	0.29	—	0.30	—	—	0.19	—	0.19
ZrO_2	—	—	—	—	—	—	—	0.00	0.04	0.00	—	—	0.04	—	0.19	0.08	—	—	—
Total	100.5	99.0	100.7	100.5	99.2	99.8	100.0	98.88	99.74	98.66	99.78	98.82	99.43	99.13	99.27	98.30	100.67	99.54	100.36
Cation Formula Based on 4 Oxygens (Ideal Spinel = 3 Cations per 4 Oxygens)																			
Ti	0.926	0.951	0.112	0.120	0.734	0.829	0.924	0.127	0.082	0.069	0.502	0.612	0.631	0.845	0.908	0.923	0.043	0.063	0.107
Al	0.100	0.069	0.493	0.491	0.153	0.109	0.091	0.646	0.781	0.840	0.254	0.192	0.188	0.097	0.092	0.059	0.418	0.434	0.480
Cr	0.024	0.005	1.291	1.281	0.423	0.207	0.035	1.063	1.020	0.989	0.740	0.541	0.498	0.133	0.029	0.010	1.447	1.433	1.266
V	0.009	0.007	—	—	—	—	—	0.019	0.017	0.015	—	—	0.013	—	0.000	0.001	0.036	—	—
Fe	1.936	1.968	0.758	0.781	1.559	1.838	1.938	0.947	0.875	0.801	1.429	1.456	1.585	1.881	1.948	2.017	0.680	0.750	1.019
Mg	0.007	0.000	0.331	0.308	0.097	0.017	0.011	0.204	0.227	0.292	0.037	0.173	0.084	0.048	0.037	0.015	0.360	0.312	0.121
Mn	0.009	0.009	0.011	0.011	0.012	0.012	0.013	0.008	0.007	0.005	0.016	0.023	0.022	0.013	0.013	0.015	0.008	0.012	0.013
Ca	—	—	—	—	—	—	—	—	—	—	0.002	0.005	—	0.003	—	—	0.002	—	0.001
Si	—	—	—	—	—	—	—	—	—	—	0.011	0.010	—	0.011	—	—	0.006	—	0.007
Zr	—	—	—	—	—	—	—	0.000	0.001	0.000	—	—	0.001	—	0.003	0.001	—	—	—
Total	3.011	3.009	2.996	2.992	2.978	3.012	3.012	3.014	3.010	3.011	2.991	3.012	3.022	3.031	3.030	3.041	3.000	3.004	3.014

TABLE A5.13. (continued).

	A-15 ol								L-16 Soil			L-16 Al		L-20 Soil					
	39.	40.	41.	42.	43.	44.	45.	46.	47.	48.	49.	50.	51.	52.	53.	54.	55.	56.	57.
Chemical Composition (Weight Percent)																			
TiO_2	6.10	10.01	13.85	18.12	21.10	26.40	28.14	31.56	0.83	6.14	6.93	24.14	30.16	5.25	3.99	15.22	0.54	1.10	0.16
Al_2O_3	11.35	9.66	8.04	6.23	5.03	3.81	2.82	1.95	17.36	9.55	23.33	4.06	1.90	9.37	11.88	6.67	45.50	54.43	64.70
Cr_2O_3	42.79	37.69	30.54	25.57	19.85	13.36	9.16	4.84	49.00	43.07	30.76	18.08	6.68	49.18	45.91	36.32	18.47	10.06	2.29
V_2O_3	—	—	—	—	—	—	—	—	—	—	—	0.53	0.18	—	—	—	—	—	—
FeO	34.35	40.29	42.71	46.12	50.11	53.61	56.19	61.42	25.33	37.81	30.11	50.07	60.04	29.55	28.43	35.70	24.18	15.93	10.70
MgO	3.35	2.01	3.23	2.72	2.20	2.15	1.58	0.40	7.05	1.01	7.90	1.72	0.17	5.02	8.43	4.89	10.76	17.31	21.59
MnO	0.46	0.41	0.33	0.49	0.44	0.43	0.45	0.44	0.53	0.55	0.38	0.47	0.31	0.49	0.44	0.35	0.20	0.13	0.04
CaO	0.20	0.03	0.33	0.17	0.29	0.04	0.23	0.02	0.20	0.35	0.01	0.19	0.05	0.19	0.13	0.07	0.16	0.02	0.07
SiO_2	0.41	0.19	0.48	0.36	0.31	0.28	0.45	0.33	0.41	0.57	0.13	0.15	0.15	0.29	0.13	0.17	0.43	0.10	0.18
ZrO_2	—	—	—	—	—	—	—	—	—	—	—	—	—	—	—	—	—	—	—
Total	0.99.01	100.29	99.51	99.78	99.33	100.08	99.02	100.96	100.71	99.05	99.55	99.41	99.64	99.34	99.34	99.39	100.24	99.08	99.73
Cation Formula Based on 4 Oxygens (Ideal Spinel = 3 Cations per 4 Oxygens)																			
Ti	0.159	0.263	0.367	0.484	0.574	0.714	0.776	0.866	0.020	0.165	0.116	0.655	0.840	0.116	0.104	0.379	0.012	0.022	0.003
Al	0.465	0.398	0.334	0.261	0.214	0.161	0.122	0.084	0.664	0.401	0.875	0.173	0.083	0.358	0.422	0.279	1.526	1.719	1.919
Cr	1.175	1.043	0.852	0.719	0.567	0.380	0.266	0.140	1.257	1.213	0.774	0.516	0.196	1.382	1.258	0.989	0.415	0.213	0.046
V	—	—	—	—	—	—	—	—	—	—	—	0.015	0.005	—	—	—	—	—	--
Fe	0.998	1.179	1.260	1.371	1.515	1.611	1.724	1.873	0.688	1.126	0.801	1.510	1.861	0.897	0.824	1.058	0.575	0.357	0.225
Mg	0.174	0.105	0.170	0.144	0.119	0.115	0.086	0.022	0.341	0.054	0.375	0.092	0.009	0.217	0.384	0.258	0.456	0.691	0.810
Mn	0.014	0.012	0.010	0.015	0.013	0.013	0.014	0.014	0.015	0.017	0.010	0.014	0.010	0.015	0.013	0.011	0.005	0.003	0.001
Ca	0.007	0.001	0.012	0.006	0.011	0.002	0.009	0.001	0.007	0.013	0.000	0.007	0.002	0.007	0.007	0.003	0.005	0.001	0.002
Si	0.014	0.007	0.017	0.013	0.011	0.010	0.017	0.012	0.013	0.020	0.004	0.005	0.006	0.011	0.005	0.006	0.012	0.003	0.005
Zr	—	—	—	—	—	—	—	—	—	—	—	—	—	—	—	—	—	—	—
Total	3.007	3.008	3.022	3.013	3.024	3.006	3.014	3.012	3.005	3.009	2.955	2.987	3.012	3.003	3.017	2.983	3.006	3.009	3.011

*Analyses 22 to 26 show the core-to-rim zonation in one spinel crystal.

Analysis #1 is from sample 10020 (*Haggerty et al.,* 1970); #2 and 3 are from sample 10058 (*Brown et al.,* 1970); #4 is from sample 12009 (*Brett et al.,* 1971); #5 is from sample 12052 (*Champness et al.,* 1971); #6 is from sample 12063 (*El Goresy et al.,* 1971b); #7 is from sample 12021 and #8 is from sample 12022 (*Weill et al.,* 1971); #9 is from sample 12063 (*El Goresy et al.,* 1971b); #10 is from sample 12022 (*Cameron,* 1971); #11 is from sample 12018, #12 is from sample 12002 (*El Goresy et al.,* 1971b); #13 is from sample 12018 (*El Goresy et al.,* 1971b); #14 is from sample 12022 (*Weill et al.,* 1971); #15 is from sample 12063 (*El Goresy et al.,* 1971b); #16 is from sample 12035 (*Reid,* 1971); #17 is from sample *12002* (*El Goresy et al.,* 1971b); #18 is from sample 12065 (*Cameron,* 1971); #19 is from sample 12052 (*Champness et al.,* 1971); #20 and 21 are from sample 12065 (*Cameron,* 1971); #22 to 26 are from sample 12052 (*Gibb et al.,* 1970); #27 is from sample 14053 (*El Goresy et al.,* 1971a); #28 is from sample 14072 (*El Goresy et al.,* 1972); #29 is from sample 14053 (*El Goresy et al.,* 1971a); #30 and 31 are from sample 14053 (*Haggerty,* 1972a); #32 is from sample 14053 (*El Goresy et al.,* 1972); #33 is from sample 14310 (*Haggerty,* 1972a); #34 is from sample 14310 (*El Goresy et al.,* 1972); #35 is from sample 14073 (*El Goresy et al.,* 1972); #36 is from sample 15597 (*Weigand,* 1972); #37 is from sample 15085 (*Brown et al.,* 1972); #38 to 46 are from sample 15555 (*Haggerty,* 1972b); #47 to 49 are from Luna 16 soil (*Haggerty,* 1972c); #50 and 51 are from Luna 16 soil (*Albee et al.,* 1972); #52 to 57 are from Luna 20 soil (*Haggerty,* 1973b).

TABLE A5.14. Armalcolite analyses from lunar rocks and soils.

	Armalcolite Type 1: Fe-Mg Armalcolite														
	A-11 HK		Frag br	Reg br	A-11 Soil	Reg br	A-14 Soil	A-17 Soil		A-17 Basalt					
	1.	2.	3.	4.	5.	6.	7.	8.	9.	10.	11.	12.	13.	14. core*	15. rim*
Chemical Composition (Weight Percent)															
TiO_2	70.9	73.4	75.6	72.0	71.9	75.15	69.41	73.4	73.2	73.23	72.93	71.61	73.91	74.3	72.5
FeO	16.9	15.3	11.9	14.7	11.32	14.30	21.23	16.0	15.7	15.35	16.39	16.30	14.44	13.5	17.6
MgO	8.6	7.70	8.12	8.7	11.06	6.95	3.59	6.63	6.77	6.20	5.77	6.63	7.75	7.95	5.32
CaO	—	0.01	—	0.32	—	0.16	0.31	0.28	—	—	—	0.44	0.03	—	—
MnO	0.02	0.08	—	0.07	0.01	0.09	0.10	0.11	0.10	0.08	0.08	0.09	0.17	0.00	0.02
Al_2O_3	1.8	1.62	1.87	1.48	0.97	1.80	2.60	1.96	2.00	1.87	1.87	1.77	1.99	1.93	1.91
Cr_2O_3	1.3	2.15	1.81	1.94	1.26	1.88	2.05	1.65	1.78	1.83	1.62	1.69	2.01	2.17	1.43
V_2O_3	—	<0.5	—	0.07	—	—	—	—	0.71	—	—	0.27	0.05	—	—
SiO_2	—	—	—	—	—	0.40	0.21	—	—	—	—	0.30	0.08	—	—
Nb_2O_5	—	—	—	—	—	—	0.17	—	—	—	—	—	—	—	—
Y_2O_3	—	—	—	—	—	0.05	0.05	—	—	—	—	—	—	—	—
ZrO_2	—	—	—	—	—	0.05	0.38	—	—	—	—	—	—	—	—
Total	99.52	100.26	99.30	99.28	96.52	100.83	100.10	100.03	100.26	98.56	98.66	99.10	100.43	99.85	98.78
Cation Formula Based on 5 Oxygens (Ideal Armalcolite = 3 Cations per 5 Oxygens)															
Ti	1.897	1.968	2.012	1.917	1.938	1.926	1.919	1.979	1.967	1.954	1.927	1.952	1.970	1.984	1.993
Fe	0.506	0.456	0.352	0.438	0.342	0.408	0.653	0.480	0.469	0.448	0.482	0.494	0.427	0.397	0.538
Mg	0.459	0.409	0.428	0.462	0.595	0.353	0.197	0.354	0.361	0.323	0.302	0.357	0.409	0.421	0.290
Ca	—	0.000	—	0.012	—	0.006	0.012	0.011	—	—	—	0.016	0.000	—	—
Mn	0.001	0.002	—	0.002	0.000	0.003	0.003	0.003	0.003	0.002	0.002	0.002	0.004	0.000	0.001
Al	0.076	0.068	0.077	0.062	0.041	0.072	0.113	0.083	0.084	0.050	0.045	0.048	0.082	0.081	0.082
Cr	0.037	0.061	0.051	0.055	0.036	0.051	0.060	0.047	0.050	0.050	0.045	0.048	0.056	0.061	0.041
V	—	—	—	0.002	—	—	—	—	0.020	—	—	0.007	0.001	—	—
Si	—	—	—	—	—	0.014	0.008	—	—	—	—	0.010	0.002	—	—
Nb	—	—	—	—	—	—	0.003	—	—	—	—	—	—	—	—
Y	—	—	—	—	—	0.001	0.001	—	—	—	—	—	—	—	—
Zr	—	—	—	—	—	0.083	0.007	—	—	—	—	—	—	—	—
Total	2.976	2.964	2.920	2.950	2.952	2.917	2.976	2.957	2.954	2.827	2.803	2.934	2.951	2.944	2.945

TABLE A5.14. (continued).

	Type 2: Cr-Zr-Ca Armalcolite					Type 3: Zr Armalcolite			
	Cryst br	A-15 Soil	Cryst br	A-15 Soil	L-20 Soil	A-15 Soil	A-15 Soil	A-15 Soil	A-15 Soil
	16.	17.	18.	19.	20.	21.	22.	23.	24.
Chemical Composition (Weight Percent)									
TiO_2	66.52	68.58	71.2	68.8	65.42	67.94	68.16	71.84	71.72
FeO	9.33	9.78	9.1	13.4	10.66	17.61	17.33	14.08	13.44
MgO	2.31	2.38	1.9	1.7	1.98	7.09	6.78	8.80	9.41
CaO	3.40	3.72	3.1	3.1	3.40	0.35	0.35	0.33	0.35
MnO	0.13	0.21	—	0.2	0.10	0.08	0.02	0.08	0.08
Al_2O_3	1.49	2.12	1.7	0.9	1.48	0.97	0.97	0.94	0.98
Cr_2O_3	10.31	9.67	8.8	4.3	7.67	1.46	1.49	1.49	1.45
V_2O_3	—	—	—	—	—	—	—	—	—
SiO_2	0.23	0.47	0.6	0.2	0.27	0.18	0.23	0.23	0.19
Nb_2O_5	0.37	<0.05	—	—	—	0.65	0.58	0.20	0.44
Y_2O_3	<0.05	<0.05	—	—	—	0.53	0.53	0.01	0.01
ZrO_2	6.01	4.4	4.4	6.1	6.55	3.76	3.92	2.76	2.39
REE	—	—	—	1.3	—	—	—	—	—
Total	100.10	101.33	100.8	100.0	97.53	100.62	100.36	100.76	100.46
Cation Formula Based on 5 Oxygens (Ideal Armalcolite = 3 Cations per 5 Oxygens)									
Ti	1.834	1.849	1.915	1.921	1.855	1.871	1.880	1.927	1.923
Fe	0.286	0.293	0.272	0.416	0.336	0.539	0.531	0.420	0.401
Mg	0.126	0.127	0.101	0.094	0.111	0.387	0.371	0.468	0.500
Ca	0.134	0.143	0.119	0.123	0.137	0.014	0.014	0.013	0.013
Mn	0.004	0.006	—	0.006	0.003	0.002	0.001	0.002	0.002
Al	0.064	0.090	0.072	0.039	0.066	0.042	0.042	0.040	0.041
Cr	0.299	0.274	0.249	0.126	0.229	0.042	0.043	0.042	0.041
V	—	—	—	—	—	—	—	—	—
Si	0.009	0.017	0.021	0.007	0.010	0.007	0.008	0.008	0.007
Nb	0.008	—	—	—	—	0.011	0.010	0.003	0.007
Y	—	—	—	—	—	0.010	0.010	0.000	0.000
Zr	0.108	0.077	0.077	0.110	0.120	0.067	0.070	0.048	0.042
REE	—	—	—	0.017	—	—	—	—	—
Total	2.872	2.876	2.826	2.859	2.867	2.992	2.980	2.971	2.977

*Analyses 14 to 15 show the core-to-rim variation in one spinel crystal.

Analysis #1 is from sample 10022 (*Anderson et al.,* 1970); #2 is from sample 10071 (*Anderson et al.,* 1970); #3 is from sample 10059, #4 is from sample 10068 (*Anderson et al.,* 1970); #5 is from sample 10084 (*Anderson et al.,* 1970); #6 is from sample 10021 (*Haggerty,* 1973a); #7 is from sample 14191 (*Haggerty,* 1973a); #8 is from sample 74241 (*Taylor et al.,* 1973c); #9 is from sample 75081 (*Taylor et al.,* 1973c); #10 and 11 are from sample 74242 (*Williams and Taylor,* 1974); #12 is from sample 70017, #13 is from sample 70215 (*El Goresy et al.,* 1974); #14 and 15 are from sample 70035 (*Papike et al.,* 1974); #16 is from sample 66156, #17 is from sample 15102 (*Haggerty,* 1973a); #18 is from sample 60335 (*Levy et al.,* 1972); #19 is from sample 15102 (*Peckett et al.,* 1972); #20 is from sample 22001 (*Reid et al.,* 1973); #21 to 24 are from sample 15102 (*Haggerty,* 1973a).

TABLE A5.15. Analyses of other oxides from lunar rocks and soils.

	Rutile					Baddeleyite				
	A-11 LK	A-12 Soil	Frag br	Cryst br	L-20 Soil	A-12 ilm		A-12 pig	Melt Rock	L-20 Soil
	1.	2.*	3.	4.	5.	6.	7.	8.	9.	10.
	Chemical Composition (Weight Percent)									
SiO_2	—	—	0.93	—	0.13	0.39	0.12	<0.01	—	0.18
TiO_2	96.62	87.9	87.29	98.0	97.23	1.97	3.13	2.4	—	1.82
Al_2O_3	1.91	—	0.13	—	0.02	—	—	<0.01	—	0.54
Cr_2O_3	0.30	3.2	0.56	0.3	0.48	—	—	—	—	0.13
V_2O_3	—	0.4	—	—	—	—	—	—	—	0.06
FeO	0.22	—	7.45	0.1	2.34	3.25	0.96	7.4	—	0.45
MnO	0.03	—	0.14	—	0.01	<0.02	<0.02	—	—	0.17
MgO	0.05	—	3.20	<0.1	0.04	<0.02	0.18	—	0.06	0.14
CaO	0.37	—	0.28	<0.1	0.10	—	—	<0.1	—	0.16
Nb_2O_5	—	6.4	0.55	1.6	—	—	—	—	—	0.49
ZrO_2	—	—	0.07	0.1	—	91.9	93.2	90.3	98.23	94.7
HfO_2	—	—	—	—	—	3.23	1.60	—	1.70	1.65
REE	—	1.2	—	—	—	—	—	—	—	—
Total	99.50	99.1	100.60	100.1	100.35	100.74	99.19	100.1	99.99	100.49
	Cation Formula Based on 2 Oxygens (Ideal Rutile or Baddeleyite = 1 Cation per 2 Oxygens)									
Si	—	—	0.013	—	0.002	0.008	0.002	—	—	0.004
Ti	0.971	0.915	0.898	0.984	0.980	0.030	0.048	0.037	—	0.028
Al	0.030	—	0.002	—	0.000	—	—	—	—	0.013
Cr	0.003	0.035	0.006	0.003	0.005	—	—	—	—	0.002
V	—	0.004	—	—	—	—	—	—	—	0.001
Fe	0.002	—	0.085	0.001	0.026	0.056	0.016	0.126	—	0.008
Mn	0.000	—	0.002	—	0.000	—	—	—	—	0.003
Mg	0.001	—	0.065	—	0.001	—	0.005	—	0.002	0.004
Ca	0.005	—	0.004	—	0.001	—	—	—	—	0.003
Nb	—	0.040	0.003	0.010	—	—	—	—	—	0.004
Zr	—	—	0.000	0.001	—	0.915	0.929	0.900	0.989	0.933
Hf	—	—	—	—	—	0.019	0.099	—	0.010	0.010
REE	—	0.006	—	—	—	—	—	—	—	—
Total	1.012	1.000	1.078	0.999	1.015	1.028	1.099	1.063	1.001	1.013

*Also 0.2% Ta_2O_5.

Analysis #1 is from sample 10058 (*Agrell et al.,* 1970b); #2 is from sample 12070 (*Marvin,* 1971); #3 is from sample 14321 (*Haggerty,* 1973a); #4 is from sample 15445 (*Anderson,* 1973); #5 is from sample 22003 (*Haggerty,* 1973b); #6 and 7 are from sample 12036 (*Keil et al.,* 1971); #8 is from sample 12038 (*Simpson and Bowie,* 1971); #9 is from sample 14310 (*El Goresy et al.,* 1971a); #10 is from sample 22002 (*Brett et al.,* 1973).

TABLE A5.16. Analyses of sulfide minerals from lunar rocks and soils.

	Troilite				Chalcopyrite	Cubanite	Bornite	Sphalerite	
	A-12 ilm		A-12 ol		A-12 pig		A-16 Soil	Cryst br	
	1.	2.*	3.	4.	5.	6.	7.	8.	9.
	Chemical Composition (Weight Percent)								
Ti	0.15	0.05	0.24	0.27	—	—	—	—	—
Cr	0.02	0.02	—	—	—	—	—	—	—
Fe	63.2	63.1	63.4	63.58	30.0	40.4	12.7	14.8	17.6
Cu	—	—	—	—	33.6	22.8	60.7	—	—
Mg	—	—	—	0.04	—	—	—	—	—
Zn	—	—	—	—	—	—	—	51.0	48.2
Ni	0.03	0.03	0.10	0.02	—	—	0.07	—	—
Co	0.08	0.06	0.12	0.11	0.85	0.87	0.2	—	—
S	36.4	36.0	36.4	35.66	35.2	35.7	26.2	33.0	33.7
P	—	—	—	—	—	—	0.1	—	—
Total	99.88	99.26	100.26	99.68	99.65	99.77	99.97	98.8	99.5
	Atomic Formulae: *Ideal troilite = FeS, chalcopyrite = $CuFeS_2$, cubanite = $CuFe_2S_3$, bornite = Cu_5FeS_4, sphalerite = (Zn,Fe)S*								
Ti	0.003	0.001	0.004	0.005	—	—	—	—	—
Cr	0.000	0.000	—	—	—	—	—	—	—
Fe	0.996	1.002	0.996	1.007	0.986	1.964	1.133	0.256	0.300
Cu	—	—	—	—	0.971	0.974	4.758	—	—
Mg	—	—	—	0.001	—	—	—	—	—
Zn	—	—	—	—	—	—	—	0.752	0.701
Ni	0.000	0.000	0.001	0.000	—	—	0.006	—	—
Co	0.001	0.001	0.002	0.002	0.026	0.040	0.017	—	—
S	0.999	0.996	0.996	0.984	2.016	3.022	4.071	0.992	0.999
P	—	—	—	—	—	—	0.016	—	—
Total	1.999	2.000	1.999	1.999	3.999	6.000	10.001	2.000	2.000

Analysis #1 and 2 are from sample 12063 (*Taylor et al.*, 1971); #3 is from sample 12004 (*Taylor et al.*, 1971); #4 is from sample 12021 (*Weill et al.*, 1971); #5 and 6 are from sample 12021 (*Taylor and Williams*, 1973); #7 is from sample 68841 (*Carter and Padovani*, 1973); #8 is from sample 66095 (*El Goresy et al.*, 1973); #9 is from sample 66095 (*Taylor et al.*, 1973a).

TABLE A5.17. Analyses of native Fe metal from lunar rocks and soils.

	A-11 LK	A-11 Soil		A-12 pig	A-12 ilm	A-12 ol	Melt Rock	A-15 Soil			Fan	Glassy br	Cryst br	Melt Rock	Cryst br		Melt Rock
	1.	2.	3.	4.	5.	6.	7.	8.	9.	10.	11.	12.	13.	14.	15.	16.	17.
Fe	98.95	99.2	85.82	97.54	95.7	67.4	91.71	88.4	82.74	37.8	91.33	92.66	94.69	90.45	93.31	94.94	78.41
Ni	—	0.1	13.4	0.61	1.72	26.7	7.45	4.7	5.0	60.0	6.52	4.74	4.45	0.91	5.46	4.16	20.23
Co	0.80	0.7	0.48	1.24	2.59	2.37	—	6.9	11.8	1.3	0.41	0.43	0.30	7.86	0.54	0.39	0.78
P	—	—	—	—	—	—	—	0.02	0.02	0.02	0.31	1.44	0.29	0.01	0.19	0.10	0.14
Si	0.12	—	0.14	0.16	—	—	—	—	—	—	—	—	—	—	—	—	—
Cr	0.09	—	0.04	0.05	—	0.03	—	—	0.46	—	—	—	—	—	—	—	—
Mn	—	—	0.07	0.07	—	—	—	—	—	—	—	—	—	—	—	—	—
S	—	—	—	—	—	—	—	—	—	—	0.06	0.02	0.02	0.05	0.01	0.02	0.03
Σ	100.0	100.0	99.86	99.67	100.01	96.47	99.16	100.0	100.0	100.0	98.63	99.29	99.75	99.28	99.51	99.59	99.59

Analysis #1 is from sample 10058 (*Brown et al.,* 1970); #2 is from sample 10084 (*Agrell et al.,* 1970b); #3 is from sample 10085 (*Brown et al.,* 1970); #4 is from sample 12021 (*Weill et al.,* 1971); #5 is from sample 12051 (*Keil et al.,* 1971); #6 is from sample 12004 (*Taylor et al.,* 1971); #7 is from sample 14276 (*Gancarz et al.,* 1971); #8 is from sample 15261, #9 is from sample 15071, #10 is from sample 15261 (*Axon and Goldstein,* 1973); #11 is from sample 61016 (*Misra and Taylor,* 1975a); #12 is from sample 69935 (*Misra and Taylor,* 1975a); #13 is from sample 68115 (*Misra and Taylor,* 1975a); #14 is from sample 62295 (*Misra and Taylor,* 1975a); #15 is from sample 66095 (*Misra and Taylor,* 1975a); #16 is from sample 60335 (*Misra and Taylor,* 1975a); #17 is from sample 68415 (*Misra and Taylor,* 1975a).

TABLE A5.18. Analyses of lunar phosphates.

	Whitlockite					Apatite			
	Soil	Soil	Cryst br	Melt Rock	Cryst br	Soil	Cryst br	Melt Rock	Cryst br
	1.	2	3.	4.	5.	6.	7.	8.	9.
	Chemical Composition (Weight Percent)								
CaO	40.4	40.9	39.31	42.50	42.70	52.0	52.14	56.79	54.36
P_2O_5	43.9	44.1	42.14	45.62	46.65	40.6	39.40	39.70	39.11
FeO	0.90	0.90	1.03	3.68	0.90	0.83	0.35	1.47	0.92
MgO	3.29	3.38	2.91	2.50	2.99	0.39	0.11	–	0.35
Na_2O	1.11	0.60	0.14	0.75	–	0.01	0.10	–	–
K_2O	0.01	0.04	0.02	–	–	0.02	–	–	–
SiO_2	0.76	0.31	0.41	–	–	0.75	1.38	–	0.72
TiO_2	0.07	0.11	–	–	–	0.09	–	–	–
Al_2O_3	0.50	0.10	–	–	–	0.07	0.04	–	–
Y_2O_3	2.76	2.98	3.66	1.68	–	0.10	0.81	–	1.47
La_2O_3	0.91	0.92	1.46	0.69	0.91	0.08	0.28	–	–
Ce_2O_3	2.26	2.45	3.78	1.62	2.69	0.10	0.66	–	–
Nd_2O_3	1.90	2.16	2.30	1.04	1.60	0.12	–	–	–
Cl	0.01	0.01	0.04	–	–	1.40	1.38	0.84	1.80
F	0.10	0.07	0.14	–	–	2.75	2.59	1.10	1.12
Total	98.88	99.03	97.34	100.08	98.44	99.31	99.24	99.90	99.85
	Cation Formula Based on 8 Oxygens (Whitlockite) or 12.5 Oxygens (Apatite)								
Ca	2.31	2.35	2.33	2.385	2.400	4.80	4.86	5.325	5.110
P	1.98	2.00	1.98	2.023	2.071	2.97	2.90	2.941	2.904
Fe	0.04	0.04	0.048	0.161	0.039	0.06	0.026	0.108	0.065
Mg	0.26	0.27	0.240	0.195	0.234	0.05	0.014	–	0.046
Na	0.12	0.06	0.015	0.019	–	–	0.017	–	–
K	–	–	0.002	–	–	–	–	–	–
Si	0.04	0.02	0.022	–	–	0.06	0.120	–	0.063
Ti	–	–	–	–	–	0.01	–	–	–
Al	0.03	0.01	–	–	–	0.01	0.004	–	–
Y	0.04	0.05	0.108	0.045	–	–	0.038	–	0.069
La	0.02	0.02	0.030	0.013	0.017	–	0.009	–	–
Ce	0.04	0.05	0.077	0.031	0.051	–	0.021	–	–
Nd	0.04	0.04	0.045	0.019	0.029	–	–	–	–
Total Cations	4.92	4.91	4.897	4.891	4.841	7.96	8.009	8.374	8.257
	Anion Contents Including CL and F (Analyzed) and O (Assumed)								
Cl	–	–	0.004	–	–	0.20	0.204	0.125	0.267
F	0.02	0.01	0.025	–	–	0.75	0.711	0.304	0.311
O	8	8	8	8	8	12.5	12.50	12.5	12.5

*Represents oxide sum of 99.78 less O = Fl, Cl(1.52).

Analyses #1 and 2 are from sample 10085-LR- 1 (*Albee and Chodos,* 1970); #3 is from sample 12013 (*Lunatic Asylum,* 1970); #4 is from sample 14310 (*Friel and Goldstein,* 1977); #5 is from sample 14321 (*Friel and Goldstein,* 1977); #6 is from sample 10085-LR-1 (*Albee and Chodos,* 1970); #7 is from sample 12013 (*Lunatic Asylum,* 1970); #8 is from sample 14310 (*Friel and Goldstein,* 1977); #9 is from sample 14321 (*Friel and Goldstein,* 1977).